Technische Universität München

Department für Biowissenschaftliche Grundlagen

In situ sampling rates of virtual organisms for lipophilic organic compounds

Pokem Cedrique Temoka

Vollständiger Abdruck der von der Fakultät Wissenschaftszentrum Weihenstephan für Ernährung, Landnutzung und Umwelt der Technischen Universität München zur Erlangung des akademischen Grades eines

Doktors der Naturwissenschaften (Dr. rer. nat.)

genehmigten Dissertation.

Vorsitzender:	Prof. Dr. Wolfgang Liebl
Prüfer der Dissertation:	1. apl. Prof. Dr. Karl-Werner Schramm
	2. Prof. Dr. Jean Charles Munch

Die Dissertation wurde am 15.11.2017 bei der Technischen Universität München eingereicht und durch die Fakultät Wissenschaftszentrum Weihenstephan für Ernährung, Landnutzung und Umwelt am 01.02.2018 angenommen.

Table of Contents

List of Figures

List of Tables

Acknowledgements

"There is nothing more practical than a good theory."
Ludwig Boltzman

Following the wisdom of Dr Boltzman, I have spent a great deal of my time in this project performing a theory. As anyone involved in science knows, not much can be accomplished without the support of others. Therefore it is in place to mention, in no special order, some of all the people who have helped, supported and in other ways contributed to my work.

Primary thanks must be extended to Prof Karl-Werner Schramm who gave me the opportunity to work in his PPM-MEX group. I want to thank for his trust, his expertise and his guidance in all aspects of the research that went into preparing this dissertation. His door was always open for questions and suggestions, and I have tried to learn as much as possible from his deep knowledge of organic contaminant science and analytical chemistry. Also I would like to extend deserved thanks to Dr Gerd Pfister and Mr. Bernhard Henkelmann for their technical advice at all stages throughout this study.

I am very grateful to Dr Jingxian Wang and Dr Yonghong Bi who collected all the samples that I used for the Three Gorges Reservoir project.

Our PPM_MEX group was a good environment to work. My thanks go to my dear colleagues Silke Bernhöft, Claudia Corsten, Norbert Fischer, Felix Antritter, Jacques Ehret, Joachim Nagler, Dr Florian Mertes, Dr Dominik Deyerling Dr John Mumbo, Dr Meri De Angelis, Dr Marchela Pandelova, Dr Walkiria Levy, Dr Zhenlan Xu and Prof Dieter Lenoir for their input during this period. I would also like to thank the Helmholtz Centre in Munich for access to their laboratories and equipment and of course the Research Department Bioscience for giving me the opportunity to achieve my PhD.

Lastly I would like to say special thanks to my parents Dr Dieudonné and Bernadette Temoka, my lovely husband Gerond Kwenda, my daughters Waris and Kendis (my greatest achievement), my precious sisters Frederique and Myriam and brothers Erick, Patrice and Daniel, my dearest cousins Stephanie, Christian and Dany and my extended family, for having faith and encouraging me to complete this work when times were hard but also for helping me to keep my feet on the ground and not get too ahead of myself.
May those who are not mentioned here forgive me, and know I will always be thankful to all those who have helped me.

Zusammenfassung

Diese Studie untersucht die Anwendung eines virtuellen Organismus (VO), wie beispielsweise einer semi-permeablen Membranvorrichtung (SPMD), welche ein nützliches Werkzeug zur Überwachung von Spurenkonzentrationen (pg/L) von hydrophoben organischen Verunreinigungen einschließlich polychlorierten Dibenzo-p-dioxinen und Furanen (PCDD/F), polychlorierten Biphenylen (PCB), polycyclischen aromatischen Kohlenwasserstoffen (PAK) und Organochlorpestiziden (OCP) in Wasser und Luft darstellt. Bei der Diffusion dieser Chemikalien durch die VO-Membran handelt es sich um einen isotropen Prozess, bei dem die Aufnahmerate (*ku*) und die Eliminationsrate (*ke*) in chemischen Austausch gleiche Widerstände gegenüber der Massenübertragung in beide Richtungen haben. Diese Erkenntnis ermöglicht die Entwicklung von Leistungsreferenzverbindungen (PRC). PRC werden verwendet, um die Wirkungen von VO-Membran-Biofouling auf die Aufnahmeraten der hydrophoben organischen Verunreinigungen zu bestimmen. Die Eliminationskinetik konnte durch das gleiche Massentransfergesetz beschrieben werden wie die Akkumulationskinetik. Somit kann die Geschwindigkeit des PRC-Verlustes während einer Aussetzung verwendet werden, um in situ-Kinetiken der Analyten von Interesse zu bestimmen. Huckins (Huckins et al., 2002a) beschreibt ein quantitatives Modell auf Basis von Kalibrierungsdaten, das benötigt wird, um zeitgewichtete durchschnittliche Wasserkonzentration von Zielverbindungen zu schätzen. Dieses Modell zeigt mehrere Defizite bei der Extrapolation der Kinetik von nur einem PRC zu anderen Molekülen.

In der vorliegenden Studie wurden 16 ^{13}C-makierte PAH-PRC und vier PCB-PRC Verbindungen mit mittleren und hoher Hydrophobizität untersucht, um Informationen von möglichen Variationen in den VO-Parametern oder Einwirkungsfaktoren zu gewinnen, die einen Einfluss auf die Leistung der Eliminationsrate von PRC $ke_{,PRC}$ haben. Diese Experimente wurden in mehreren Feldversuchen und in früheren Untersuchungen in unserem Labor durch den Einsatz von VO durchgeführt. Das Aufnahmeverhalten der VO ist abhängig von den physikalisch-chemischen Eigenschaften der jeweiligen Verbindungen. Die Verbindungen mit log $K_{ow} > 5.18$ haben zu niedrige Verluste gezeigt, sogar für eine lange Exposition. Die anderen Verbindungen mit log $K_{ow} \leq 5.18$ präsentierten signifikante Werte von $ke_{,PRC} \neq 0$. Nach 30 Tagen Einsatz waren die Verbindungen mit niedrigerem Octanol-Wasser-Verteilungskoeffizienten log K_{ow} im Gleichgewicht, während Verbindungen mit intermediären

log K_{ow} im linearen oder nicht-linearen Bereich lagen. So konnte eine Beziehung zwischen K_{ow} und $ke_{,PRC}$ nachgewiesen werden.

Lagerungstudien zeigten, dass keine möglichen Reaktionen in dem VO auftreten, die zur PRC Abnahme beitragen können, denn diese Verbindungen wurden vollständig erhalten in VO, wenn sie in Glasampullen niedriger Temperatur ausgesetzt waren.

Die Konzentration von PRC hat sich nach einer langen Exposition der VO in Brunnenwasser von über einem Jahr kaum verändert. Jedoch ergab eine Vergleich von VO und aktive Wasserprobenahme mit XAD-2 für die quantitativen Bestimmungen von hydrophoben organischen Verunreinigungen in klarem Wasser von Freiluft-Brunnen. Diese Ergebnisse zeigen guter Übereinstimmung die Präzision der passiven VO-Probenahme-Methode und Auswertung, die in dieser Arbeit für die Schätzung der Wasserkonzentration der Analyten entwickelt wurde.

Die Eliminationsrate *ke* von PCDD/F in VO steigt mit dem Grad der Chlorierung in VO ausgesetzt in Luft und in verschlossenen Aufbewahrungsgefäße aus Glas. Dieses Verhalten steht in Widerspruch mit anderen höher chlorierten Homologen der PCB. Die Dominanz der höher chlorierten Spezies in dem atmosphärischen Muster von PCDD/F kann diese Diskrepanz erklären. Die weniger chlorierten PCDD/F partitionierten vorzugsweise mit Aerosolen, und sind so auch in der Gasphase vorhanden. Jedoch ist das Verhalten von hoch chlorierten PCDD/F in VO immer noch mehrdeutig. Die Verwendung von PCB als PRC für die Schätzung der PCDD/F-Konzentration ist nicht zuverlässig.

Im Gegensatz zu vorhergehenden Experimenten mit nativen PCDD/F war der Prozentsatz der Rückgewinnung von Radioaktivität für ^{14}C-OCDD während 16 Tagen Expositionszeit der VO stabil in Luft und in verschlossene Aufbewahrungsgefäße aus Glas,, so dass kein messbarer Verlust von OCDD, in die Atmosphäre aufgetreten war. Die Ergebnisse zeigen, dass VO derzeit noch nicht zuverlässig für PCDD/F-Verbindungen geeignet sind.

In dieser Arbeit wurde ein alternatives Verfahren mit in-situ-Daten von 16 ^{13}C-PAH-PRC und vier PCB-PRC Verbindungen mit niedrigen bis hohen log K_{ow} von 3,4 bis 7,2 für die Abschätzung der Konzentration der Verunreinigung in Wasser wie PAHs, OCP und PCB entwickelt. Blindwert PRC Daten wurden mithilfe von Schätzungen des minimalen gesammelten Wasservolumens pro Zeit (R_{min}) modelliert, wenn die Messung der Eliminationsrate $ke_{,PRC}$ nach einer Einsatzzeit nicht möglich war. Die Beziehung zwischen log

K_{ow} und $Rs_{,PRC}$ wurde zur Bestimmung der Eliminationsrate respektive des gesammelten Wasservolumens des Analyten $R_{analyte}$ (N) der Verbindungen mit mittleren und hohen Hydrophobizität eingeführt. Ein Vergleich von Huckins Modell mit dem alternativen Verfahren ergab einen relevanten Unterschied für Verbindungen mit hohem log $K_{ow} \geq 5.18$. $R_{analyte}$ *(N)* von Verbindungen mit log K_{ow} von 5,18 bis 7,24 ergeben mehr als das 30-fache des gesammelten Wasservolumens von Huckins $R_{analyte}$*(H).* Unsere Methode vergleicht sich mit der PAK Wasserkonzentration von XAD-2 zeigte Genauigkeit

Das alternative Modell wurde auf die OCP Wasserkonzentration im Drei-Schluchten-Stausee (TGR) während der Probenahme-Kampagnen in den Jahren 2009 und 2011 angewendet. Die gemessenen Konzentrationen variierten im Bereich von 410 bis 1418 pg/L. Die höchste Gesamt OCP-Konzentration wurde in Wanzhou gemessen, während die niedrigste flussabwärts in Maoping in der Nähe des Drei-Schluchten-Damm (TGD) ermittelt wurde. Darüber hinaus wurde eine Untersuchung des OCP-Massenflusses des Yangtzes vorgenommen. Es ergaben sich Massenflüsse im Bereich von 9,6 mg/s in Wanzhou bis 2,97 mg/s in Maoping. Obwohl mehrere Faktoren die Reduktion der OCP-Wasserkonzentration in TGR 2008-2009 erklären könnte, könnte die frühere Anwendung der Huckins Methode bei der Probenahme-Kampagne im Jahr 2008 zur Bestimmung der gesamten OCP zu einer erheblichen Überschätzung der Wasserkonzentration geführt haben.

.

Abstract

This study involves the application of a Virtual Organism (VO), such as a Semi Permeable Membrane Device (SPMD), as a useful tool for monitoring trace (pg/L) concentrations of hydrophobic organic contaminants including polychlorinated dibenzo-p-dioxins and furans (PCDD/F), polychlorinated biphenyls (PCB), polycyclic aromatic hydrocarbons (PAH) and organochlorine pesticides (OCP) in water and air media. Diffusion of these chemicals through the VO is an isotropic process, in which the uptake rate (*ku*) and the elimination rate (*ke*) in chemical exchange have equal resistances to mass transfer in either direction. This finding permits the development of the performance reference compounds (PRC) approach. The PRC compounds are used to determine collected water volume of VO membranes despite biofouling and other effects on the uptake rates of the hydrophobic organic contaminants. The elimination kinetic was governed by the same mass transfer as the uptake kinetic. Hence, the rate of PRC loss during an exposure could be used to estimate in situ sampling rates of the analytes of interest. Huckins (Huckins et al., 2002a) described a quantitative model based on calibration data needed to estimate time-weighted average water concentrations of target compounds. This model reveals several shortcomings when extrapolating the sampling rate of only one PRC to other molecules.

In this present study, the investigation of 16 ^{13}C-PAH-PRC and four PCB-PRC labelled compounds with moderate and high hydrophobicity was established with the aim of providing information of potential variations in VO parameters or exposure factors that have an impact in the variability of the elimination rate of PRC $ke,_{PRC}$. This experiment was achieved through the deployment of VO in several field deployments from previous research in our laboratory. The uptake behaviour of VO depends on the physicochemical properties of the compounds of interest. The PRC compounds with log $K_{ow} > 5.18$ have exhibited too low a dissipation even for a long exposure time. The other compounds with log $K_{ow} \leq 5.18$ presented relevant values of $ke,_{PRC}$. After 30 days of deployment, compounds with lower octanol-water partition coefficient log K_{ow} were in equilibrium, while compounds with intermediary log K_{ow} were in linear or curvilinear stage. Hence, a relationship between K_{ow} and $ke,_{PRC}$ was assessed.

No potential reactions occurred in the VO that may contribute to the PRC elimination since these compounds were completely retained in VO when they were exposed inside the glass ampules at low temperature.

Concentrations of PRC were not affected after a long exposure time of over a year. However, a comparison of VO and active water sampling with XAD-2 for the quantitative determinations of hydrophobic organic contaminants in clean water from outdoor wells showed the accuracy of the passive sampling method developed in this work for the estimation of the analyte water concentration.

The uptake rate of PCDD/F in VO increased with the degree of chlorination in VO exposed in air and in glass vial. This behaviour contradicts the other higher chlorinated homologues such as PCB. The predominance of higher chlorinated species in the atmospheric pattern of PCDD/F may explain this discrepancy. The lower chlorinated PCDD/F partitioned preferentially with particles in air and is more pronounced in the gas phase. However, the release of high chlorinated PCDD/F in VO is still ambiguous and the use of PCB as PRC for the estimation of PCDD/F concentration was indicated as improper.

In contrast to the precedent experiment, the percentage of recovery of radioactivity for ^{14}C-OCDD was stable during sixteen days of exposure time of VO exposed in air and in glass vials, indicating that no loss of OCDD, the highest chlorinated compound of PCDD had occurred into the atmosphere. This result reveals the VO deficiency to accumulate PCDD/F compounds properly.

An alternative method was developed in this work using in-situ data of the sixteen ^{13}C PAH-PRC and four PCB-PRC, with log K_{ow} ranging from 3.4 to 7.2, for the estimation of water contaminant concentrations such as PAH, OCP and PCB. Blank PRC data to allow estimation of minimal sampling rate R_{min} were utilized when the measurement of PRC sampling rate $Rs_{,PRC}$ after a deployment time was not obtainable. The relationship between log K_{ow} and $Rs_{,PRC}$ was established for determining the analyte sampling rate $R_{analyte}(N)$ of compounds with moderate and high hydrophobicity. Comparison of Huckins model and the alternative method revealed a relevant difference for compounds with high log $K_{ow} \geq 5.18$. $R_{analyte}(N)$ of compounds with log K_{ow} ranging from 5.18 to 7.24 were reported to be more than 30-fold higher than the analyte sampling rate from Huckins $R_{analyte}(H)$. Our method compares with the XAD-cartridge presented accuracy.

The alternative model was applied to assess the OCP water concentration in Three Gorges Reservoir (TGR) during the sampling campaigns in 2009 and 2011. The measured concentrations varied between 410 and 1418 pg/L. The highest total OCP concentration was

found in Wanzhou while the lowest was downstream from Maoping near the Three Gorges Dam (TGD). Furthermore, investigation of OCP mass flux at Yangtze presented values ranged from 9.6 mg/s in Wanzhou to 2.97 mg/s in Maoping. Although several factors might explain the reduction of OCP water concentration in TGR from 2008 to 2009, the previous application of Huckin's method during the sampling campaign in 2008 to determine total OCP may have led to a substantial overestimation of the water concentration.

List of Publications

Author: Manuscript I, II

I. **Temoka C**, Wang J, Bi Y, Deyerling D, Pfister G, Henkelmann B, Schramm K-W (2016): Concentrations and Mass Fluxes estimation of Organochlorine Pesticides in Three Gorges Reservoir with virtual organisms using in situ PRC-based sampling rate, Chemosphere 144, 1521–1529

II. **Temoka C**, Pfister G, Henkelmann B, Schramm K-W (2017): Adapting current model with field data of related performance reference compounds in passive samplers to accurately monitor hydrophobic organic compounds in aqueous media. Environ Monit Assess 189:543-555 doi: 10.1007/s10661-017-6252-4

Coauthors: Manuscripts III, IV, V

III. Bergmann A, Bi Y, Chen L, Flöhr T, Henkelmann B, Holbach A, Hollert H, Hu W, Kranzioch I, Klumpp E, Küppers S, Norra S, Ottermanns R, Pfister G, Roß-Nickoll M, Schäffer A, Schleicher N, Schmidt B, Scholz-Starke B, Schramm K-W, Subklew G, Tiehm A, **Temoka C**, Wang J, Westrich B, Wilken R-D, Wolf A, Xiang X, Yuan Y (2011a) The Yangtze-Hydro Project: a Chinese-German environmental program. Environ Sic Pollute R. doi: 10.1007/s11356-011-0645-7

IV. Chen L, Bi Y, Zhu K, Hu Z, Zhao W, Henkelmann B, Bernhöft S, **Temoka C**, Schramm KW (2013) Contamination status of dioxins in sediment cores from the Three Gorges Dam area, China. Environ Sci Pollut Res Int. doi:10.1007/s11356-012-1447-2

V. Schramm, K.-W., Wang, J., Bi, Y., **Temoka, C**., Pfister, G., Henkelmann, B., Scherb, H., (2013) Chemical-and effect-oriented exposomics: Three Gorges Reservoir (TGR). Environmental Science and Pollution Research 20, 7057-7062.

VI. Wang J, Henkelmann B, Bi Y, Zhu K, Pfister G, Hu W, **Temoka, C**., Schramm, K.W., (2013) Temporal variation and spatial distribution of PAH in water of Three Gorges Reservoir during the complete impoundment period. Environmental Science and Pollution Research 20, 7071-7079.

Abbreviations and Acronyms

Ace	Acenaphthylene
Acy	Acenaphthene
Alox	Aluminum Oxide
Ant	Anthracene
BaA	Benzo[a]anthracene
BAF	Bioaccumulation factors
BaP	Benzo[a]pyrene
BbF	Benzo[b]fluoranthene
BkF	Benzo[k]fluoranthene
BghiP	Benzo[g,h,i]perylene
BD1/2	Badong ½
CDF	Chlorinated dibenzofuran
Chr	Chrysene
CQ	Chongqing
CS	Changshou
DahA	Dibenzo[a,h]Anthracene
DDD	Dichlorodiphenyldichloroethane
DDE	Dichlorodiphenyldichloroethylene
DDR	Deutsche Demokratische Republik
DDT	Dichlorodiphenyltrichloroethane
DJR	Danjiangkou Reservoir
DN1/2	Daning (Wushan) 1/2
DPM	Disintegrations per minute
EPA	Environmental Protection Agency
FEN	Phenanthrene
FJ	Fengjie
Fle	Fluorene
Flu	Fluoranthene
GC-MS	Gas Chromatography-Mass Spectrometry
GJB	Guojiaba
HCB	Hexachlorobenzene
HCH	Hexachlorocyclohexane
HMGU	Helmholtz Zentrum München
HRGC	High Resolution Gas Chromatography
HRMS	High Resolution Mass Spectrometer
IND	Indeno(1 2 3-cd)pyrene
LDPE	Low Density Polyethylene
LOD	Limit of Detection
LOQ	Limit of Quantification
MEX	Molecular EXposomics
MP	Maoping
MW	Megawatts

B	Constant
Cc	Carbon column
C_{min_tr}	Minimum concentration of analyte of a tributary
C_{SP}	Analyte concentration adsorbed on soil
$CV(\%)$	Coefficient of variation
C_W	Analyte concentration in water
$C_W(N)$	Analyte concentration in water from new procedure
$C_W(H)$	Analyte concentration in water from Huckins
$C_{W(eq)}$	Analyte concentration in water from $K_{VO\text{-}W}$
$C_{W(Rs)}$	Analyte concentration in water from $Rs_{analyte}\,(N)$
C_t	Analyte concentration in water and suspended particles
$D(x,t)$	Discharge upstream of the Yangtze dependent on the location x and time t
$D(x+1,t)$	Discharge downstream of the Yangtze dependent on the location x+1 and time t
f_{oc}	Fractional soil organic carbon content
h	Distance
K_{oa}	Octanol/air partition coefficient
K_{oc}	Soil Organic Carbon/Water partition coefficient
K_{ow}	Octanol/water partition coefficient
ke	Elimination rate constant
$ke_{,PRC}$	PRC release rate constant
K_H	Henry´s law constant
K_{TW}	Triolein-water partition coefficient
K_{LPDEW}	LPDE-water partition coefficient
$K_{VO\text{-}W}$	VO-water partition coefficient
ku	Uptake rate constant
m	Mass of the sampler
m_{SP}	Mass of analyte in water bound to suspended particles
m_{DOC}	Mass of analyte in water bound to DOC
m_w	Mass of analyte in water in its freely dissolved form
MF_{OCP}	OCP mass flux

Naph	Naphthalene
NLS	Nonlinear squares
PAH	Polycyclic Aromatic Hydrocarbons
PCP	Pentachlorophenol
PE	Polyethylene
PeCA	Pentachloroanisol
PeCB	Pentachlorobenzene
Pyr	Pyrene
OCP	Organochlorine Pesticides
OCS	Octachlorostyrene
TCDD	Tetrachlorodibenzo-*p*-dioxins
PCB	Polychlorinated Biphenyls
PCDD	Polychlorinated dibenzo-p-dioxins
PCDF	Polychlorinated dibenzofurans
POP	Persistent Organic Pollutants
PRC	Performance Reference Compounds
SC	Scintillation Cocktail
SPMD	Semi-permeable Membrane Device
SPE	Solid Phase Extraction
SV	Scintillation Vial
TWA	Time weighted average
TGR	Three Gorges Reservoir
TGD	Three Gorges Dam
UNEP	United Nations Environment Programme
US	United States
USEPA	United States Environmental Protection Agency
VO	Virtual Organism
VO(N)	Concentration in VO from new method
VO(H)	Concentration in VO from Huckins
VOC	Volatile Organic Compound
XJ1/2	Yunyang 1/2
WBL	Water Boundary Layer
WZ	Wanzhou
XAD	Polystyrene-based absorption resin

ΔMF_{OCP}	Mass fluxes difference from upstream to downstream
MW *or* M	Molecular Weight
n	Number of blank used for the measurement
N *or* N_{VO}	Amount of analyte accumulated after a given exposure time
r	Radius
R^2	Coefficient of correlation
$Rs_{,PRC}$	PRC sampling rate
$Rs_{analyte}(H)$	Analyte sampling rate from Huckins
$Rs_{analyte}(N)$	Analyte sampling rate from the alternative theory
Rs^{300}	Analyte sampling rate with molar mass of 300 g/mol
Sc	Sandwich column
S_{CV}	Standard error of CV
Sn	Standard deviation
S_{SP}	Concentrations of PAH in suspended particles
S_{DOC}	Mean value of daily discharge of DOC
u	Dissipation of PRC during exposure time
$\bar{u}$	Average dissipation of PRC
u_i	Obtained values in percent for the blank sample i
u_{max}	Largest possible deviation from ū
u_o	Obtained values
u_w	Expected values
Vs	Volume of the VO/SPMD
V_T	Volume of the triolein
V_{LPDE}	Volume of the membrane LPDE
Vm	LeBas Molar Volume of target analyte
$Vm_{,PRC}$	LeBas Molar Volume of the selected PRC
y	Uncertainty

1 Chapter I: Introduction

Persistent organic pollutants (POP) are organic contaminants, generally halogenated or aromatic with low water solubility and high lipid solubility. This affinity for the adipose tissues leads to their accumulation, persistence and bioconcentration. The level of POP in the environment is a global matter of great concern as these compounds generated a cycle of volatilization and deposition due to their resistance to breakdown reactions in air. Humans can be exposed to POP through diet, occupational accidents and the environment. Exposure to POP, either acute or chronic, can be associated with a wide range of adverse health effects, including illness and death. Laboratory investigations and environmental impact studies in the wild have implicated POP in endocrine disruption, reproductive and immune dysfunction, neurobehavioral and disorders and cancer. Due to their persistence, toxicity, bioaccumulation and long range transport potential, POP are on the lists of substances which have been banned or severely restricted under the United Nations Environmental Program (UNEP) Stockholm Convention.

The monitoring of POP is highly important for the control of water and air quality to assess human exposure. Analysis of POP can be difficult because in water, they partition strongly to organic matter, avoiding the aqueous phase and in the atmosphere, they partition between gas phase and aerosols depending on the physico-chemical properties of the chemical and ambient temperature. Several methods are currently used for monitoring POP. The direct use of tissue samples is useful as it provides a measure of exposure but circumstances such as issues of metabolism, depuration, low bioaccumulation potential of a chemical, avoidance of contaminated areas, death of the organism or episodically appearance of contaminants in water column can all cause inaccuracies in estimating the chemical concentration. The common alternative sampling techniques to investigate non-polar lipophilic chemical are the application of passive sampling technologies such as a semipermeable membrane device SPMD. SPMD is a man-made device with which the concentration of chemicals is mediated by the diffusion of volatile organic compounds (VOC) into the sampler, which allows for the estimation of time-weighted average trace concentrations (sub-parts-per-trillion) from site-specific environmental conditions. The original models, in which the uptake rate is used to estimate the time-weighted average concentrations, relied on sampling rates determined under a specific condition in the laboratory (Huckins et al., 1993). Consistent differences between experimental-derived sampling rates and in situ sampling rates were observed as the diffusion into the monitor is

affected by the environmental conditions such as water turbulence, temperature and biofilm covering the membrane surface. Also the size of very hydrophobic organic compounds may play a dominant role in dictating the sorption kinetics in and out of the sorbent phase.

The research of this study was designed to establish an alternative approach that allows us to estimate accurate values of time-integrated dissolved concentration of POP in the air or in water exposure media using the in-situ sampling rate values of fifteen ^{13}C PAH-PRC compounds and four PCB-PRC with log K_{ow} ranged from 3.38 to 7.2. The new model was compared with the Huckins method and was applied for investigating organic pollutants in the Yangtze River (China). The Yangtze River Project and POP of interest to this study are briefly described below, while evaluation of the behaviour of these pollutants in the passive sampler is discussed in more detail in chapter 2

1.1 Yangtze River Project

The Yangtze River is the longest river in both China and Asia and is also the third longest river in the world in terms of its length (6,300 km) and flux (9.6×1011 m3 year−1). The river provides about 70% of water transportation, runs through more than 25% of the farmlands and over 30 industrial cities are located along its coast. More and more people in cities and towns along the river explore the river water as the sources of their drinking water.

The Three Gorges Dam (TGD), which was constructed on the Yangtze River, is the world's largest hydroelectric power generator with a total generating capacity of 18,200 MW. The dam produces electricity, increases the Yangtze River's shipping capacity and reduces the potential for floods downstream by offering flood storage space. The Three Gorges reservoir (TGR) created by TGD has an area of 1080Km2, 700km length with the backwater ending in Chongqing city (Fig.1.1.1). The highest water level reached 175 m in flood season after the final impoundment in October 2010.

TGR, said to be one of the most polluted reservoir in the world, has been concern about certain measures as discharge of industrial wastes, promoted the application of fertilizers, pesticides in farming, as well as heavy metal pollution (Wong et al., 2007). As a consequence, the cities close to the TGD may experience drastic environmental alterations such as changes in the whole ecosystem structure and functioning(Wu et al., 2004). One billion tons of sewage is flowing into the TGR each year. Pollution in the river itself will increase, as the dam will slow waterflow, stopping the river's natural cleaning mechanisms.

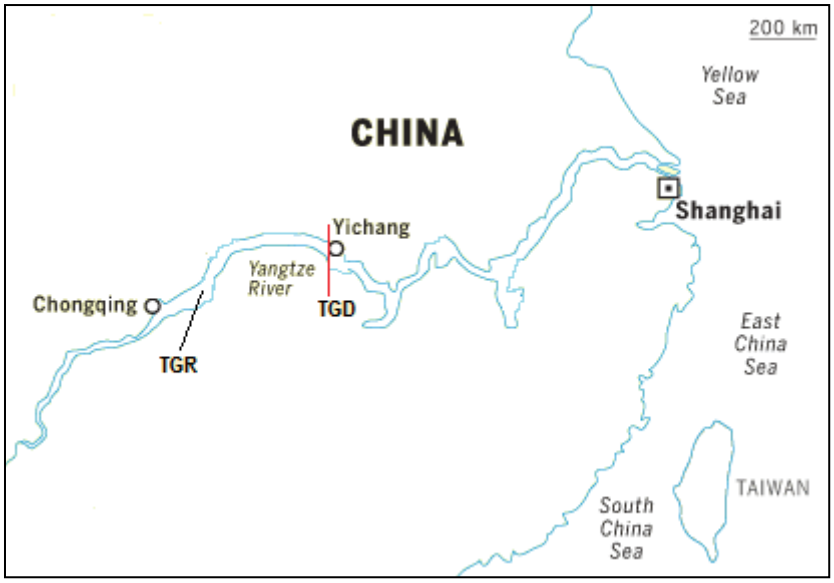

Fig. 1.1.1: Yangtze River, Three Gorges Reservoir (TGR), Three Gorges Dam (TGD)

Water Quality in TGR is of great concern as the electricity produced by the dam should not be produced by a dirty Chinese coal-burning power plants leading to serious environmental impacts. Although the government officials took some measures to improve water quality in TGR, they note that eutrophic conditions and algal blooms continue to occur throughout the basin (Cai and Hu, 2006).

The Yangtze-hydro Project is an agreement settle in 2010 between Chinese and German scientist from universities, institutes and research centre, which aims to provide an environmental research on the area of the TGR. Hence, investigations on water quality deterioration and eutrophication, and sediment quality have been launched (Bergmann et al., 2012).

The role of our research group PPM-MEX on this project included the study of the behaviour and transformation of non-polar pollutants in water and in air, using SPMD-based Virtual organism (VO), a virtual tool used for the measure of all exposures like persistent organic pollutants to molecules (Schramm et al., 2013).

1.2 Overview of persistent organic pollutants (POP)

POP possesses in general high lipophilicity, which means POP can concentrate in the fat and lipid of marine organisms. The lipophilicity of POP is related to the octanol-water partition coefficient K_{ow}. K_{ow} is defined as the ratio of chemical concentration in octanol in relation to its concentration in water when the two phases are in equilibrium. Log K_{ow} can be used as a

measure of a compounds lipophilicity or hydrophobicity which can then be associated with its potential bioavailability. Studies of the past 15 to 20 years have provided evidence of the widespread distribution of these non-polar organic chemicals (Meijer et al., 2003; Moeckel et al., 2008; Dreyer et al., 2009) and their analysis allows managers to assess the quality and safety. To date, the concentration and distribution of these substances have been estimated in different sources of many countries (Reid et al., 2000; Carrera et al., 2001; Manz et al., 2001; Wang et al., 2009).

There is a wide range of POP of interest to the environmental scientist; however this study will concentrate on compounds that are covered by legislation or conventions (Parliament, 2008) such as Organochlorine Pesticides (OCP), PCDD/F and Polychlorinated biphenyls (PCB) and others substances possessing the POP characteristics such as Polycyclic Aromatic Hydrocarbons (PAH).

1.2.1 Polycyclic Aromatic Hydrocarbons (PAH)

1.2.1.1 Physical and Chemical Properties

The PAH compounds are one of the most widespread forms of organic pollutants in the environment, significantly affect air, water and soil quality.

PAH originate from both natural and anthropogenic burning processes and have increased steadily due to human impact. PAH are composed of two or more fused benzene rings (Neff, 1985). Aromatic rings are fused when they share two carbon atoms. The lowest molecular weight PAH, Naphthalene ($C_{10}H_8$), consisting of two fused aromatic rings (Figure 1.2.1) is commonly found in air and water. The physical and chemical characteristics of PAH vary with the molecular weight (Table 1.2.1), the highest molecular weight PAH (6 benzene rings) tend to be extremely persistent in soil as their water solubility and mobility decrease substantially with their increasing molecular weight. The United States Environmental Protection Agency currently listed the 16 most hazardous PAH

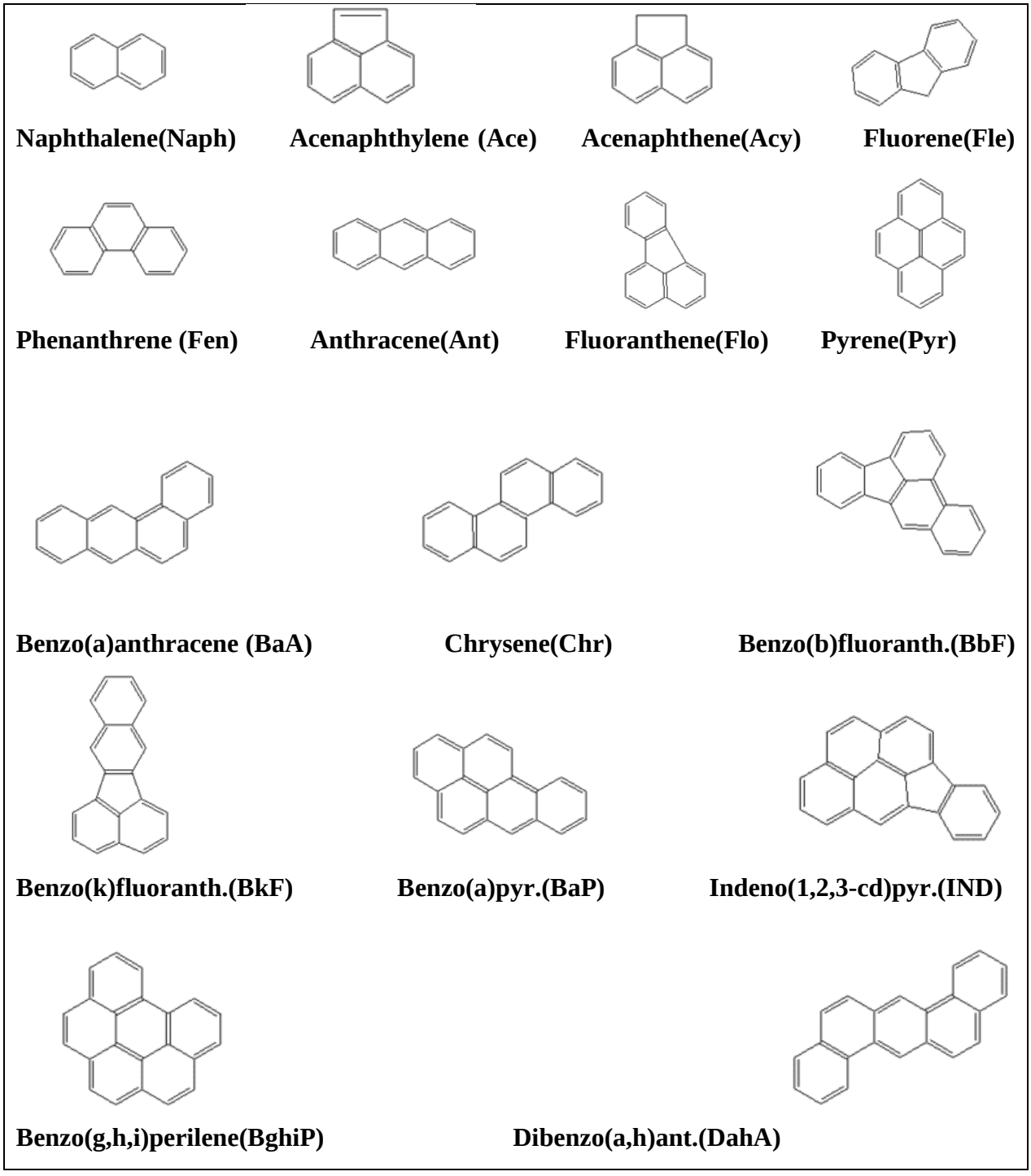

Fig. 1.2.1: Chemical structures of sixteen priority polycyclic aromatic hydrocarbons (PAH) *(Anyakora et al., 2011)*

Table 1.2.1: Octanol-water partition coefficient log K_{ow} at 25°C and molecular weight of sixteen EPA PAH(Mackay et al., 1992)

Chemical Name	log K_{ow}	MW (g/mol)
Naph	3.38	134
Ace	4.07	158
Acy	3.92	160
Fle	4.1	172
Fen	4.46	184
Ant	4.54	184
Flo	4.84	208
Pyr	5.18	208
BaA	5.6	234
Chr	5.84	234
BbF	6.44	258
BkF	6.44	258
BaP	6.42	256
IND	6.42	282
BghiP	6.63	288
DahA	6.5	284

Log K_{ow} increases with increasing molecular weight, whereas the aqueous solubility of these compounds decreases. However, it becomes increasingly difficult to accurately estimate aqueous solubility and partition coefficients as the molecular weight increases. Therefore, measures of these physical properties from literature vary over a range of several orders of magnitude (Güsten et al., 1991; Mackay et al., 1992; Meador et al., 1995; De Maagd et al., 1998)

1.2.1.2 Sources

PAH are used in medicines, plastics and pesticides and may be synthetized by a variety of mechanisms (Neff, 1979). Hence, pyrogenic PAH are formed by a rapid incomplete combustion or pyrolysis of organic materials, in a very high temperature, around 700 °C, petrogenic PAH are formed by very slow rearrangement and transformation of biogenic materials at moderate temperatures of 100-300 °C to form fossil fuels, diagenetic PAH are formed by a relatively rapid (days to years) transformation of certain classes of organic compounds in soil and sediments and biogenic PAH are formed by a direct biosynthesis.

Many PAH are known or suspected carcinogens. A wide variety of organic compounds containing fused-ring polyaromatic systems are synthesized by organisms, particularly bacteria, fungi, higher plants and some insects (Fetzer, 2007). Most of these compounds are not true

PAH because they contain oxygen, nitrogen or sulfur substituents. Direct biosynthesis is not a quantitatively important source of PAH in the marine environment

1.2.1.3 Fate and Transport

PAH are transported from superficial water to sediment (Rojo-Nieto et al., 2013). Because of their low solubility in water and hydrophobicity, PAH in the marine environment are rapidly bound to organic and inorganic suspended particles, and afterwards, they are deposited in sediments. As PAH solubility decreases with increasing molecular weight, organisms are often enriched in the lower molecular weight PAH, relative to the water. This is because the heavier molecular weight compounds are preferentially adsorbed on sediment or associated with particulate matter while the lighter molecular weight PAH are dissolved in the water, although all of them are hydrophobic (Baumard et al., 1999).

1.2.2 Organochlorine Pesticides (OCP)

1.2.2.1 Physical and Chemical Properties

OCP are chlorinated hydrocarbons used extensively from the 1940s through the 1960s for the purpose of killing or otherwise deterring "pest" species in agriculture control.

OCP investigated in this study include hexachlorocyclohexanes (HCH), dichlorodiphenyltrichloroethane (DDT) and its related organochlorines, chlordane and its related organochlorines and chlorobenzenes (Fig.1.2.2).

Hexachlorocyclohexanes (HCH), a commercial insecticide, consists of a mixture of five configurational isomers (primarily α, β, γ, δ, and ε isomers). It was introduced in 1942 and was banned in the Federal Republic of Germany in 1977. Lindane or technical-grade hexachlorocyclohexane containing the γ isomer is used primarily as an insecticide in the treatment of wood and wooden structures, seed grains, and live-stock (Dorsey, 2005; Bank, 2009). The molecular formula of HCH is $C_6H_6Cl_6$.

Hexachlorobenzene with the molecular formula C_6Cl_6 was found to be a more environmentally persistent molecule. This pollutant is mainly emitted by combustion and is still detectable in marine environments and organisms. It is used as a wood preservative and as a fungicide on grains, especially wheat.

Pentachlorobenzene (PeCB) was previously used as a fungicide and chemical intermediate such as the production of quintozene (a soil fungicide). It is unintentionally produced during combustion in thermal and industrial processes and appears as an impurity in products such as solvents or pesticides. The molecular formula of PeCB consists of a benzene ring substituted with five chlorine atoms C_6HCl_5.

Pentachloroanisole (PeCA) is formed mainly from biomethylation of pentachlorophenol (PCP) by bacteria and fungi in the environment. PeCA is easily evaporated, quite stable in the atmosphere and has a very high potential to bioaccumulate. Although it does not meet internationally recognized persistence criteria, its semi-volatile nature has made him ubiquitous and susceptible to long range transport. The molecular formula of PeCA is $C_7H_3Cl_5O$.

Octachlorostyrene (OCS) is formed as a by-product from waste material burning at temperatures between 600-800 °C. It was consistently found in fish and sediment. The molecular formula is C_8Cl_8.

Dichlorodiphenyltrichloroethane (DDT) is one of the best known pesticides, synthesized first by a German chemist named Othmar Zeidler in 1874 and used later by Paul Hermann for its insecticidal properties. It was the most effective agent known for eradicating diseases that are transmitted by insects. It is highly hydrophobic, colorless, crystalline and solid with a weak odour. It is soluble in most organic solvents, fats and oils. DDT has the molecular formula $C_{14}H_9Cl_5$. DDT degrades into two metabolites: are dichlorodiphenylethane (DDE) and dichlorodiphenyldichloroethane (DDD). The major metabolite is DDE.

Endosulfan is an insecticide of the cyclodiene group, chemically similar to Aldrin, chlordane and heptachlor. Technical endosulfan is a mixture of stereoisomers designated endosulfan-I (α) and endosulfan-II (β). Endosulfan-I is the more stable of the two and it is about three times more toxic than endosulfan-II. The principal metabolite of endosulfan is endosulfan sulfate. The sulfate is equally toxic and more persistent than the parent isomers (Lubick, 2010). Endosulfan has as molecular formula $C_9H_6Cl_6O_3S$.

Chlordane, from its past use as pesticide, has adhered strongly to soil particles at the surface. It has the molecular formula $C_{10}H_6Cl_8$. Chlordane has the ability to stay in the soil for over 20 years and can leave soil by evaporation to the air. Its metabolites include cis-chlordane and trans-chlordane that are resistant to metabolism and have a strong affinity for lipid and biomagnify in aquatic food webs.

Heptachlor is one of the cyclodiene insecticides, used to kill cotton insects, grasshoppers, termites and malaria-carrying mosquitoes. It has a highly stable structure, therefore can persist in the environment for decades. Its molecular formula is $C_{10}H_5Cl_7$. The metabolites of heptachlor include cis-heptachlorepoxide and trans-heptachlorepoxide. They are more persistent and dissolve more easily in water than its parent compound.

Aldrin is an insecticide that was widely used to treat seeds and soil until the 1970s when it was banned in most countries. Exposure to it is mostly from eating contaminated foods. It has the molecular formula $C_{12}H_8Cl_6$. Sunlight and bacteria rapidly change aldrin instantly to dieldrin in the body and the environment.

Endrin is a colourless, odourless solid that could also be used as a rodenticide. It is a stereoisomer of dieldrin and has as molecular formula $C_{12}H_8Cl_6O$.

Methoxychlor is an insecticide that is used to protect crops, ornamentals, livestock and pets against fleas, mosquitoes, cockroaches and other insects. It is a pale-yellow powder with a slight fruity or musty odour. It has a relatively low toxicity and does not lead to bioaccumulation. It has a short persistence in biological systems but it is very persistent in soil and its half-life is greater than six months. Methoxychlor has as molecular formula $C_{16}H_{15}Cl_3O_2$.

Mirex is an insecticide, white crystalline odourless solid that was used to control fire ants and termites. It is highly resistant to microbiological degradation and slowly dechlorinates to a mono-hydroderivative by anaerobic microbial action in sewage sludge and by enteric bacteria. Mirex also is highly accumulative, present in aquatic and terrestrial food chains to harmful levels. Mirex has as molecular formula $C_{10}Cl_{12}$.

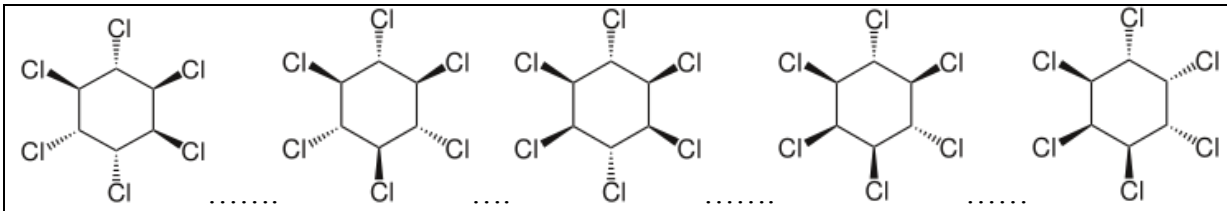

α-HCH **β-HCH** **γ-HCH** **δ-HCH** **ε-HCH**

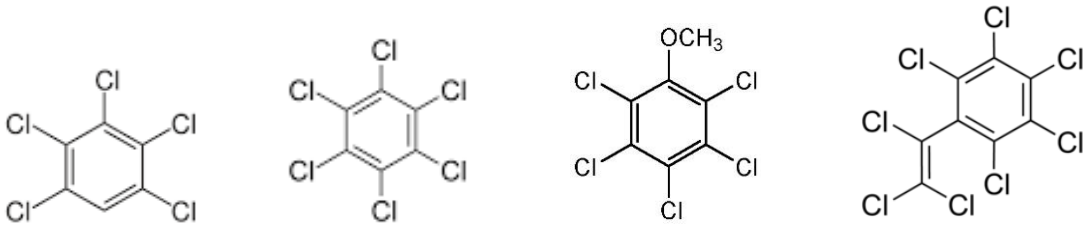

PeCB **HCB** **PeCA** **OCS**

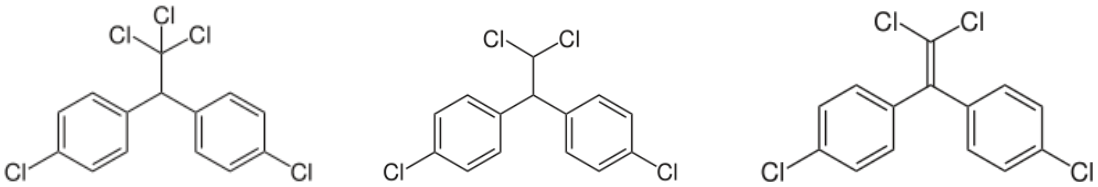

p,p'-DDT **p,p'-DDD** **p,p'-DDE**

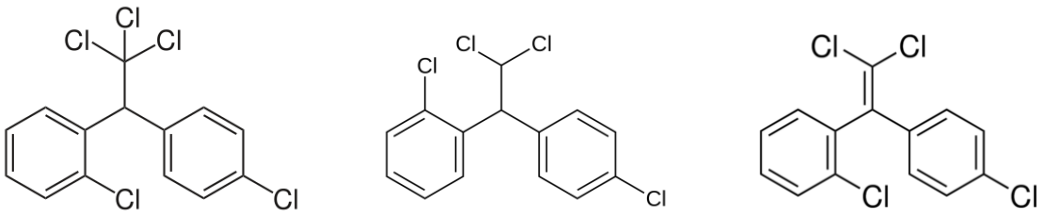

o,p'.DDT **o,p'-DDD** **o,p'-DDE**

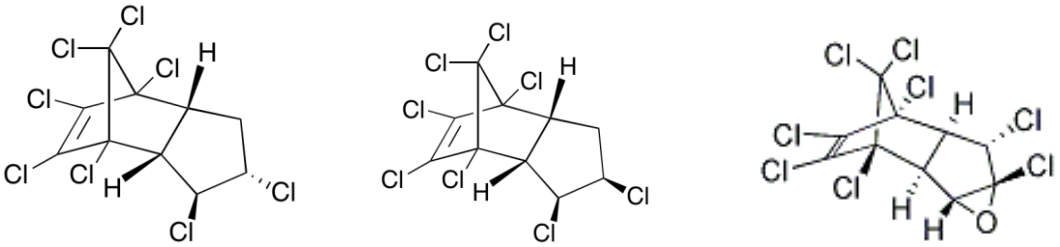

trans-chlordane **cis-chlordane** **oxy-chlordane**

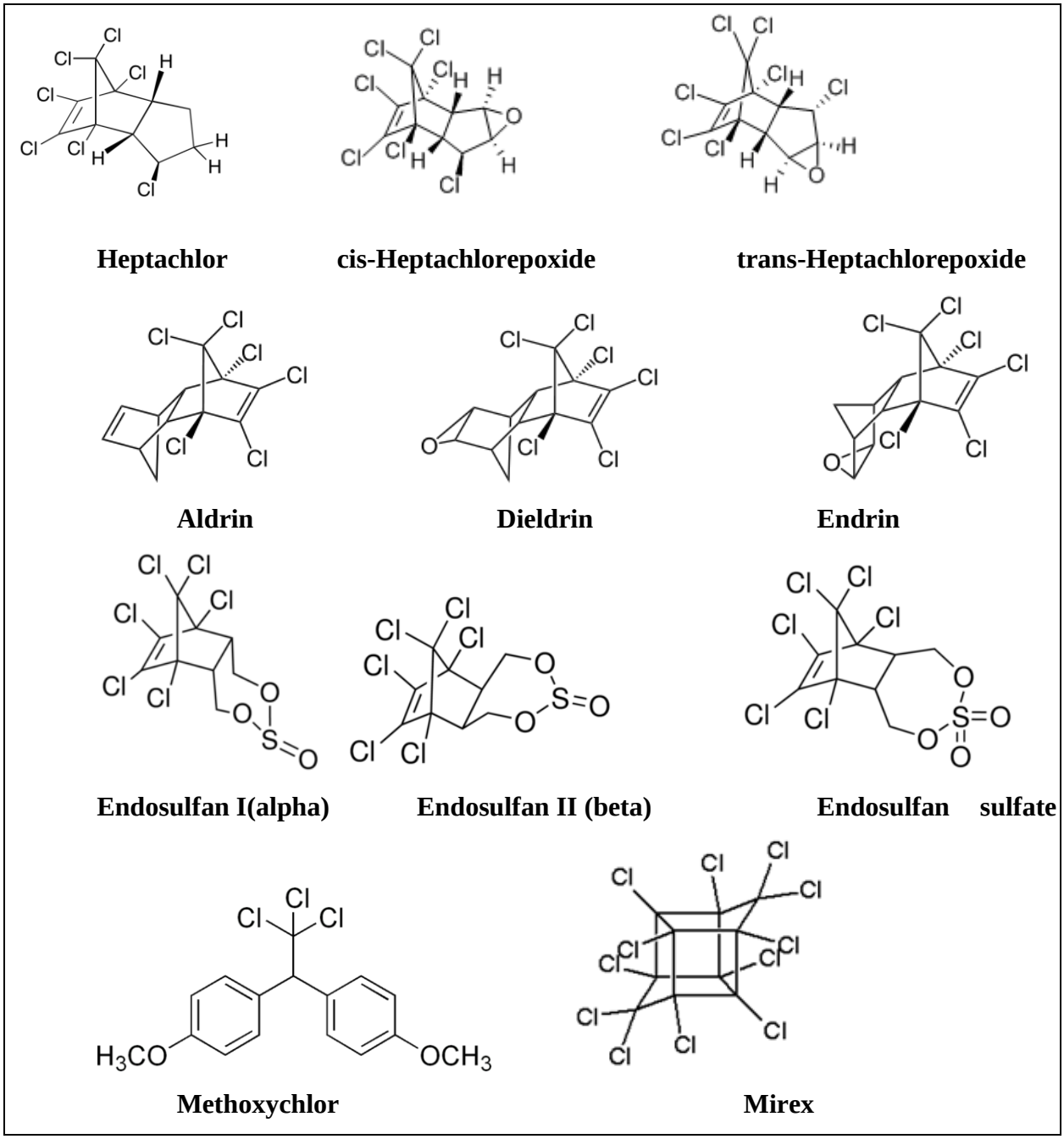

Fig. 1.2.2: Chemical structures of the organochlorine pesticides (OCP) *(Wikipedia)*

OCP exhibit high Log K_{ow} values (Table 1.2.2) indicating low water solubility and are not found in high levels in the water column as they are adsorbed to suspended particulate matter in water and by aquatic plants.

Table 1.2.2: Octanol-water partition coefficient log K_{ow} and molecular weight of twenty nine OCP. (Mackay et al., 1992)

Chemical Name	log K_{now}	MW (g/mole)
Chlorobenzene		
PeCB	5.19	250
HCB	5.64	285
PeCA	5.48	280
OCS	6.2	380
1,2,3,4,5,6-HCH		
α-HCH	3.94	291
β-HCH	3.84	291
γ-HCH	3.7	291
δ-HCH	4.14	291
ε-HCH	4.14	291
DDT-metabolites:		
4,4'-DDT	5.47	355
2,4'-DDT	5.59	355
4,4'-DDD	5.75	320
2,4'-DDD	6.08	320
4,4'-DDE	6.14	318
2,4'-DDE	5.56	318
Endosulfan		
Endosulfan-I	4.94	407
Endosulfan-II	4.78	407
Endosulfan-sulfate	4.78	423
Chlordane-related organochlorines		
trans-Chlordane	5.38	410
cis-Chlordane	5.38	410
oxy-Chlordane	5.48	420
Heptachlor	5.94	373
cis-Heptachlor epoxide	4.51	389
trans-Heptachlor epoxide	4.51	389
Aldrin	6.24	365
Dieldrin	4.76	381
Eldrin	4.71	381
Methoxychlor	4.95	346
Mirex	7.13	546

OCP break down slowly in the environment and accumulate in the fatty tissues of animals. They are endocrine disrupting chemicals, meaning they have slight toxic effects on the body's hormonal systems. As neurotoxicants, they have been banned, although a few are still used in many countries

1.2.2.2 Sources

DDT was involved during 1983-84 in a forest spraying program in the former East Germany (DDR) (Eriksson et al., 1989; Jensen et al., 1992). Other parts of the world continue to introduce OCP in agricultural practices and in disease-control programs. Once they are released into the environment as a pesticide, they will partition between environmental media according to their physical and chemical properties and the ultimate sink is sediment (Moore and Ramamoorthy, 2012).

1.2.2.3 Fate and Transport

The most common route of OCP exposure is through the diet, particularly fatty foods such as fish, meat and dairy products. The continued use of these pesticides in some countries further contributes to worldwide environmental contamination. OCP can accumulate to high levels in the soil, sediments, plants, animals, fishes and humans. Analyses of blood and urine are the most common methods for detecting OCP exposure. It can also be measured in fatty tissues and breast milk.

1.2.3 Dioxin

1.2.3.1 Physical and Chemical Properties

The halogenated aromatic hydrocarbons Polychlorinated dibenzo-para-dioxins (PCDD) and polychlorinated dibenzofurans (PCDF), commonly known as Dioxin are formed as unintentional by-products through a variety of chemical reactions and combustion processes. The basic structure of both compounds is the triple ring molecule, which consists of two benzene rings connected by a third oxygenated ring. For PCDD, the benzene rings are connected by a pair of oxygen atoms while for CDF via a single oxygen atom (Fig. 1.2.3).

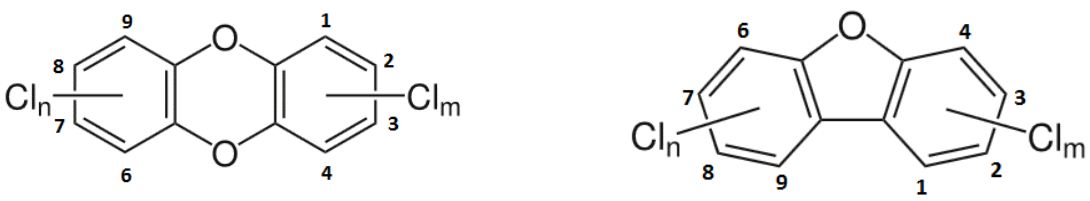

Fig. 1.2.3: Polychlorinated dibenzo-para-dioxins (left) and dibenzofurans (right) structures *(Wikipedia)*

The class of PCDD contains 75 congeners, in which are present 22 tetraCDD (TCDD), 14 pentaCDD (PeCDD), 10 hexaCDD (HxCDD), 2 heptaCDD (HpCDD), and a single octaCDD (OCDD) (Ryan et al. 1991). The class of PCDF contains 135 congeners, in which are include 4 monoCDF, 16 diCDF, 28 triCDF, 38 tetraCDF (TCDF), 28 pentaCDF (PeCDF), 16 hexaCDF (HxCDF), 4 heptaCDF (HpCDF), and a single octaCDF (OCDF). The numbers indicate the positions for chlorine substitutions. For this study, six PCDD and ten PCDF were investigated: one TCDD, three HxCDD, one HpCDD and OCDD; one TCDF, 2 PeCDF, 4 HxCDF, 2HpCDF and OCDF.

PCDD and PCDF possess low vapor pressures and water solubility. Its high Log K_{ow} partition coefficient values are ranged between ~6.5 and 8.5 (Table 1.2.3). Chemicals with these physical properties, when combined with a stable structure, allowing persistence in the environment, have shown long range transport capabilities combined with the ability to bioaccumulate and can be toxic to animals and humans alike (Geyer et al., 2000).

Table 1.2.3: Octanol-water partition coefficient log K_{ow} and molecular weight of 2,3,7,8 – substituted PCDD/F. (Mackay et al., 1992)

Chemical Name	log K_{ow}	MW (g/mol)
PCDD		
2,3,7,8-TCDD	6.8	322
1,2,3,7,8-PeCDD	6.84	357
1,2,3,4,7,8-HxCDD	7.8	391
1,2,3,6,7,8-HxCDD	7.58	391
1,2,3,7,8,9-HxCDD	7.58	391
1,2,3,4,6,7,8-HpCDD	7.66	425
OCDD	8.48	460
PCDF		
2,3,7,8-TCDF	6.46	306
1,2,3,7,8-PeCDF	6.99	340
2,3,4,7,8-PeCDF	7.11	340
1,2,3,4,7,8-HxCDF	7.53	375
1,2,3,6,7,8-HxCDF	7.57	375
1,2,3,7,8,9-HxCDF	7.76	375
2,3,4,6,7,8-HxCDF	7.65	375
1,2,3,4,6,7,8-HpCDF	8	409
1,2,3,4,7,8,9-HpCDF	8.23	409
OCDF	8.03	444

PCDD and PCDF exist as colourless solids or crystals in the pure state. They have a low solubility in water, a low volatility and an affinity for particulates in air, water, and soil.

The more toxic compounds appear to be the 2,3,7,8-substituted tetra-, penta-, hexa, hepta and octachloro compounds. They have been defined as POP under the Stockholm Convention as they tend to bioaccumulate through the food chain and can pose a serious matter to human health and environmental ecology, even at trace concentrations (Fiedler, 2003). Dioxins produce many carcinogenic, immunotoxic, and reproductive effects in the host organism. Since dioxin is ubiquitous, there are background levels in humans at an average body burden (EPA, 1994). In adult humans, the estimated half-life is 7.78 years for 2,3,7,8-TCDD, 12.6 years for 1,2,3,7,8-PeCDD, 26-45 years for HxCDD, 80-102 for HpCDD, and 112-1 32 years for OCDD (Geyer et al., 2002). The majority of human accumulation originates from the diet (95%) with smaller percentages deriving from inhalation and dermal exposure (Gilman et al., 1991). In humans, elevated levels of dioxin exposure have been associated with chloracne, cancer, decreased testosterone, decreased testicle size and altered glucose tolerance (EPA, 1994).

1.2.3.2 Sources

PCDD and PCDF are not commercially produced but are commonly inadvertently formed during the production of other chemicals, such as chlorinated phenols and their derivatives, chlorinated diphenyl ethers and polychlorinated biphenyls (PCB). Ongoing or earlier use of pentachlorophenol is considered to be a major source of PCDD in many industrialized countries (Koning et al., 1993). PCDD and PCDF are also formed during combustion processes such as waste incineration and in the production of steel and iron. An important source in low concentrations of PCDD and PCDF, found in earlier paper products, has been Chlorine bleaching of pulp (Beck et al., 1989; Wiberg et al., 1989). Other sources are chlorine-alkali plants using graphite electrodes (Rappe et al., 1991) and car exhausts from leaded petrol in which chlorinated solvents have been used as so-called “scavengers” (Ballschmiter et al., 1986). Sewage sludge and garden composts have also been identified as sources of PCDD and PCDF (Öberg et al., 1992; Öberg et al., 1993).

1.2.3.3 Fate and transport

The fate and transport of dioxin follow many complex and poorly understood pathways. In the atmosphere, dioxin travels by adsorbing to particulates and aerosols. The EPA has discovered the estimated amount of dioxin released by emissions is less than the amount that is being precipitated by deposition (USEPA, 1998). More than likely, this discrepancy is a result of a lack of reliable monitoring rather than formation in the atmosphere. Nonetheless, researchers are attempting to determine possible photochemical formation in the atmosphere (Whitefield and Hagen, 1995). The ultimate sinks for dioxin are soils, sediments, and organic matter (Czuczwa and Hites, 1986). Hence, because of their semi-volatile nature, ambient air is the most important medium for their distribution and transport in the atmospheric environment (Alcock and Jones, 1996). However, a number of possible dioxin pathways exist as sources in water medium as described above. Due to dioxin's high partitioning affinity to particulate organic carbon, it can be transported effectively in the water column. Therefore, transport of dioxin in surface water is a function of biotic, physical, hydrodynamic, and chemical properties.

1.2.4 Polychlorinated biphenyl (PCB)

1.2.4.1 Physical and chemical properties

PCB is stable chlorinated aromatic compounds that were commercially produced as complex mixtures for a variety of applications, including dielectric fluids for capacitors and transformers. Approximately 2 million tons of PCB were produced worldwide (Erickson and Kaley II, 2011).209 possible congeners have been identified, which differ in the number as well as in the position of chlorine atoms located in the biphenyl structure (Fig.1.2.4)

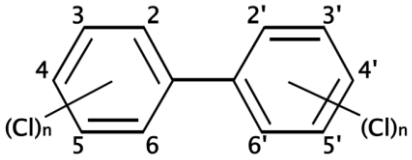

Figure 1.2.4: Polychlorinated biphenyl structure. *(Wikipedia)*

The differences in the amount and location of the chlorine atoms also result in different physical and chemical properties, such as Henry's Law constant, octanol-water partition coefficient and vapour pressure (Hawker and Connell, 1988; Dunnivant et al., 1992; Li et al., 2003). The PCB assume a dioxin-like structure when they have chlorine in a minimum of four of the lateral positions (i.e., 3, 3', 4, 4', 5, 5') and none (non-) or only one (mono-) of the ortho positions (i.e., 2, 2', 6, or 6') of the biphenyl. There are twelve PCB which the structure-activity relationships underlying the distinction of dioxin-like PCB from the other PCB. The non ortho substituted chlorine PCB are often referred to as co-planar PCB (Table 1.2.4)).

Table 1.2.4: Octanol-water partition coefficient log K_{ow} and molecular weight of PCB (Mackay et al., 1992)

PCB #	Chemical Name	Log K_{ow}	*MW* (g/mol)
non-ortho substituted PCB			
77	3,3',4,4'-tetra-CB	6.48	292
81	3,4,4',5-tetra-CB	6.24	292
126	3,3',4,4',5-penta-CB	6.67	327
169	3,3',4,4',5,5'-hexa-CB	7.41	361
mono-ortho substituted PCB			
105	2,3,3',4,4',-penta-CB	6.61	327
114	2,3,,4,4',5-penta-CB	6.47	327
118	2,,3',4,4',5-penta-CB	6.49	327
123	2',3,4,4',5'-penta-CB	6.5	327
156	2,3,3',4,4',5-hexa-CB	7.11	361
157	2,3,3',4,4',5'-hexa-CB	6.97	361
167	2,3',4,4',5,5'-hexa-CB	6.82	361
189	2,3,3',4,4',5,5'-hepta-CB	6.15	395
Indicator PCB:			
28	2,4,4'/2,5,4'-tri-CB	5.66	258
52	2,2',5,5'-tetra-CB	5.91	292
101	2,2',4,5,5'-penta-CB	6.33	327
138	2,2',3,4,4',5'-hexa-CB	7.22	361
153	2,2',4,4',5,5'-hexa-CB	6.87	361
180	2,2',3,4,4',5,5'-hepta-CB	7.16	396

Due to the presence of chlorine atoms in the biphenyl molecule, PCB persists in the environment and because they are lipophilic, they tend to bioconcentrate, biomagnify in the food chain, and bioaccumulate in organisms, including humans. PCB are listed in the Stockholm Convention on Persistent Organic Pollutants (POP) (UNEP, 2005). This international treaty establishes the measures to reduce or eliminate the production and use of these chemicals around the globe. PCB are probable animal carcinogens and endocrine disruptors, and new evidence links PCB exposure to neurodevelopment disorders and autism (Roegge et al., 2004; Pessah et al., 2010).

1.2.4.2 Source

In most countries, commercial PCB and products containing PCB are no longer produced anymore. But for the retrospective consideration of emission, this group is important. In the production of capacitors for example, PCB losses reached to 10–20 % of dielectric used for filling. Polychlorinated biphenyls still have relatively various applications in closed systems, including dielectric liquids in capacitors and transformers, in hydraulic and cooling equipment, cables, and are used additionally for paper impregnation, paints manufacture, etc. Some PCB sources include contaminated soils, various PCB-containing wastes, bottom sediments, waters that perform as secondary sources of PCB emissions and various thermal processes where PCB are formed like dioxins. Others sources were enumerated by the European PCB emission inventory for 1990 (Berdowski et al., 1997): coal combustion, steel smelting (open-hearth, converter, electric), sintering, waste incineration, electrical equipment (capacitors and transformers).

1.2.4.3 Fate and transport

The fate of individual PCB congeners is determined by both environmental processes and the physical-chemical properties of individual congeners. In general, PCB congeners that are more highly chlorinated and have fewer ortho substitutions are less volatile, less water-soluble, bind more readily to organic particulate matter and are more amenable to anaerobic dechlorination processes (typically in buried sediments). Thus, these congeners are more prominent in soils and sediments, less prominent in water and in the atmosphere, and have higher bioaccumulation factors (BAF). Congeners that are less chlorinated and have more ortho substitutions are more volatile, more water soluble and are much more readily metabolized in mammals. Consequently, these congeners are more prominent in the atmosphere, surface waters and in fish from temperate waters. Hydrophobicity is the most important chemical property that controls bioavailability from water, sediment or soils. Hydrophobicity can be estimated by the octanol-water partition coefficient, K_{ow}. Generally, log K_{ow} for PCB increase from approximately 3 to 9 as the degree of chlorination increases(Hansen et al., 1999). Hence, lower chlorinated PCB compounds having lower K_{ow} are more bioavailable than higher chlorinated congeners having higher K_{ow}. PCB compounds that are highly hydrophobic are difficult to measure in water because of the very small concentrations in solution. Conversely, concentrations in surficial sediments or soils are often measurable and can be used effectively to reference each PCB congener’s distribution to abiotic and biotic components of the

ecosystem. In aquatic ecosystems, concentrations measured in surficial sediments can be used to estimate average concentrations in water.

1.3 Sampling methods

In situ analysis methods have developed significantly in recent decades, increasing the ability to understand and model ecosystems, allowing us to be able to better protect them. Passive samplers are one of these in situ techniques, in which fractionation and accumulation of the analyte occur in situ but the analysis of the accumulated fraction is carried out in a subsequent step at the laboratory (Dunn et al., 2007). The passive samplers have been used for the determination of wide range of analyte in various applications in air, water and soil for years (Morrison, 1987). One major advantage of passive sampling is its inherent specificity towards the analyte of interest. They have the ability to sample species that would dissociate within the timescale of transport across the diffusion pathways. These species have stability constant lower than the stability constant of the compound formed as a result of the binding to the samplers receiving phase. The fraction accumulated by passive sampling reflects the analyte's behaviour in the investigated environment, yielding valuable information not only on its content but also on its chemical status, thereby contributing to the more accurate assessment of the environmental impact of the analyte (Garofalo et al., 2004). Other advantages are that passive samplers can be deployed for several days at a time (up to several months) and provide a time-averaged representation of analyte concentrations at the sampling stations.

The passive sampler covers multiple subgroups, in which the kinetic passive sampler is designed to continuously accumulate the analyte by maintaining a concentration gradient and a mass flux of analyte during an exposure period. Semi Permeable Membrane Device (SPMD) is one subgroup of the kinetic passive sampler, to which the target class of analyte is the organic non-polar compounds (Fig.1.3.1).

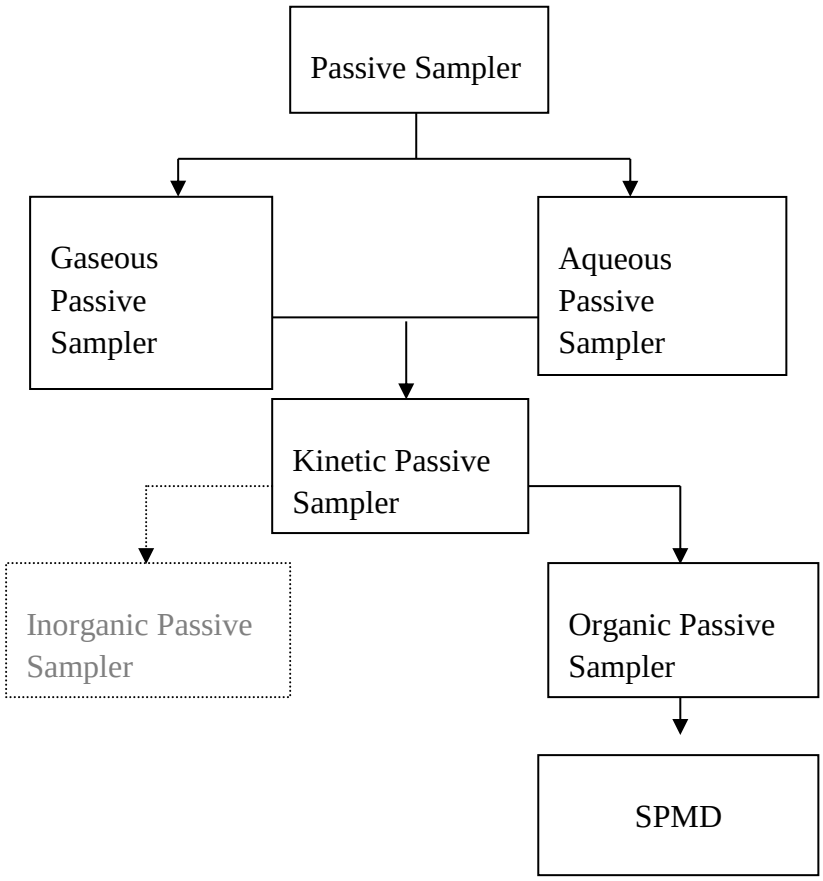

Fig.1.3.1: Passive sampler structure

1.3.1 Passive sampler SPMD

Common semipermeable membrane devices (SPMD) are polymeric membrane (LPDE) lay flat tubes with 91cm length, 2.5 cm wide and a wall thickness 75-90 μm (Fig.1.3.2), enclosing a thin film (1 mL) of a high purity neutral lipid called triolein and having a capacity to concentrate organic compounds from air, water, soil, and sediments (Huckins et al., 1996). Organic chemicals can pass through the polyethylene membrane and partition into the lipid. Chemicals with a log octanol-water partition coefficient (log K_{ow}) higher than three and a diameter less than 10 Å are preferentially sampled from air and water by SPMD. The use of triolein, a natural symmetrical triglyceride with 885.4 g/mol molar mass, over other lipids offers multiple physiochemical advantages being its high purity (95-99%), its melting point of 0 °C allowing exposures in cold water and its ability to solubilize non-polar organics. Chiou (1985) established a close correlation between the equilibrium triolein-water partition coefficient K_{TW} and the equilibrium octanol water partition coefficient K_{ow} of hydrophobic contaminants. The low LDPE membrane permeability ensures no loss of lipid during exposure and dialysis (Meadows et al., 1993). These characteristics make then SPMD suitable sampler

for hydrophobic organic compounds with lower than 600 Dalton. Contaminants partitioned with the particulate material are mainly not absorbed in the device. The transport of the contaminant into SPMD is over three different barriers. The first one is the diffusion layer, a region where molecular diffusion becomes increasingly important relative to eddy diffusion and convection. After crossing this layer, contaminant may encounter an organic or inorganic macrofauna called biofilm, in which transport takes place via molecular diffusion, or in some cases by internal ventilation by the organism present. Once past the biofilm, contaminants will either diffuse through the membrane and partition to the triolein or concentrate into the LDPE itself (Gale, 1998). The sequestered contaminant into the triolein remains partitioned until equilibrium with ambient environmental concentration is reached. The uptake kinetic of SPMD is affected by the environmental factors such as flow velocity or wind-speed, biofilm, temperature (Petty, 2000). Thus, a high flow velocity in water or wind speed in air can increase the volume sampled per day by the SPMD; the existence of a biofilm on the SPMD during the exposure will expand the width of the membrane, increasing the energy required to impregnate the matrix, by that slowing the uptake rate. There is a correlation between high temperature and high biofouling (Shoven, 2001). The water chemistry (pH, salinity…) can also affect the migration of contaminants through the SPMD but without altering the barriers.

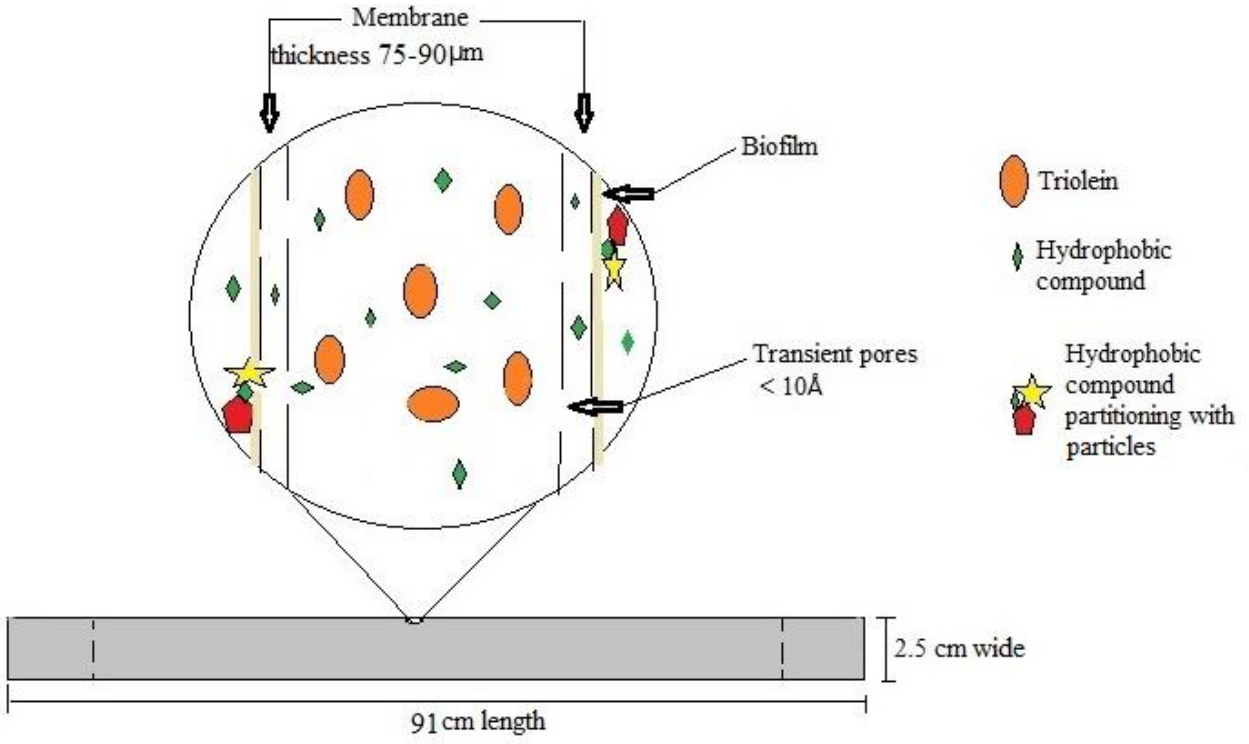

Fig.1.3.2: Schematic representation of standard SPMD

Chemical Reaction kinetics and Mass Transfer Coefficient are two models applied to describe the SPMD-air/water exchange of contaminant. The used one is the kinetic model, where exchange between chemical concentrated in the device and contaminant in the sampled media following three patterns, depending on the air/ water partition coefficient of compound. The first phase is linear or integrative, where no significant accumulation residues are observed; followed by curvilinear or partly integrative phase, where elimination residues from SPMD achieve importance and finally the equilibrium phase where the uptake amount is equal to the release amount per unit time (Fig.1.3.3). In the linear stage, the device is called kinetic sampler and parameters such as exposure time, film thickness, sampler area and sampler volume are essential to define its accumulation capacity. Passive samplers operating in this regime require that the sampler capacity is to be kept well below that found in the sampled media to avoid saturation and that the devices response time must be shorter than any fluctuations being measured in the environmental medium. The basic requirements of the equilibrium sampler approach are that stable concentrations of contaminants are reached during a known time period.

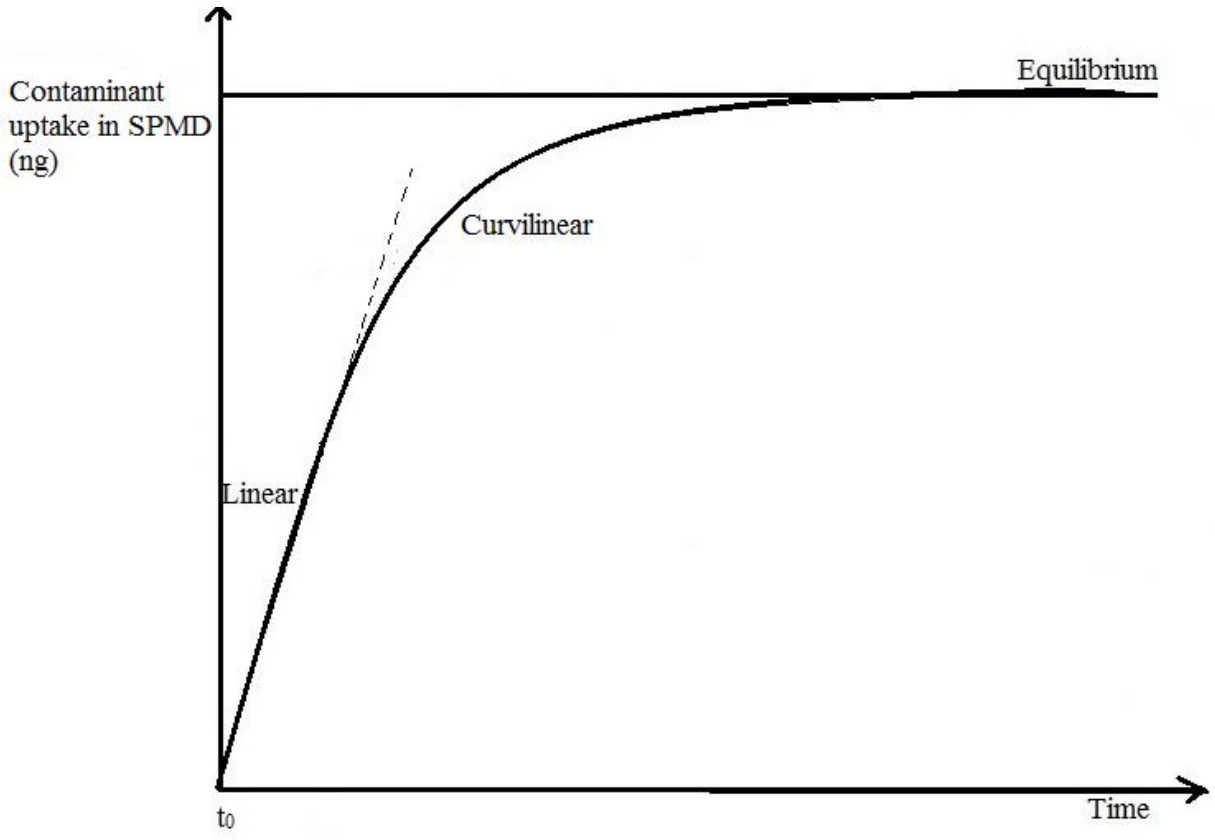

Fig. 1.3.3: The general uptake stage of contaminant concentration over time in SPMD

The uptake in the air is based on the contaminant concentration difference between the air and the SPMD. The compound uptake is restricted by two barriers: the boundary air layer and the membrane. Compounds with high octanol-air partition coefficient K_{oa} on turbulence conditions are absorbed into SPMD during exposure in air under membrane control and compound with low K_{oa} and thicker air-membrane layer are absorbed under air boundary layer control. The biofilm effect in the compound-SPMD mass transfer is neglected in contrary for the deployment of the devices in aquatic media.

1.3.1.1 Use of SPMD in water

Huckins et al, 2002 suggest two types of rate limiting SPMD uptake models in water. The first model is when compounds are under water boundary layer WBL by log K_{ow}> 4.4, where analyte concentration occurs by diffusion through a static layer of water and analytes are retained once they pass in the samplers and the other is when compounds are under membrane control by log K_{ow} < 4.4, where accumulation occurs through a porous or non-porous membrane. In general, the exchange of integrative phase between SPMD and the water phase can be described as a first order for the solute concentration giving by:

$$C_S(t) = K_{SW} C_W \left[1 - \exp(ke.t)\right] \qquad \text{Eqn.1.1}$$

Where $C_s(t)$ is the concentration of the analyte in the SPMD at time t, K_{SW} is the SPMD-water partition coefficient ((L.L^{-1}); C_W (mass.L^{-1}) is the analyte concentration in aqueous media and *ke* is the elimination rate constant of the chemical in SPMD per day (d^{-1}).

In the equilibrium sampling regime, the equilibrium partitioning co-efficient *Ksw* can be used to estimate the concentration of pollutants in the medium by measuring the concentration in the sampler. Then, the analyte water concentration C_W is giving as:

$$C_w = \frac{N}{V_S K_{SW}} \qquad \text{Eqn.1.2}$$

Where N (mass) is the amount of analyte accumulated after a given exposure time and V_S is the volume of the receiving phase

In kinetic sampling regime, the analyte concentration in SPMD C_S increases linearly with time. The device is characterized by a high capacity for collecting contaminants during the sampling period. It is assumed that the mass transfer of contaminants from the sampled media to the

receiving phase is proportional to the difference between the chemical activity of the contaminant in the sampled media compared to that in the receiving phase (Stuer-Lauridsen, 2005). In the initial uptake phase the rate of desorption from the sampler receiving phase to the surrounding media is considered negligible hence the time-weighted average TWA concentration of an analyte in water is giving as:

$$C_w = \frac{N}{R_S t} \qquad \text{Eqn.1.3}$$

Where the sampling rate R_S is the product of a first order constant for uptake of a contaminant (*ku*) and the volume of water that gives the same chemical activity as the volume V_S. *Vs* is the total volume in the SPMD and includes the volume of the triolein V_T and the volume of the membrane LPDE $V_{LPDE.}$ R_S can be interpreted as the volume of water cleared of analyte per unit of time by the SPMD. R_S is not affected by the concentration present in the water phase (C_W) but is affected by water flow and turbulence as well as bio-fouling and temperature(Booij et al., 2006).

The introduction of performance reference compound PRC provided a tool for the prediction of the sampling rate(Booij et al., 2002). These compounds, added prior the exposure into SPMD, are non-interfering organic chemical with medium to high affinity for triolein (Huckins et al., 2002a). The evaluation of the uptake rate is then based on the amount of dissipation PRCs and those found at the beginning of the sampling. Thus, under conditions of isotropic exchange, PRC elimination rate $ke,_{PRC}$ is giving by:

$$ke,_{PRC} = -\frac{\ln(N_{t,PRC} / N_{0,PRC})}{t} \qquad \text{Eqn.1.4}$$

Where $N_{0,PRC}$ is the retained PRC fraction at the beginning of the exposure period and $N_{t,PRC}$ is the retained PRC fraction after the exposure period t.

The PRC sampling rate $Rs,_{PRC}$ is characterized by the individual contaminants of interest under the prevailing environmental conditions during the sampling period and can be estimated using the volume of the chemical *Vs*, the PRC's release rate constant (ke, $_{PRC}$) and K_{SW} as following:

$$Rs,_{PRC} = VsK_{SW}ke,_{PRC} \qquad \text{Eqn.1.5}$$

1.3.2 Virtual Organism

Some changes to SPMD mode were introduced in this study. To investigate potential toxicity in the fat compartment, the term SPMD is replaced with Virtual Organism (VO), the same passive sampler with different dimensions such as the filled length of 23 cm and the wall thickness of 67 µm (Fig.1.3.4). VO is defined as artificial property-tool, and is reflecting exposomic processes in compartments (fat, protein, membranes etc.) of real organisms (Schramm et al., 2013). In comparison with the mass fraction of 20% triolein of a standard SPMD, the mass transfer of our VO is 44% to gain more power for the accumulation of lipophilic compounds per sampler. This is meant to improve the sensitivity for the chemicals under investigation and achieves better results.

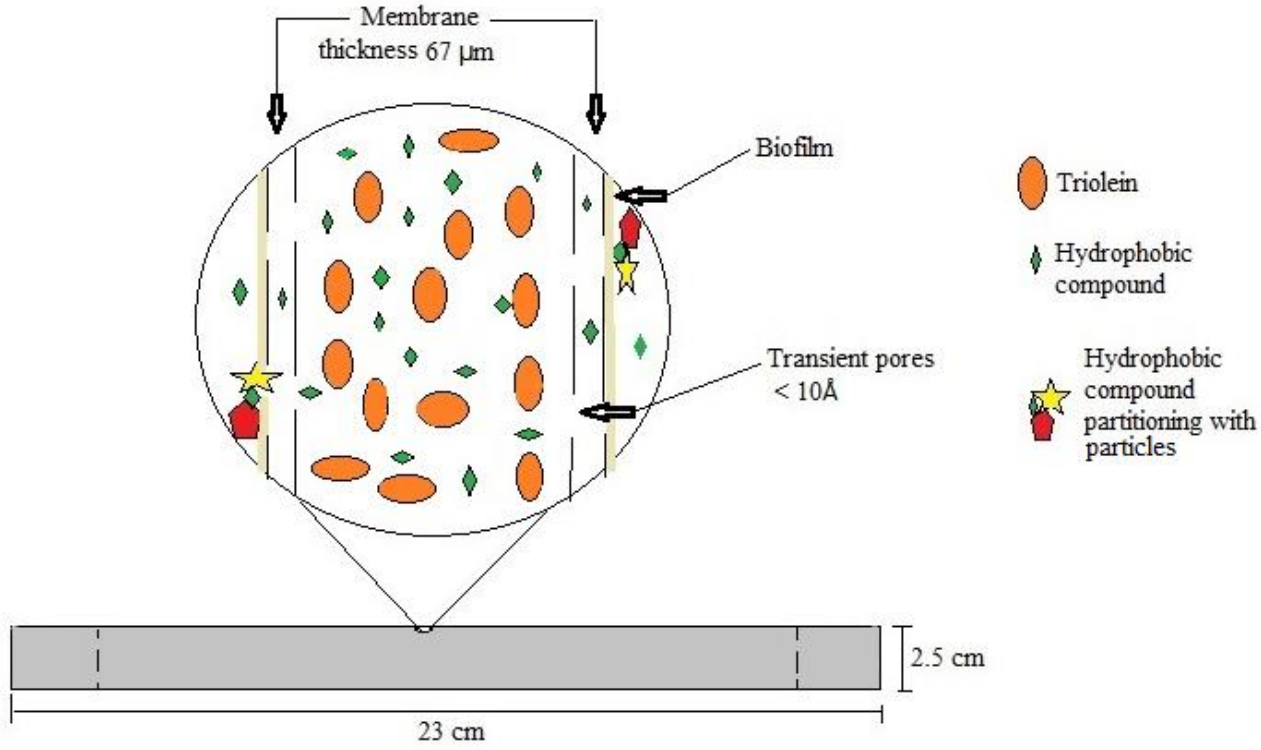

Fig.1.3.4: Schematic representation of VO

To evaluate K_{VO_W} with 44% triolein, the theory of Mackay and Paterson, 1982 has been used. Considering two compartments: Low Density Polyethylene (LPDE) and triolein in which the solute has different concentration and fugacity, resistance is controlled by the boundary layer, and equilibrium exists between the membrane (LPDE) and lipid (triolein) phases(Gale, 1998). K_{VO_W} equation for our VO (triolein mass 44% of total mass, resp. volume due to nearly identical densities) is represented as:

$$K_{V0-W} = \frac{K_{TW}V_T + K_{LPDE.W}V_{LPDE}}{V_T + V_{LPDE}}$$ Eqn.1.6

Where: V_T is the volume of the triolein (L), $_{VLPDE}$ the volume of LPDE (L), K_{TW} is the triolein-water partitioning coefficient (mass/L/ (mass/L) and K_{LPDEW} is the LPDE-water partitioning coefficient (mass/L/ (mass/L)

$$\log K_{TW} = 1.00 \log K_{ow} + 0.105$$ Eqn.1.7 (Chiou, 1985)

and

$$\log K_{LPDE.W} = 1.05 \log K_{ow} - 0.59$$ Eqn.1.8 (Booij and Smedes, 2010)

1.4 Material and Method

1.4.1 VO preparation before deployment

The LDPE lay flat tubing was cut into 29 cm pieces and was heat-sealed at one end and a distance of 2.5 cm from this end. In 2008, into each piece of tubing 700 μL of triolein (Sigma, Munich, Germany, 99%) was pipetted with 3^{13}C PAH-PRC and 3 PCB-PRC (anthracene-$^{13}C_6$, benzo(a)pyrene-$^{13}C_4$, benzo(g,h,i)perylene-$^{13}C_{12}$, PCB60, PCB127, PCB159). From 2009, the triolein was spiked with 16 ^{13}C-labeled PAH-PRC, which was different to the previous sampling campaign in 2008 (naphthalene-$^{13}C_6$, acenaphthylene-$^{13}C_6$ acenaphthene-$^{13}C_6$, fluorene $^{13}C_6$, phenanthrene-$^{13}C_6$, anthracene-$^{13}C_6$, fluoranthene-^{13}C6, pyrene-^{13}C3, benzo(a)anthracene-^{13}C6, chrysene-^{13}C6, benzo(b)fluoranthene-$^{13}C_6$, benzo(k)fluoranthene-$^{13}C_6$, benzo(a)pyrene-$^{13}C_4$, indeno(1,2,3-cd)pyrene-$^{13}C_6$, benzo(g,h,i)perylene-$^{13}C_{12}$, dibenzo(a,h)anthracene-$^{13}C_6$). This large range of PRC compounds with of log K_{ow} from 3 to 6 allowed then a better choice of PRC used to calculate sampling rate of the analyte. Air was removed first by squeezing the triolein towards the sealed end using a triangle stainless steel loaf, and then pushing the triolein front towards the open end. A third heat-seal was applied just above the triolein front at a distance of 23 cm from the second seal and another at the upper end of the tubing. Mounting loops were made at the empty end parts of the tubing. The triolein-containing part of the sampler (i.e., excluding the mounting loops) had an area of 115 cm2. VO was prepared in a purified glovebox under nitrogen atmosphere to avoid contaminations. The prepared VO were stored at 30°C in sealed heat cleaned 10 mL glass vials wrapping in aluminium foil and kept cool during transportation until deployment.

VO preparation for ^{14}C OCDD Test

To 25.14 g (27.26 mL) of triolein were added 1.7 mL (1.474 g) of a given solution of ^{14}C-OCDD (3237.5 ng / 1.85 mL) in toluene and thoroughly mixed by magnetic stirring in a conical flask for about 16 h. So, the total amount of ^{14}C-OCDD in the mixture should be given as 3030.135 ng and the concentration of ^{14}C-OCDD therefore 3030.135 ng / 28.96 ml = 104.6317 ng/mL or 3030.135 ng / 26.614 g = 113.855 ng/g.

Radioactivity measurement of the mixture gave an average value (N=2, 3 measurements each) of 8355 DPM / 0.1g triolein, i.e. 2223600 DPM in the total mixture. Then, based on the data available, the specific radioactivity in the mixture was 734 DPM/ng ^{14}C-OCDD or 0.0013627 ng/DPM.

The triolein was used to fill PE lay-flat tubing (0.7 mL each) in a common way to prepare the VO, but with the safety precautions necessary for work with radioactive substances. All work with radioactivity in this study was done in a special authorized laboratory HMGU-Institute of Soil Ecology. As usual, each VO was encased in a storage glass directly after preparation and the glasses controlled for outside radioactive contamination. After preparation and weight measurement VO were frozen and stored at -80 °C.

1.4.2 PAH, OCP and PCB preparation

For chemical analysis, all organic solvent were of picograde quality and were obtained from LGC standards (Wesel, Germany). The VO was cut into small pieces before extraction. The sample was extracted in a 250 mL Erlenmeyer flask overnight by soaking in 100 mL of cyclohexane at 200 rpm on a constant left-right shaker. At the beginning of the extraction, internal standards with a range of deuterated and ^{13}C-labeled compounds were spiked into to the cyclohexane (Naphthalene-D_8, Acenaphthylene-D_8, Acenaphthene-D_{10}, Fluorene-D_{10}, Phenanthrene-D_{10}, Anthracene-D_{10}, Fluoranthene-D_{10}, Pyrene-D_{10}, Benzo(a)anthracene-D_{12}, Chrysene-D_{12}, Benzo(b)fluoranthene-D_{12}, Benzo(k)fluoranthene-D_{12}, Benzo(a)pyrene-D_{12}, Indeno(1,2,3-c,d)pyrene-D_{12}, Benzo(g,h,i)-perylene-D_{12}, Dibenzo(a,h)anthracene-D_{14}) and PCB (IUPAC Nos. 28, 52, 77, 81, 101, 105, 114, 118, 123, 126, 138, 153, 156, 157, 167, 169, 180, 189) and OCP (Pentachlorobenzene $^{13}C_6$, alpha-HCH $^{13}C_6$, gamma-HCH $^{13}C_6$, beta-HCH $^{13}C_6$, delta-HCH $^{13}C_6$, Pentachloroanisole $^{13}C_6$, Hexachlorobenzene $^{13}C_6$, Heptachlor $^{13}C_6$, Aldrin $^{13}C_{12}$, Octachlorostyrene $^{13}C_6$, oxy-Chlordane $^{13}C_{10}$, Heptachloroepoxide $^{13}C_{10}$, 2,4'-DDE $^{13}C_{12}$, 4,4'-DDE $^{13}C_{12}$, trans-Chlordane $^{13}C_{12}$, Endosulfan-I $^{13}C_9$, Endosulfan-II $^{13}C_9$,Endosulfan sulfate $^{13}C_9$, 4,4'-DDD D_8, Dieldrin $^{13}C_{12}$, 2,4'-DDT $^{13}C_{12}$, 4,4'-DDT $^{13}C_{12}$,

Methoxychlor $^{13}C_{12}$, Mirex $^{13}C_{10}$) in nonane to monitor the extraction and cleanup procedures (Fig.1.4.1). The extract was passed over anhydrous sodium sulfate to remove water. The volumes of the extraction solutions were reduced to one drop under vacuum and the mass of triolein residues was determined. The triolein was dissolved again in approximately 1–2 mL mixture of n-hexane:dichloromethane (1:1) and the samples underwent clean-up using a mixed column (grade 60; 3 cm diameter column containing, from the bottom upward, 10 g silica (silica gel from Wesel Germany), 5 g alumina with 3% H_2O, 5 g anhydrous sodium sulfate). The extracts were eluted with 100 mL mixture of *n*-hexane and dichloromethane (1:1) and reduced to 1 mL. The residues were further purified through a C_{18} SPE cartridge for which acetonitrile was used as an eluting solvent. After adding a mixture of $^{13}C_{12}$ PCB70, 111 and170 for PCB, then Pentachlorotoluene (PCT) and $^{13}C_{12}$-1,2,3,7,8,9-HxCDD for OCP and PAH as recovery standard, the extracts were concentrated with a gentle flow of nitrogen to 20 µL to be ready for analytical determination.

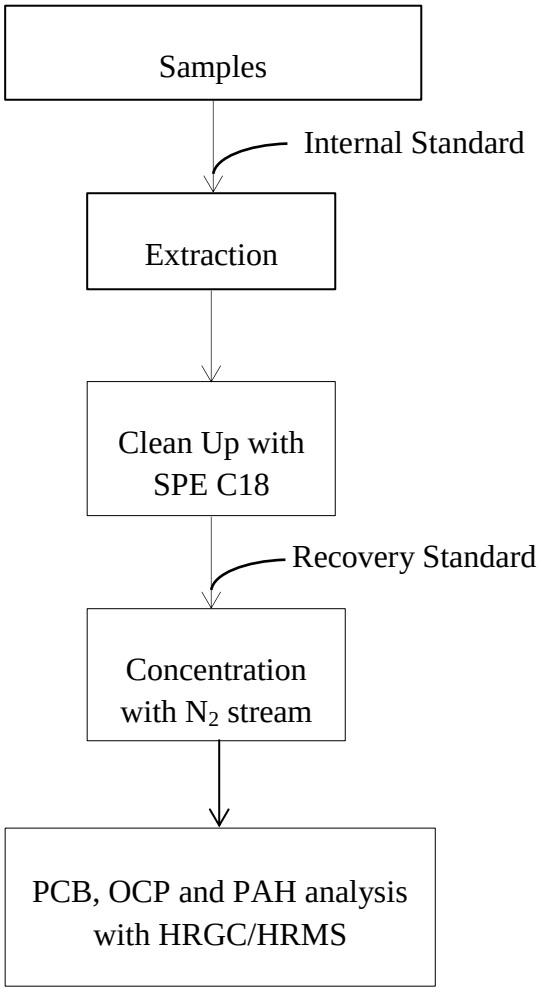

Fig.1.4.1: Sample preparation scheme for PCB, OCP and PAH

1.4.3 Dioxin and co-planar PCB preparation

Membrane devices were cut into slices and internal standards were added at the beginning of the extraction (Fig.1.4.2). For Dioxin (2,3,7,8-TCDD; 1,2,3,7,8-PCDD;1,2,3,4,7,8-HxCDD; 1,2,3,6,7,8-HxCDD; 1,2,3,7,8,9-HxCDD; 1,2,3,4,6,7,8-HpCDD; OCDD; 2,3,7,8-TCDF; 1,2,3,7,8-PCDF; 2,3,4,7,8-PCDF; 1,2,3,4,7,8-HxCDF; 1,2,3,6,7,8-HxCDF; 1,2,3,7,8,9-HxCDF; 2,3,4,6,7,8-HxCDF; 1,2,3,4,6,7,8-HpCDF; 1,2,3,4,7,8,9-HpCDF; OCDF) and for PCB (IUPAC Nos. 28, 52, 77, 81, 101, 105, 114, 118, 123, 126, 138, 153, 156, 157, 167, 169, 180, 189) (Cambridge Isotope Laboratories, USA). Then they were extracted for 24 hours with 100 ml cyclohexane each by use of a rotating shaking machine. The extracts were placed at the top of mixed columns filled with 10 g silica gel, 5 g Al_2O_3 and 2 g Na_2SO_4 from the bottom to the top and eluted with a mixture n-hexane/dichloromethane 1:1. After that, the extracts were eluted through a sandwich column composed of silica gel, silica gel treated with 44 % H_2SO_4 and anhydrous Na_2SO_4 and added with SPE-carbon column (Supelco). The sandwich column was first rinsed with 50 mL n-hexane. This column allowed the elimination of interfering organic compounds by reactions of oxidation and sulfuration with sulfuric acid as an oxidant agent. The carbon column was first rinsed with 25mL toluene and 25 mL n-hexane. The extract was eluted with 100 mL n-hexane. Both columns were later separated and the carbon column was eluted with 30 mL dichloromethane/n-hexane (1:9) to obtain co-PCB fraction and with 100 mL toluene to obtain PCDD/F fraction.

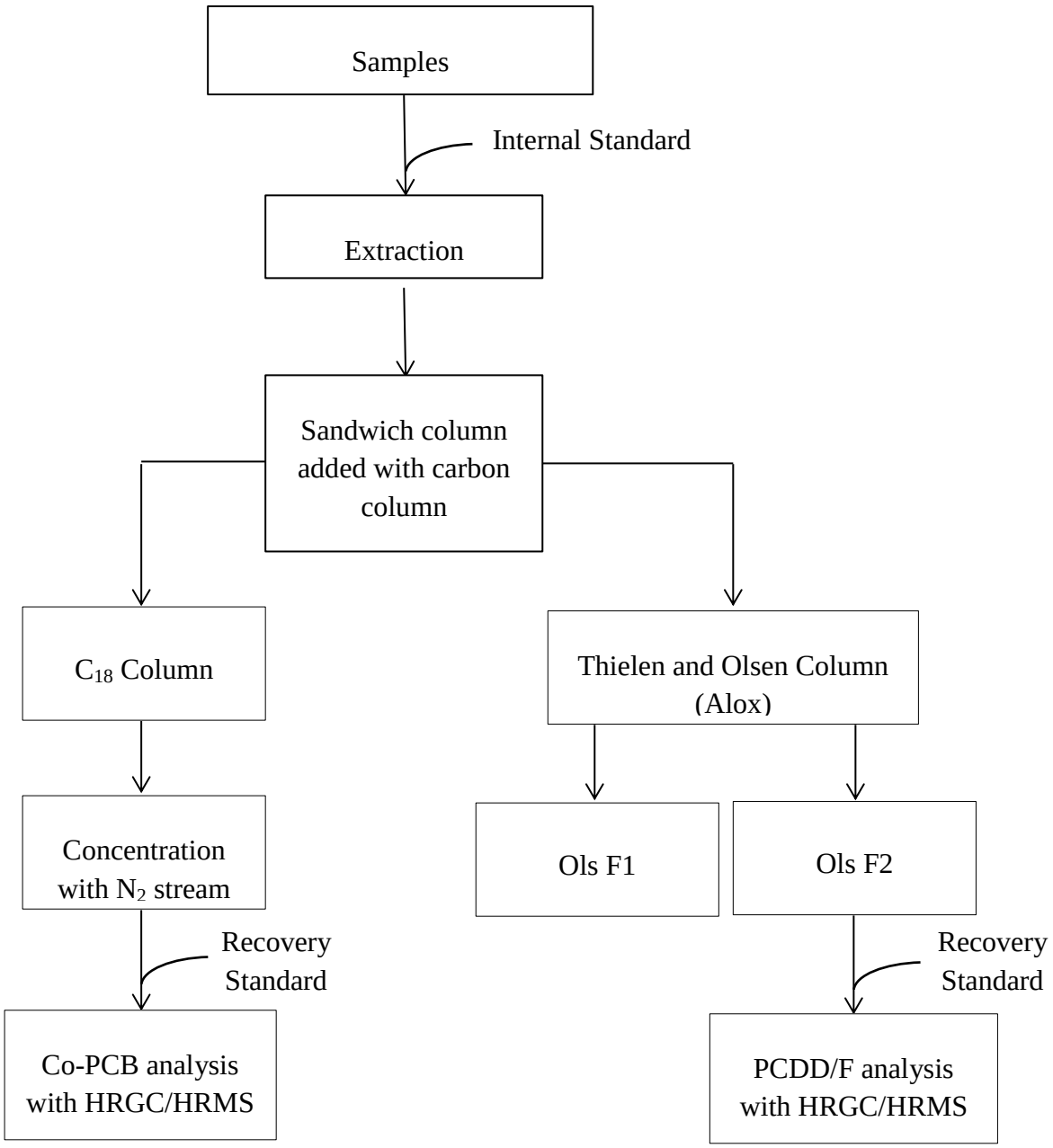

Fig.1.4.2: Sample preparation scheme for co-PCB and PCDD/F

The co-PCB extract, concentrated to 1ml, was eluted to C_{18} modified silica column with acetonitrile and reduced to 0.2 mL under nitrogen stream at 45 °C. The PCDD/F extract, concentrated to 1ml, was eluted through a Thielen and Olsen column, composed with 5g aluminiumoxide. The column was first rinsed with 20 mL n-hexane/chloroform (88:12) to obtain Ols F1 that was kept until end of analysis, then with 50 mL dichloromethane to obtain Ols F2 containing the PCDD/F fraction. Both extracts were transferred into vials and spiked with a mixture of $^{13}C_{12}$ 1,2,3,4-TCDD and $^{13}C_{12}$ 1,2,3,7,8,9-HxCDD as recovery standard.

Finally, the eluates were concentrated to 20 µL and the vials were stored at -28 °C until instrumental analysis.

1.4.4 ^{14}C OCDD Preparation

It is important to mark that all glassware used during clean-up and storage of a sample is labelled with the danger symbol for radioactivity and the individual sample number. PP scintillation vials are labelled on top of the screw cap with sample number, a sign indicating the clean-up step and number of replication of measurement sample. All work with open radioactive samples was conducted in a flat stainless steel tray inside a fume hood.

During clean-up process in the dioxin laboratory of MEX, a stopcock round flask (250 mL) was weighed and then filled with 50 mL of 100mL cyclohexane and 10 µL internal standard IS from the "PCDD/F Internal Standard 100 1000 ng/mL". Further work was conducted in the radioactive laboratory.

The frozen VO sample was first warmed up to room temperature and withdrawn from its storage glass before the beginning of clean up. The empty glass was filled with 5 mL of scintillation cocktail (SC, ULTIMA GOLD XR) closed again and vigorously shaken for 0.5 min. The cocktail was transferred then into a 5 mL PP scintillation vial (SV) and the radioactivity was measured in a scintillation counter.

A powder funnel was placed on top of the round flask, where the VO was held with forceps and opened with a scalpel by several vertical slits. The whole device was then cautiously pushed through the funnel inside the flask. All potentially contaminated tools as well as the surface of the funnel itself were rinsed with the 50 mL of cyclohexane left, into the flask. The flask was closed by its stopcock and the VO was cold extracted for 16 -18 h (overnight) according to SOPD – SP1E (preliminary, not yet released). After extraction, again a powder funnel was placed onto the flask and the VO tubing was slowly withdrawn from it through the funnel. Still above the funnel, the PE film was rinsed inside and outside thoroughly but as sparingly as possible with cyclohexane. When the dripping was stopped, the film was dried in the air stream of the fume hood and the weight was determined. Now three sections of about 2 cm in length (near first seal, middle and final seal) were cut out of the formerly triolein filled part of the PE lay flat tubing, separately transferred into pre-weighed vials and their weight determined. If not analysed immediately (incineration method), the sections and the residual PE film were stored at – 20°C. The extraction flask with a stopcock was weighed and such by

comparison with the tare weight and the weight of the extract plus washing solutions. After thorough stirring of the whole volume, two samples of 1 mL each were drawn by a pipette and transferred into pre-weighed SV and weighed therein with the closed screw cap. Then 4 mL of SC was added to each and after vigorous shaking, the sample was ready for measurement in a scintillation counter. The total radioactivity of the content inside the flask could be determined from the average of the results.

1.4.5 Instrumental analysis

The isotope dilution method of PAH, PCB, OCP and PCDD/F was used in this project to quantify a given sample. This method works by adding a known amount of labelled compounds (quantification standard) before clean up. By measuring the recovery of those substitutes, a correction factor can be made for native compounds in the sample matrix. An internal standard is introduced prior to analysis for the quantification of the substitutes. Instrumental analysis of PAH, PCB, OCP and dioxin was performed by use of a high resolution gas chromatography (HRGC) namely Agilent 5890 series II coupled to a high resolution mass spectrometer (HRMS) MAT 95 (Fig 1.4.3), following the parameters on Table 1.4.1 and Table 1.4.2.

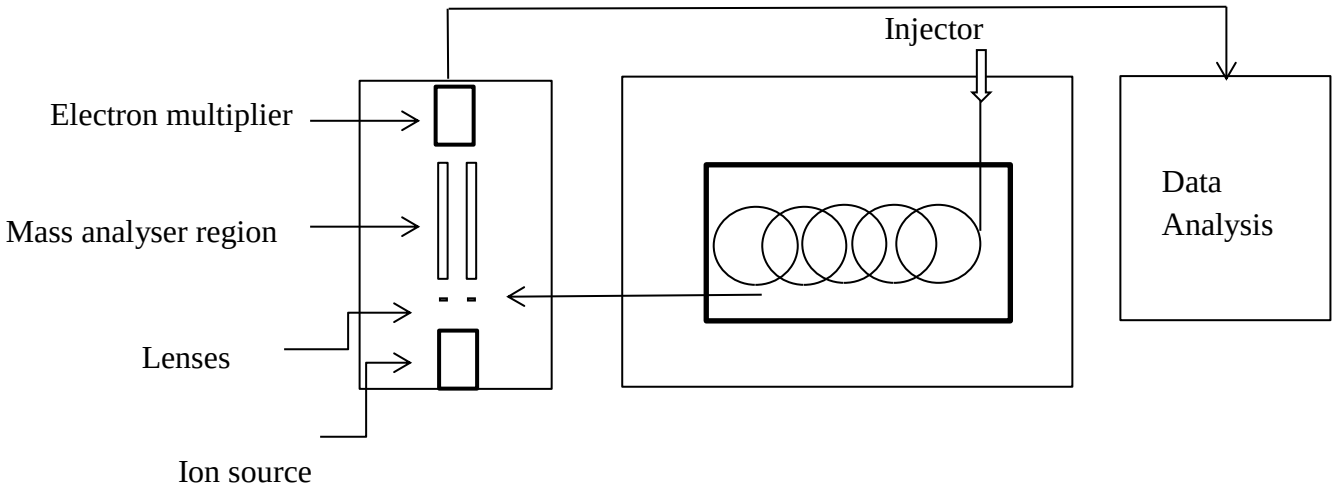

Fig.1.4.3: A block diagram of HRGC coupled to HRMS detector (Rood, 1999)

Table 1.4.1: GC/MS parameter for the isomer specific detection of PAH, PCB and organochlorine pesticides

	PAH	PCB	Organochlorine pesticides
GC:	Type: Agilent 5890 Series II; Column: Stx-CLPesticides2, 30 m, 0.25 mm ID, 0.2 µm film thickness (Restek); Temperature program: 60°C, 1.5 min, 10°C min^{-1}, 225°C, 5°C min^{-1}, 290°C, 15°C min^{-1}, 315°C, 20 min; Carrier gas: helium, head pressure: 16 psi; Injector: Cold injection system CIS 3 (Gerstel); Temperature program injector: 120°C, 12°C s^{-1}, 300°C, 5 min; Temperatur transferline: 300°C; Autosampler: MPS2 (Gerstel); Injection volume: 0.3 µl splitless	Type: Agilent 5890 Series II; Column: Stx-CLPesticides2, 30 m, 0.25 mm ID, 0.2 µm film thickness (Restek); Temperature program: 90°C, 1.5 min, 20°C min^{-1}, 170°C, 7.5 min, 3.5°C min^{-1}, 285°C, 20°C min^{-1}, 300°C, 5 min; Carrier gas: helium, head pressure: 16 psi; Injector: Cold injection system CIS 3 (Gerstel); Temperature program injector: 120°C, 12°C s^{-1}, 300°C, 5 min; Temperatur transferline: 300°C; Autosampler: MPS2 (Gerstel); Injection volume: 1 µl splitless	Type: 5890 Series II; Column: Stx-CLPesticides2, 30 m, 0.25 mm ID, 0.2 µm film thickness (Restek); Temperature program: 60°C, 1.5 min, 12°C min^{-1}, 140°C, 6°C min^{-1}, 300°C, 10 min; Carrier gas: helium, head pressure: 16 psi; Injector: Cold injection system CIS 3 (Gerstel); Temperature program injector: 120°C, 12°C s^{-1}, 300°C, 5 min; Temperatur transferline: 300°C; Autosampler: MPS2 (Gerstel); Injection volume: 1 µl splitless
MS:	Type: MAT 95S (Thermo); Ionisation mode: EI, 47 eV, 260°C ; Resolution: > 8000; Detection: SIM mode	Type: MAT 95S (Thermo); Ionisation mode: EI, 47 eV, 260°C ; Resolution: > 8000; Detection: SIM mode	Type: MAT 95S (Thermo); Ionisation mode: EI, 47 eV, 260°C ; Resolution: > 8000; Detection: SIM mode

Table 1.4.2: GC/MS parameter for the isomer specific detection of PCDD/F

	PCDD/F
GC:	Type: Agilent 6890; Column: Rtx-Dioxin2, 60 m, 0.25 mm ID, 0.25 µm film thickness (Restek); Temperature program: 130°C, 1.5 min, 25°C min^{-1}, 205°C, 4°C min^{-1}, 310°C, 15 min; Carrier gas: helium, constant flow: 1.2 ml/min; Injector: Cold injection system CIS 4 (Gerstel); Temperature program injector: 120°C, 12°C s^{-1}, 300°C, 5 min; Temperature transferline: 300°C; Autosampler: A200S (CTC); Injection volume: 1 µl pulsed splitless
MS:	Type: MAT 95XL (Thermo); Ionisation mode: EI, 45 eV, 260°C ; Resolution: > 9000; Detection: SIM mode

1.4.6 VO Quality control samples

Extra samples were analysed to ensure the quality of the field and analytical methods. The same method (SOP) was used to quantify quality control samples. VO blanks and clean-up blanks were used as an internal quality control and all results were blank-corrected using the average of VO blank values. The VO blanks are not exposed VO in the field. They can yield information on the analyte uptake that occurred during transport, deployment and subsequent retrieval of passive samplers while the clean-up blanks can yield information on the levels of contamination that can take place during the extraction and analysis of samplers. The Limit of Detection (LOD) was calculated on the basis of three times the standard deviation of the blank values. A result is valid when the margin between the sample value and the average blank is larger than the LOD and is reported as a result after subtraction of the average blank value. Data below the LOD after subtraction of the average blank were taken as no detectable and

not included in further calculation. The average recoveries of all surrogates used for quantification ranged from 40 to 120 %.

2 Chapter II: Effectiveness of VO to sample POP

2.1 Introduction

Performance Reference Compounds PRC are analytically non-interfering organic compounds with moderate to high K_{ow} that are introduced in VO preceding the membrane enclosure and the field deployment (Huckins et al., 2002a). The measured uptake rate of target compounds is based on theory and experimental evidence that PRC loss rate constant $ke,_{PRC}$ at sampling site and the uptake rate constant *ku* of the analyte are governed by first-order kinetics and that residue exchange through the VO membrane is isotropic. The rate of PRC loss during an exposure is used for the assessment of in situ sampling rates. Several scientific researchers have used the PRC model for monitoring POP (Bartkow et al., 2004; Harman et al., 2008; Monteyne et al., 2013). Booij et al. (1998) , together with Huckins et al. (1999), suggested that VO kinetic exchange of hydrophobic compounds with high log K_{ow} ≥4.4 are generally under water boundary control, implying different environmental conditions have different impacts on the sampling rate.

Some disadvantages of this approach are the stability in kinetic exchange between PRC and the target chemical. In order to obtain valuable measures of PRC loss, reproducibility between samplers need to be good because potential variations in the sampler parameters or exposure factors may have an impact in the viability of $ke,_{PRC}$ values. It appears impractical to conduct the same exposure scenarios for each sampler. Thus, information on VO performance is required in order to take adequate measures that are relevant to calibration data.

Huckins et al. (2002b) assumed that hydrophobic compounds in VO with different log K_{ow} values can adjust to one another as long as the uptake mechanism is the same. However, previous studies in our laboratory (Levy et al., 2007) reveal the difference in diffusivity between hydrophobic compounds from diverse groups such as PCDD/F and PCB. This revelation needs to be taken into consideration as some current studies are using PCB-PRC to estimate PCDD/F in situ sampling rate (Charlestra et al., 2008; Roach et al., 2009).

The objective of this work was firstly to evaluate the behaviour in the VO of sixteen PAH-PRC and four PCB-PRC compounds with different log K_{ow} values, without regard for the environments conditions. Secondly, the aim was to establish a new method using the in situ sampling rate of these PRC compounds, thereby improving the accuracy of water concentration estimates. Several experiments will be then presented, supporting the use of these PRC to assess the effects of environmental conditions such as water volume and

temperature on VO sampling and to investigate the effectiveness of VO as a sampler for dioxins.

2.2 PAHs behaviour in VO used in previous studies

PRC spiked in VO prior deployment are used to determine the kinetic uptake of the target compound. The difference in sequestered amounts and profiles of these PRC compounds need to be known in order to provide an accurate quantification of the analyte. For this work, information from previous sampling campaigns (Wang et al., 2009; Karacık et al., 2013; Wang et al., 2013a) have been used to evaluate the behaviour of sixteen $^{13}C_{12}$ PRC-PAH and four $^{13}C_{12}$ PCB regardless environment conditions.

2.2.1 Sampling sites and Experimental

2.2.1.1 Sampling sites

2.2.1.1.1 Three Gorges Reservoir TGR

TGR is reported to have drastically degraded its ecosystem during recent decades. Many cities along the river such as Chongqing, one of the most populated cities in China, flush tremendous amounts of sewage and toxic wastes into the reservoir. Pollution with slower-moving water will threaten wildlife that depends on the river for its survival. Moreover, the flow velocity and the aggregate siltation in TGD has drastically reduced, changing the biological activity and causing water degradation by reducing intrinsic depuration ability.

Data for the investigated POP such as PAH, PCB and OCP in sampling sites across the TGR in 2008 (Wang et al., 2009) and in 2011 (Wang et al., 2013a) were used in this study. During the sampling campaign in 2008, the VO was deployed for 7 days and 25 days in seven sampling sites (Fig.2.2.1): 1. Maoping (Great dam); 2.Guojiaba; 3.BadongI; 4.BadongII; 5.Wanzhou; 6.Changshou; 7.Chongqing. During the sampling campaign in 2011, The VOs were deployed for 26 days in 12 sampling sites: 1. Maoping (Great dam); 2. Guojiaba; 3. Badong I; 4. Badong II; 5. Daning I; 6.Daning II; 7. Fengxi; 8.Xiaojang I; 9. Xiaojang II; 10.Wanzhou; 11. Changshou; 12. Chongqing.

fig 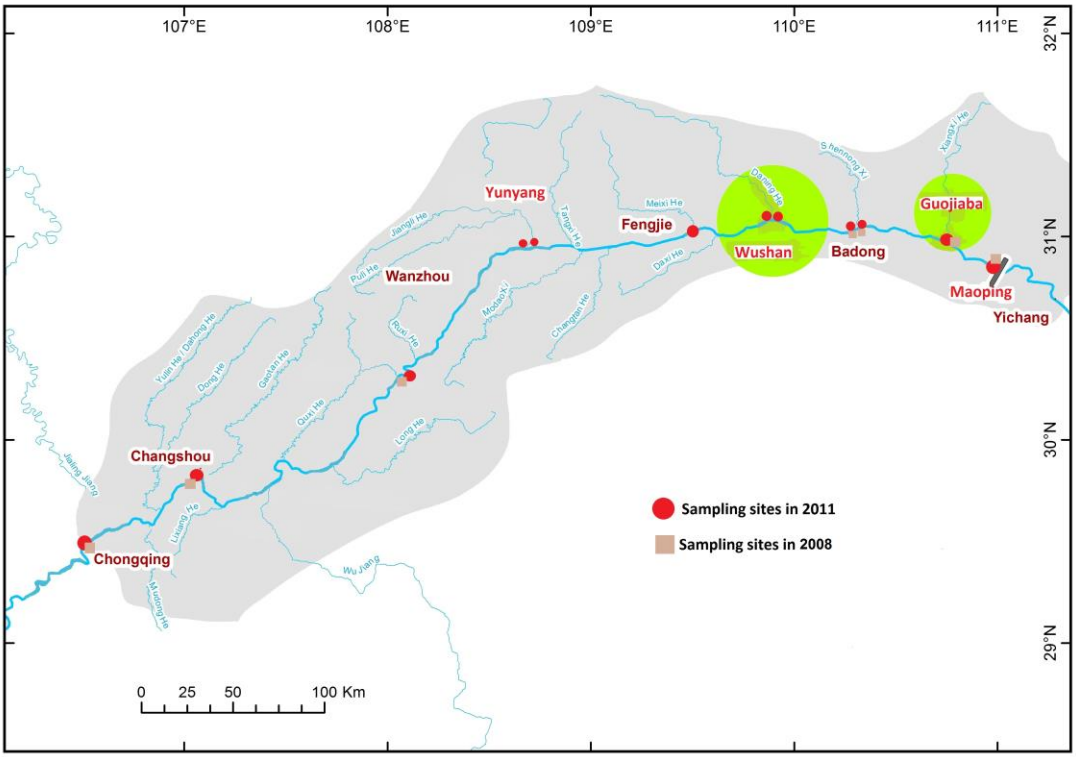

Fig.2.2.1: Sampling campaign in seven sampling sites in 2008 and in twelve sampling sites in 2011 across TGR

2.2.1.1.2 Danjiangkou Reservoir (DJR)

DJR (32°36′–33°48′N; 110°59′–111°49′E) built in 1970 with 745km^2 water surface, is located at the junction between Hubei and Henan provinces in China. This reservoir is the biggest tributary of the Yangtze River, which has a drainage area of 95,000km^2. Since 2002, the water has been transferred from the reservoir to North China for irrigation, industrial and domestic usages making the water quality of great concern (Li et al., 2008).

During sampling campaign in 2009, the VO was deployed for a minimum of 26 days and a maximum of 30 days in five different sampling sites (Fig. 2.2.2): 1.Jiangbei Bridge; 2. Hejiawah; 3. Lianhua; 4. Baqian Dam; 5. Longkou.

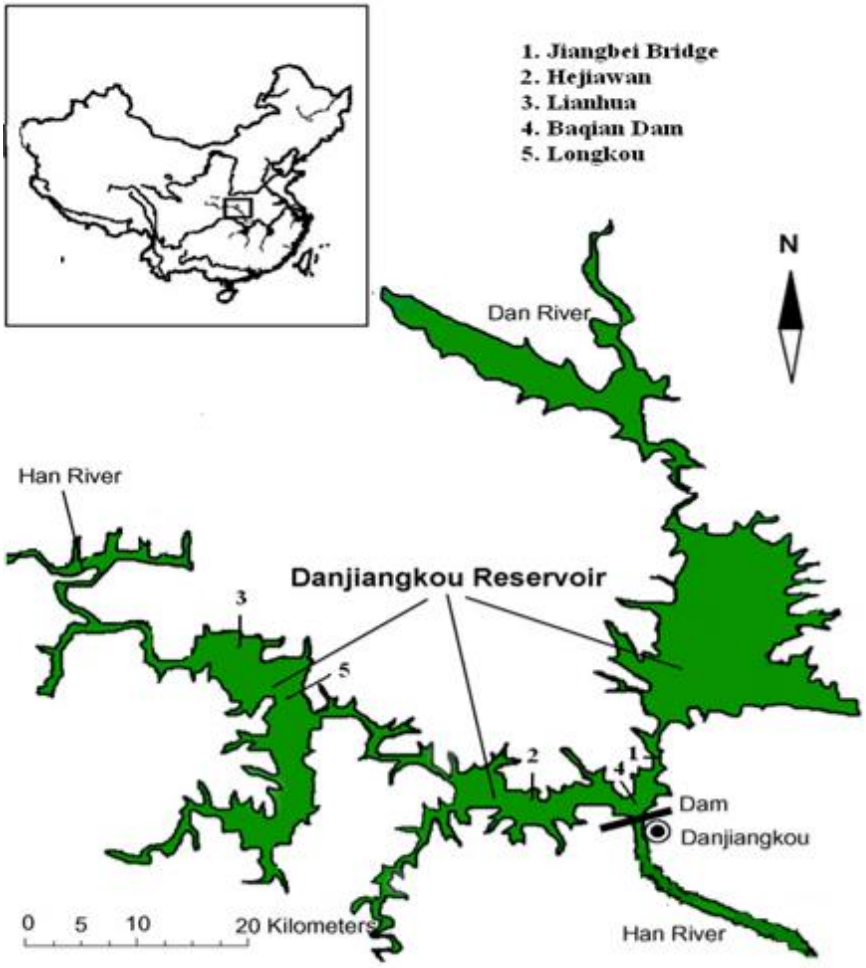

Fig 2.2.2: Sampling sites Danjiankou Reservoir during sampling campaign in 2009

2.2.1.1.3 Istanbul strait

Istanbul strait (Bosphorus) is one of the world's most strategic waterways, located between the Black Sea and the Sea of Marmara. It is an inundated valley 32 km long, 0.73-3.30 km wide and 30-120 m deep. The strait is affected by urbanization, commercial ships and oil tankers as well local fishing and passenger boats. It has an important influence on oceanographic conditions in the Black Sea and the Sea of Marmara. One of the distinct characteristics of the Bosphorus is a two layered current and density distribution. Less saline water is carried at the surface from Black Sea to the Sea of Marmara, while underlying bottom water with a higher salinity is carried in the opposite direction from the Sea of Marmara, which is originally from the Mediterranean, to the Black Sea. Investigation of pollutants in water such as PAH, PCB and OCP have been carried out by using VO during the sampling campaign in 2011 (Karacık et al., 2013). The VO was deployed for a minimum of 7 days and a maximum of 21 days in five sampling sites across the Istanbul Strait (Fig. 2.2.3): 6a. Istinye dereici; 6. Istinye; 12. Tuzla; 23. Buyukada; 24. Anadolu Feneri.

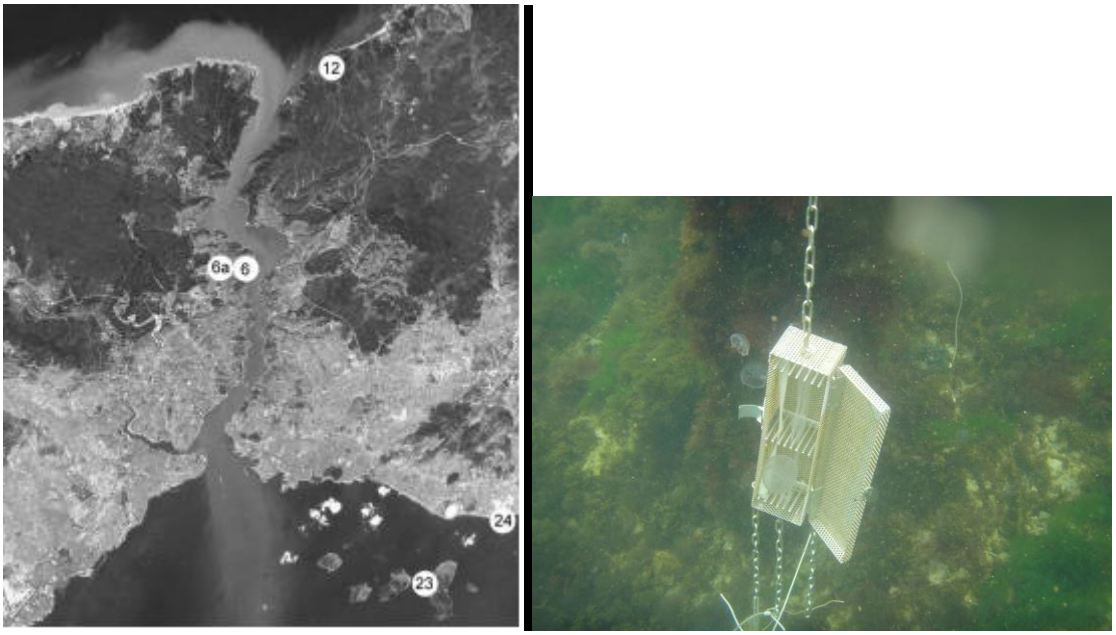

Fig. 2.2.3: Sampling site Istanbul strait (picture left, produced by Karacik et al., 2013) and VO exposed in Istanbul strait for 7 days and 21 days of deployment (picture right)

2.2.1.2 Experiments

The VO was transported to the sampling sites in clean glass vials, deployed in stainless steel cages and immersed into the water at about 1 m depth. The samplers were mounted on boats or fastened to docks which were about 10–20 m from the riverbank. The blank samples were prepared together with the other samples and transported to the sampling sites also in airtight glass vials, but they were not deployed. At the end of the sampling campaign, the VO was transported to the laboratory in the corresponding glass vials in the darkness and was kept in a freezer at -28 °C until processing.

2.2.2 Results and Discussion

To evaluate the behaviour of PAH in VO, sixteen PRC with log K_{ow} ranging from 3.4 to 6.5 from different experiments were used. Fractional losses of the PRC after different exposure time, 7 days, 21 days, 26 days and 31 days were used to find the average elimination rate $ke,_{PRC}$ for each PRC, which were assigned as the slope of the log-linear empirical function for the retained PRC fraction ln ($N_{t,PRC}$ / N_0) and the time (t) (days).

Where N_o, the PRC amount at t = 0 and ($N_{t,PRC}$), the PRC amount after exposure time t.

Naphthalene-$^{13}C_6$ with log K_{ow} = 3.38 presented the highest $ke,_{PRC}$ value with 0.24 d^{-1}, while Indeno(1,2,3-c,d)pyrene-$^{13}C_6$ with log K_{ow} = 6.42 presented the lowest $ke,_{PRC}$ value with 0.01 d^{-1}. Thus, the elimination rate ($ke,_{PRC}$) increased with the decreased log K_{ow}. Compounds with

a smaller molecular weight than fluoranthene-$^{13}C_6$ presented relevant values of $ke_{,PRC}$, while the other compounds with high K_{ow} (log K_{ow} range 5.18 to 6.5) did not perform as well for these short periods of deployments as their $ke_{,PRC}$ was between $0.02d^{-1}$ and $0.01\ d^{-1}$. From Eqn. 1.1, it was deduced in this study that equilibrium in VO is reached when $ke_{,PRC}\ t \geq 1$ and C_{VO} increased linearly with time when $ke_{,PRC}\ t < 1$. Thus, compounds with lower log K_{ow} such as naphthalene-$^{13}C_6$ and acenaphtylene-$^{13}C_6$ attained equilibrium with $k_{e,PRC}\ t > 1$ for an exposure time of 30 days while acenaphthene-$^{13}C_6$, fluorene-$^{13}C_6$, phenanthrene-$^{13}C_6$, anthracene-$^{13}C_6$ and fluoranthene $^{13}C_6$ were still in the linear stage with $k_{e,PRC}\ t < 1$ (Huckins et al., 2006b). These results were in accordance with the U.S.Environmental Protection Agency (EPA, 2009) suggesting that log K_{ow} values are generally inversely related to aqueous solubility and directly proportional to molecular weight. Results also show a linear correlation between hydrophobicity (K_{ow}) and the elimination rate ($k_{e,PRC}$), as the higher the K_{ow} was, the lower the $k_{e,PRC}$ was (Fig.2.2.4). Huckins et al., 2001 advised to exclude compounds with log K_{ow} >5.5 for obtaining measurable losses of PRC. His theory is based on the fact that the VO uptake rate of pollutant with log K_{ow} >4.4 was considered under water boundary layer control (WBL) and the effects of environmental variables on the pollutant exchange rates with a wide range of K_{ow} were concluded as constant and were reflected by changes in the loss rate of PRC with a much narrower range of K_{ow} (Booij et al., 1998; Huckins et al., 2002a). The accuracies of this approach may not be considered if the exchange rates of chosen PRC and the target analyte, both with a log K_{ow} >4.4, are not governed by the same rate-controlling mechanism. Studies found a size-disparity effect in the polymer triolein on organic compounds (Chiou, 1985) which may affect the mass transfer lipid-membrane during molecular exchange and then allow membrane control of high molecular weight rather than WBL control as expected. Besides this, the sixteen PRC were presented in a different kinetic stage after exposure; the choice of one PRC to reflect the loss rate of a wide range of target chemicals may be inappropriate as there is a high risk that the analyte does not have a diffusion and sorption matching PRC. The obtaining of a low PRC elimination rate $ke_{,PRC}$ for compounds with log K_{ow} >5.18 does not mean that there is no isotropic exchange between high hydrophobic PRC compounds and their native analogues. The change of exposure scenarios is not only limited to environmental variables but also to chemical properties of the organic pollutants. The direct measure of $ke_{,PRC}$ to estimate in situ sampling rate will insure an accurate value of the analyte water concentration.

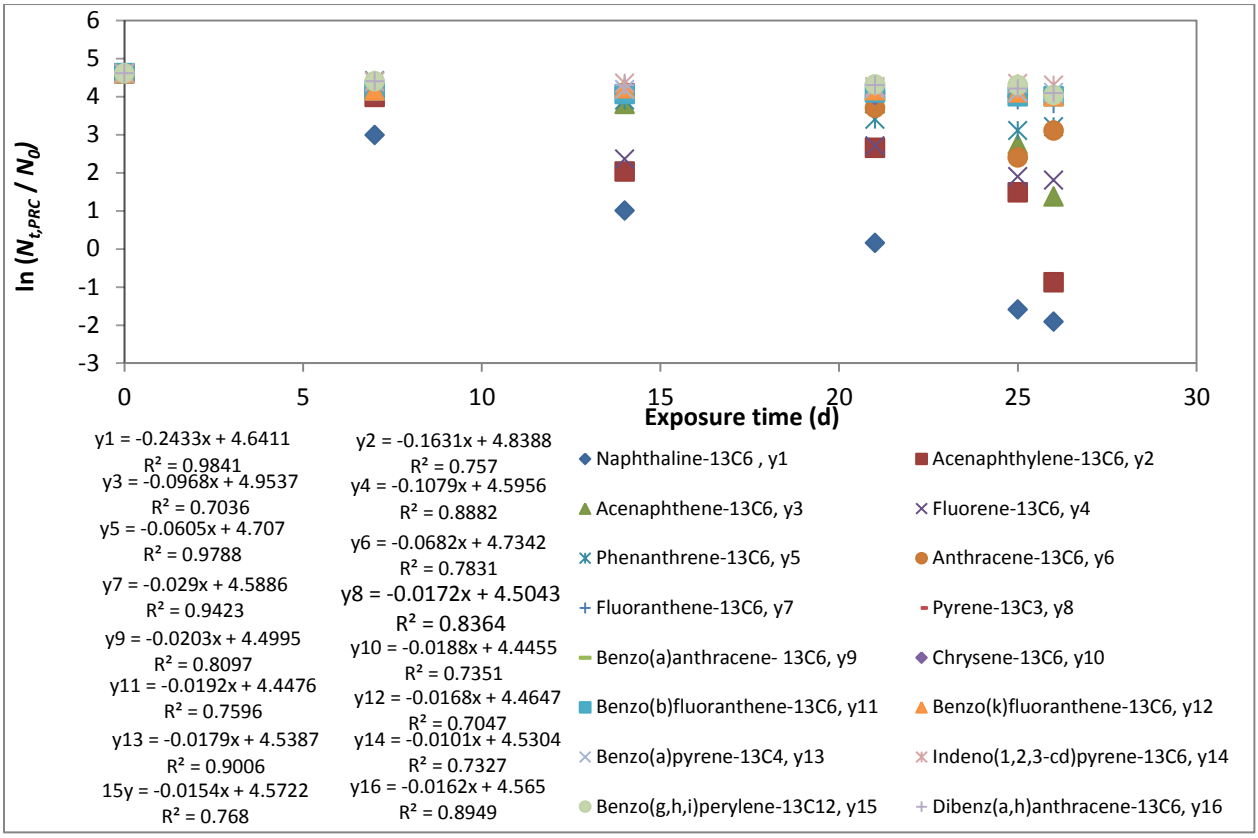

Fig.2.2.4: Exposure time as a function of retained PRC fraction at time t $N_{t,PRC}$ of sixteen PAH-PRC with log K_{ow} range 3 to 6.63: Naph-$^{13}C_6$, Acy-$^{13}C_6$, Ace-$^{13}C_6$, Fle-$^{13}C_6$, Fen-$^{13}C_6$, Ant-$^{13}C_6$, Flo-$^{13}C_6$, Pyr-$^{13}C_3$, BaA-$^{13}C_6$, Chr-$^{13}C_6$, BbF-$^{13}C_6$, BkF-$^{13}C_6$, BaP-$^{13}C_4$, IND-$^{13}C_6$, BghiP-$^{13}C_{12}$, DahA-$^{13}C_6$. Connected data points represent measurements within 3 different studies with an exposure times from 7 to 30 days (Wang et al., 2009; Wang et al., 2013 and Karacik et al., 2013).

2.2.3 Specific conclusion

This experiment assessed the relationship between hydrophobicity (K_{ow}) and elimination rate ($k_{e,PRC}$). Compounds with log K_{ow} < 5.18 presented measurable $k_{e,PRC}$ values, while higher hydrophobic compounds didn't perform as well with $ke_{,PRC}$ values lower than 0.02d^{-1}. PRC in VO can be used to evaluate the effects of chemical properties conforming to the target compound.

2.3 PAH behaviour in VO tightly sealed in glass ampules

VO has been used for many years in different sampling campaigns (Zhu et al., 2007; Levy et al., 2009; Wang et al., 2009; Karacık et al., 2013; Wang et al., 2013). One of the issues encountered during the computation process was the determination of a negative elimination rate value. The percentage of retention of blank samples didn't reach 100% as expected, so some samples presented a percentage of retention higher than a blank sample. The aim of this

study is to find out potential reactions occurring in the VO that may participate in the PRC elimination of sixteen ^{13}C- PAH-PRC and four PCB compounds.

2.3.1 Sampling sites and Experimental

Single VO with incorporated PRC (600µL PAH, 400µL PCB / 204,55g triolein) were isolated by heat, sealing it in glass ampules. Closed light protected ampules were either stored at -80°C immediately after sealing or sampled at room temperature at days 1, 4, 7, 15, 32, 63 and 125. After exposure time, samples were stored at -80°C until opening of the ampules for analysis of the VO.

2.3.2 Results and Discussion

There was no reduction of PAH- PRC amounts (Fig. 2.3.1) and PCB-PRC amounts (Fig. 2.3.2) detected during 125 days of exposure period. This observation confirmed the reliability of the isotropic exchange of the PRC. There is no isotropy exchange without the presence, in both side out and in the VO, of contaminants with similar physicochemical properties. Furthermore, the result reveals that PAH-PRC and PCB-PRC inside the VO didn't present any interaction. The dissipation of high volatile compounds such as naphthalene was influenced by environmental conditions. PRC with wide range of K_{ow} such as PCB-PRC are generally strongly bound onto the sorbent phase (triolein) through physico-chemical interaction. These compounds would be difficult to dissipate.

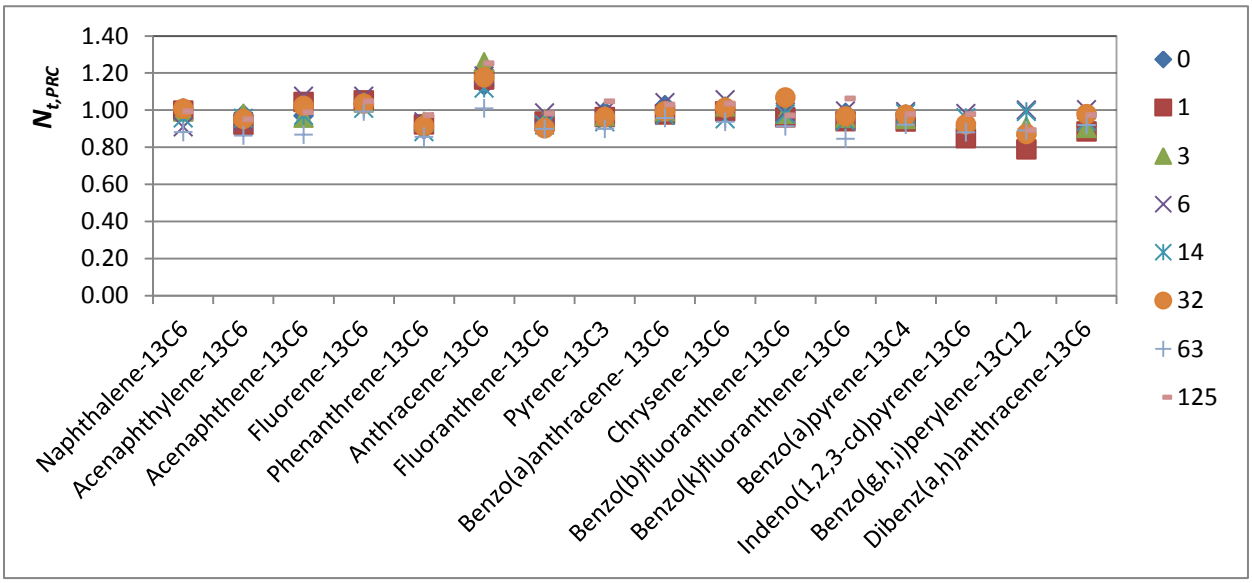

Fig. 2.3.1: Retained PAH-PRC fraction $Nt_{,PRC}$ after the exposure period of 1 d, 3 d, 6 d, 14 d, 32 d, 63 d and 125 d. The retention of B(g,h,i)p ranged from 0.22 to 0.39 because of an error factor accounted during GC-MS analysis.

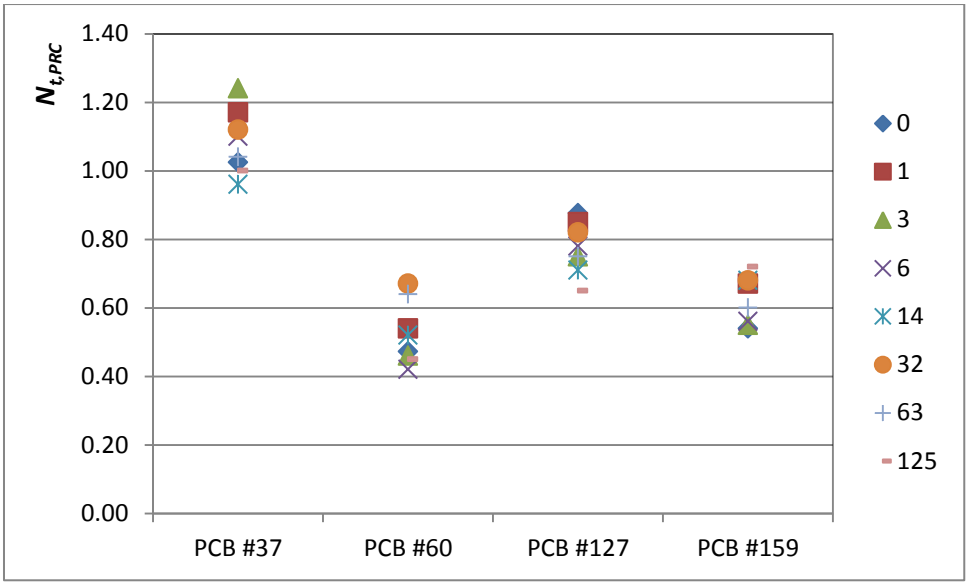

Fig. 2.3.2: Retained PCB-PRC fraction $N_{t,PRC}$ after the exposure period of 1 d, 3 d, 6 d, 14 d, 32 d, 63 d and 125 d

2.3.3 Specific conclusion

The PRC were suitable tools in the quantification of exchange-kinetics for contaminant transfer into the samplers. The PRC were completely retained in VO when they were protected from environmental effects, except temperature and when they were not in contact with contaminants with similar physicochemical properties.

2.4 PRC release in the well and comparison of VO with an active sampler XAD

The use of PRC was proposed by Huckins et al., 2002 to calibrate the SPMD sampling rate in situ and thereby assess the actual water sampling situation by predicting the site effects. This in situ calibration approach is based on the theory that PRC dissipation rate constant at sampling sites is related to the uptake rate constants of target compounds. This study provides some feedback on the release of PRC during one year of exposure time. The experiment was achieved in the clean water of an outdoor well. A complementary tool, an active sampling by XAD, was added to give access to information of concentration of PRC that were released from the VO.

2.4.1 Sampling sites and Experimental

The VO, contained in stainless steel cages, was attached to a cord that was securely fixed to the wellhead. The sampler was placed in the vertical midpoint of the screen and was immersed slowly down the well to avoid causing any damage to the polyethylene tubing. A reference point was marked on the rope at 180 cm from the cage container so that it stood at a

given depth above groundwater surface (Fig. 2.4.1). The first trial started from 27.07.12 to 08.03.13 for almost ten months. VO was sampled at days 3, 18, 53, 93, 168 and 262. The second trial started from 26.03.13 to 01.03.14 for 13 months. VO was immersed in the well water and was sampled at days 25, 30, 56, 201 and 340. The purpose of these two trials was to observe PRC behaviour after a long period of deployment. The measurements were carried out at outdoor temperature, water temperature, time and water depth (Appendix table 7) to allow the calculation of the water volume. The water was later pumped twice at times 01.03.2014 and 06.04.2014, through XAD, an active water sampling cartridge filled with Supelpak-2 XAD-2 resin with a glass frit at one side and heat-treated glass wool at the other side. VO and XAD results were both used for the evaluation of pollutant water concentration. In contrast to VO, chemicals can directly be absorbed to XAD without any barriers. The water was pumped by a battery driven peristaltic pump (Verder, Haan, Germany) at a flow rate of about 3 L/min. Consequently, the water was drawn to -40 cm of the initial water depth during 60 minutes. VO was removed in the well before the first pump. The second sampling was executed when the water reached its initial depth. Until extraction, the samples were stored at 4 °C.

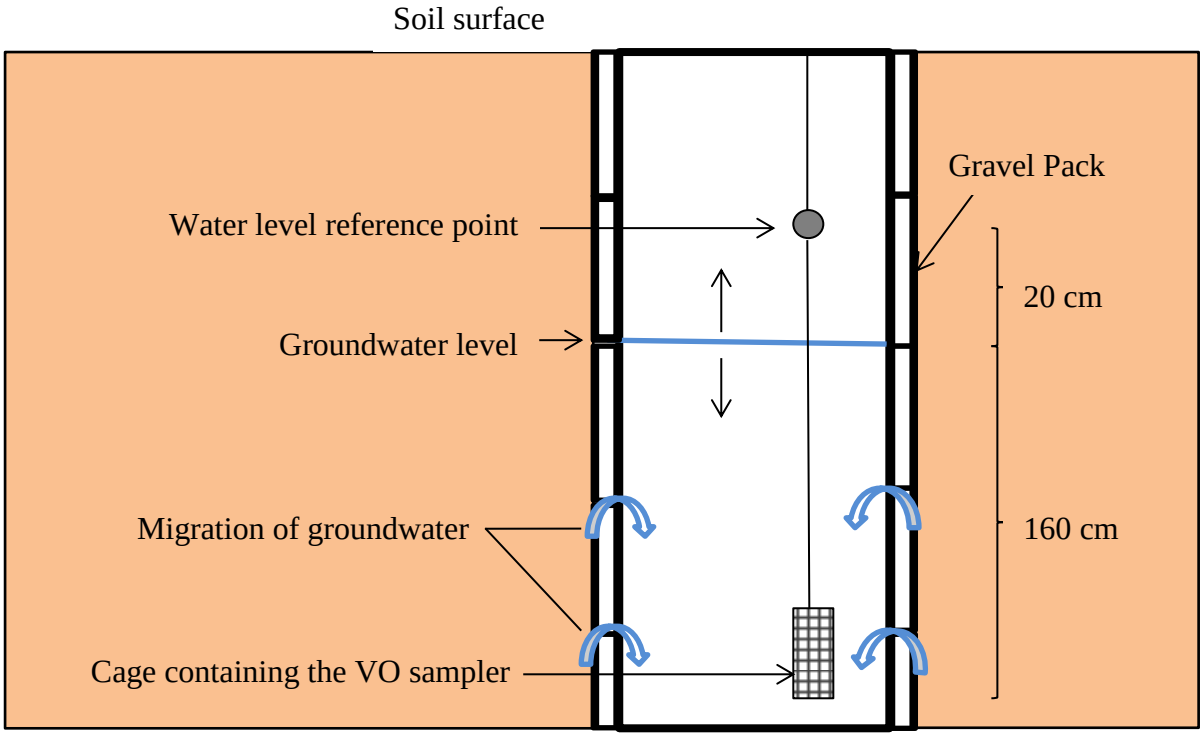

Fig. 2.4.1: Deployment scheme of the VO in the well at the beginning of the experiment

2.4.2 Results and Discussions

Reproducibility of PRC loading after a long period of deployment (262 days)

There was no detectable loss of the PRC amounts in frozen VO and field blanks during the experiment (Fig.2.4.2). For samplers deployed in the well during the first trial for 262 days, the loss rate constant increased with decreasing log K_{ow}. Therefore, only 2% of naphthalene-$^{13}C_6$, the most volatile PAH-PRC compound, remained in the sampler. This was followed by acenaphthylen-$^{13}C_6$ with 25% remaining, acenaphthen-$^{13}C_6$ with 43% remaining and fluoren-$^{13}C_6$ with 55% remaining. The amount of heavier molecule weight PRC compound remains quasi stable during this period. The results of this first trial and the PAH-PRC evaluation see above (See above, Chapter 2.2.2) presented some similarities.

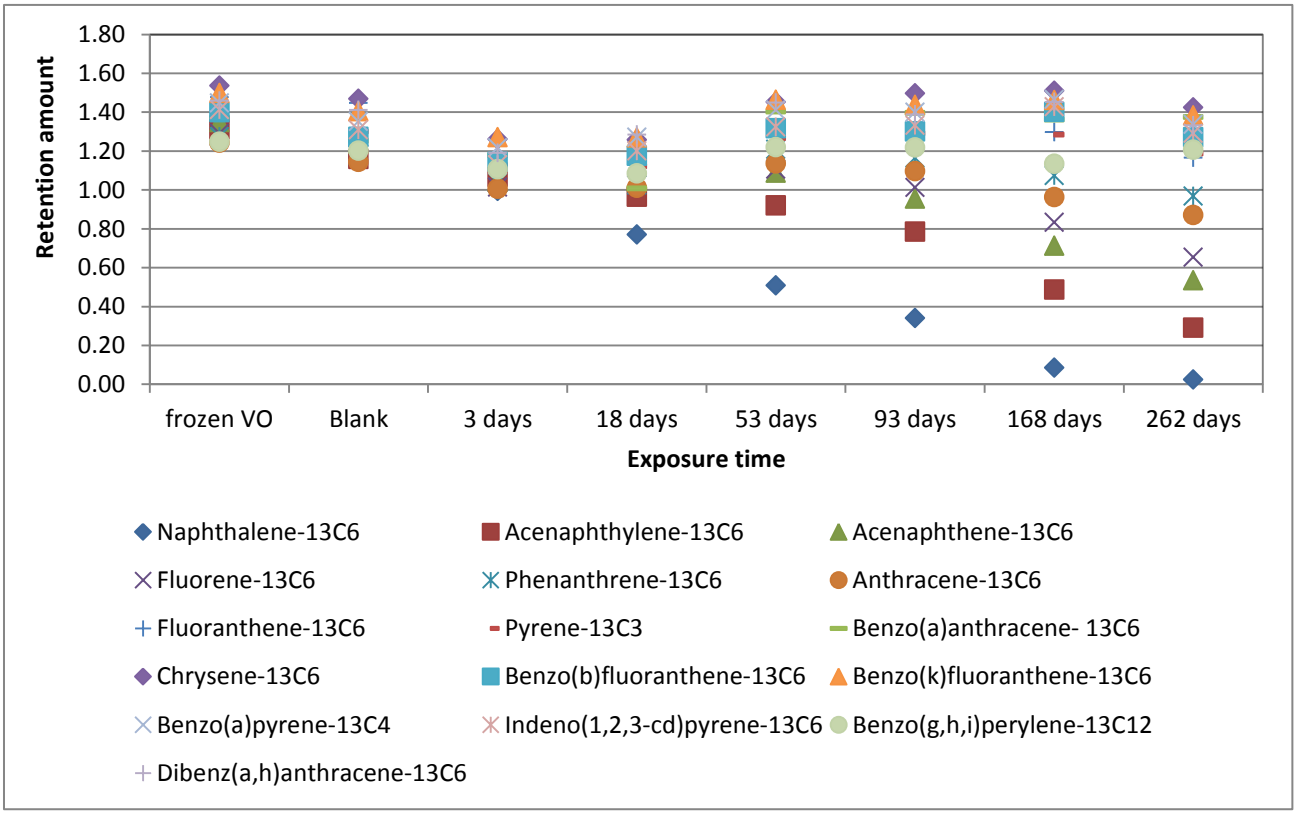

Fig. 2.4.2: Retention amounts of PRC of VO exposed in well after deployment period of 262 days during the first trial (Appendix Table 8)

The elimination rate constant for each PRC were calculated from the VO deployed during 262 days (Table 2.4.1). *ke* values increase with the decrease of log K_{ow}. Naphthalene presented the highest *ke* value (0.014 d^{-1}).The high hydrophobic compounds with log K_{ow} >5.18 presented very low *ke* values (<10^{-4} d^{-1}). Naphthalene and acenaphthylene seemed to be in equilibrium

after 262 days of deployment with ke_t, reaching 3.9 and 1.4 respectively. The rest of the compounds were still in the linear stage. This is congruent with the fact that compounds with lower K_{ow} values reach an equilibrium stage in the VO faster than those with higher K_{ow}.

Table 2.4.1: Log K_{ow} values and corresponding PRC loss after the exposure period of 262 days.

PRC	log K_{ow}	Loss rate constant *ke* (10^{-3} d^{-1})
Naphthalene-$^{13}C_6$	3.38	14.86
Acenaphthylene-$^{13}C_6$	4.07	5.26
Acenaphthene-$^{13}C_6$	3.92	3.20
Fluorene-$^{13}C_6$	4.1	2.31
Phenanthrene-$^{13}C_6$	4.46	1.05
Anthracene-$^{13}C_6$	4.54	1.04
Fluoranthene-$^{13}C_6$	4.84	0.83
Pyrene-$^{13}C_3$	5.18	0.35
Benzo(a)anthracene- $^{13}C_6$	5.6	< 0.1
Chrysene-$^{13}C_6$	5.84	< 0.1
Benzo(b)fluoranthene-$^{13}C_6$	6.44	< 0.1
Benzo(k)fluoranthene-$^{13}C_6$	6.44	< 0.1
Benzo(a)pyrene-$^{13}C_4$	6.42	< 0.1
Indeno(1,2,3-cd)pyrene-$^{13}C_6$	6.42	< 0.1
Benzo(g,h,i)perylene-$^{13}C_{12}$	6.63	< 0.1
Dibenz(a,h)anthracene-$^{13}C_6$	6.5	< 0.1

Comparison between passive sampler VO and active XAD-sampling

During analysis of VO used for the second trial, the native PAH standard were used by mistake as quantification standard. The samples were no more useful due to the reduction of the percentage of PRC retention. Only VO data of dates 25 and 340 were available for the estimation of PAH and OCP concentration in the well. At this second trial, the PRC dissipation values after 340 days of exposure were lower than the first trial (Fig 2.4.3). Besides, the analysis of ^{13}C-PAH-PRC released from VO and accumulated in XAD after

exposure period didn't present any substantial signals. An explanation of this inconsistency is still unclear.

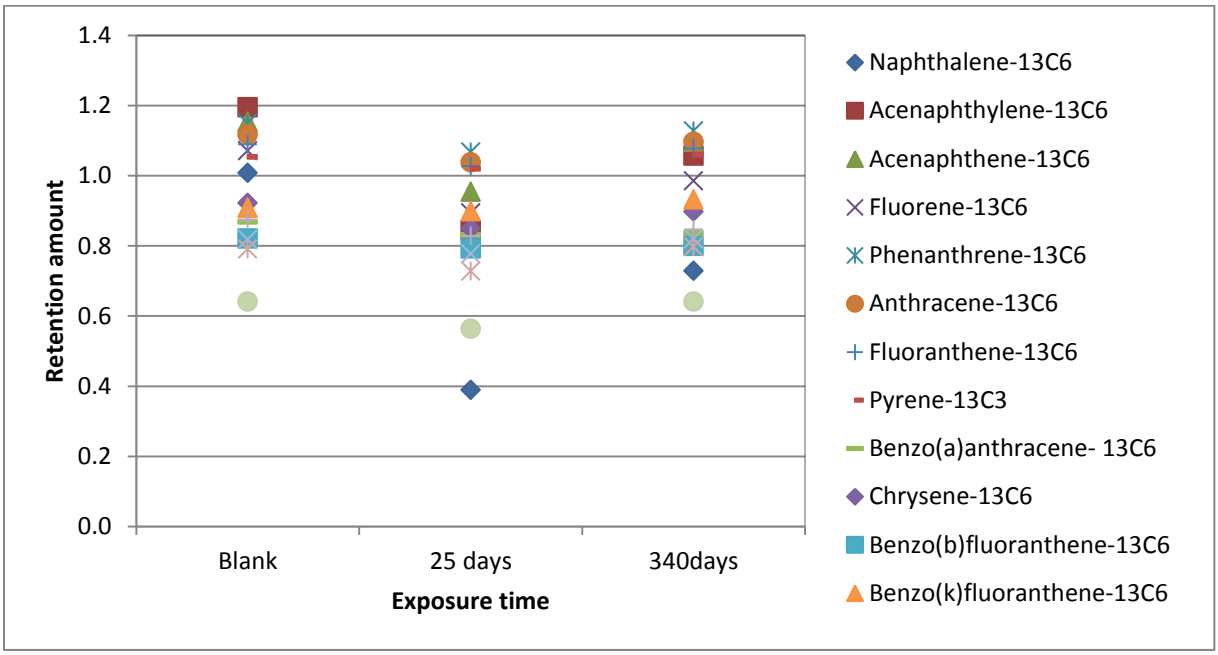

Fig. 2.4.3: Retention amounts of PRC of VO exposed in well after deployment period of 340 days during the second trial (Appendix table 9)

The water running through the XAD column involved the reduction of the volume from 6.96 m^3 to 8.13 m^3 at the first pump and from 9.32 m^3 to 9.91m^3 at the last pump (Fig. 2.4.4). The measured volume values and the real volume values are significantly different (Fig.2.4.5). The reason for this discrepancy is due to the migration of the groundwater that flows horizontally through the gravel pack, which increases the volume of the well. The measured volume depends on the dimension of the well and is given as:

$$V = \pi \times r^2 \times h \qquad \text{Eqn 2.2}$$

Where r is the radius of the well and h is the distance between the water level and the container.

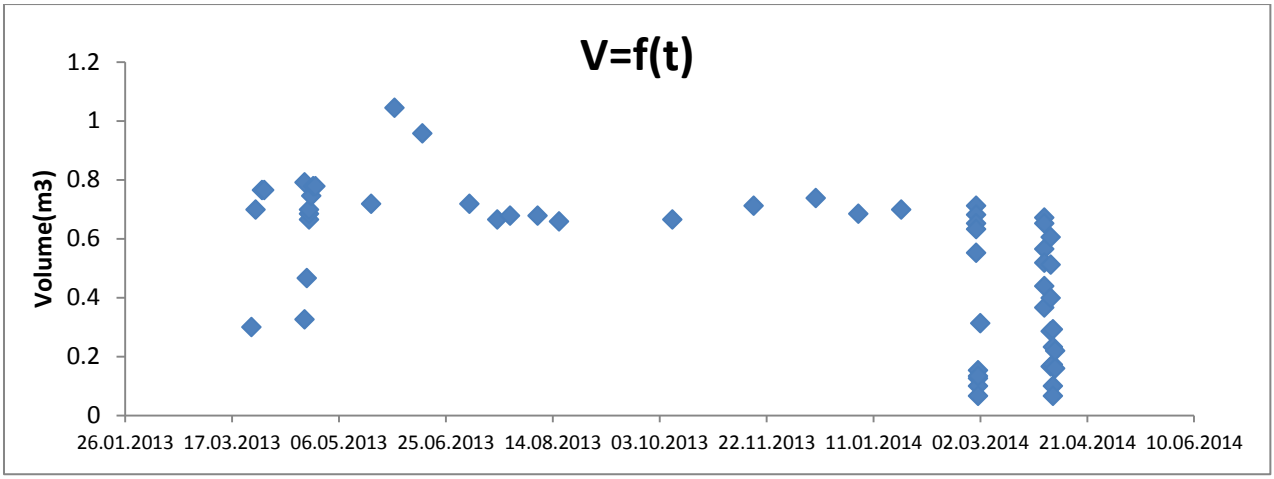

Fig 2.4.4: Water volume variation during the experiment in the well. Four water reduction with 2 at the beginning and 2 at the end of the trial are observed. XAD was used from 01.03.2014 to 06.04.2014 (Appendix Table 7).

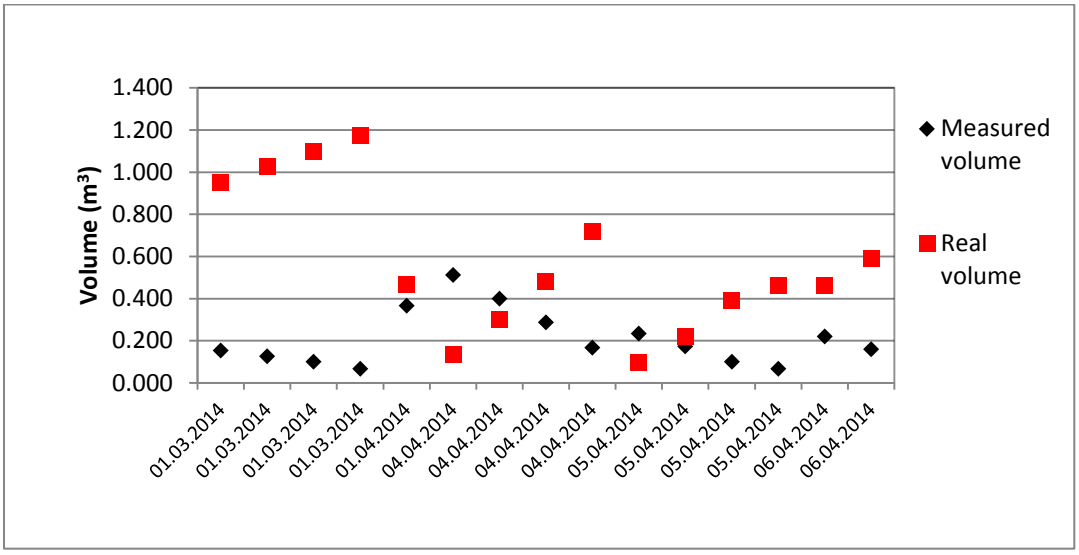

Fig.2.4.5: Comparison of measured volume and real volume during the water sampling of the well (Appendix Table 7)

The method of calculation used to estimate pollutant water concentration in VO was elaborated in chapter 3.2. The PAH concentration in VO after 25 days of deployment ranged from 763 pg/L for naphtalene to 2 pg/L for dibenzo(a,h)anthracene and after 340 days, from 1758 pg/L for naphthalene to 6 pg/L for dibenzo(a,h)anthracene (Fig.2.4.6). The total PAH bounded to XAD-2 resin after purging a water volume of 232L revealed a concentration ranged from 1043 pg/L for pyrene to 8 pg/L for dibenzo(a,h)anthracene. 83% of this total amount was found in the master side and 17% in the backup. Most PAH compounds presented a similar concentration in the VO and in XAD-2 resin especially those with log K_{ow} > 5.18. This similarity can be a proof of the accuracy of the new method developed in this

study.

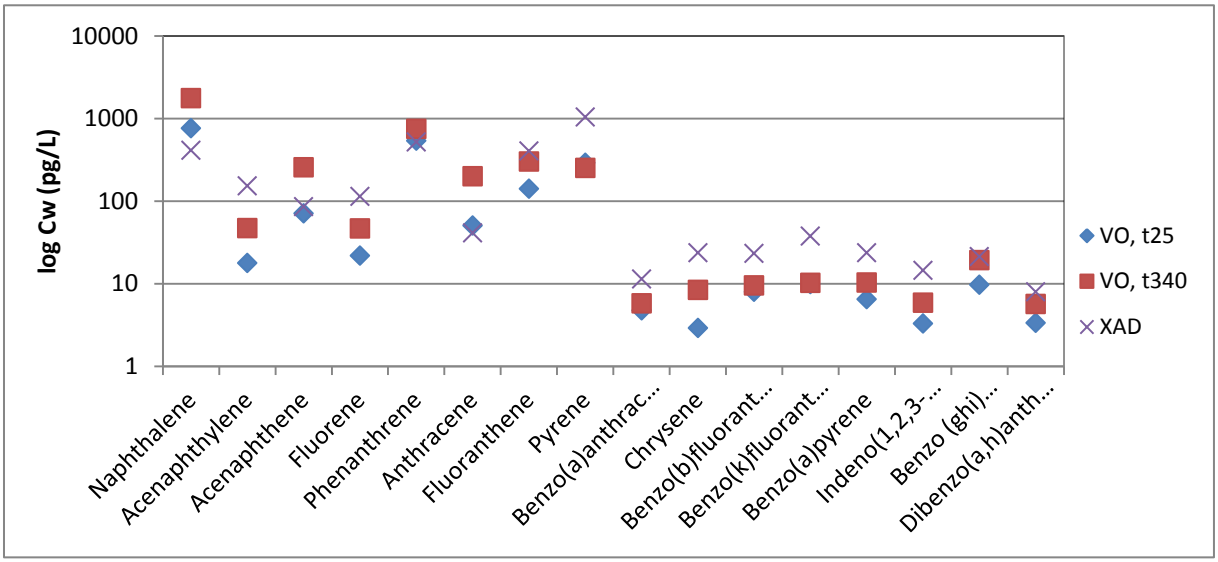

Fig 2.4.6: Comparison of PAH water concentration in VO at 25 days and 340 days and in XAD after 2 purging (Appendix Table 11)

Most of OCP compounds presented a very low concentration leading to an inconsistence in the results during the blank correction. The analyte amounts in the samples lower than in the blank, could have led to improbable concentration values. The relative lower is the pollutant concentration in water, the relative higher is the error measurements (Messinger, 2004). However, compounds with a concentration above LOQ such as γ-HCH, PeCB, 2,4-DDT, 2,4-DDE and Methoxychlor , presented similar amounts in the VO and XAD. Hence, the abundant OCP compound was γ-HCH with 332.92 pg/L in the VO after 25 days, 547.68 pg/L in the VO after 340 days and 422.83 pg/L in XAD. The lowest OCP compound was 2,4-DDE with 0.69 pg/L and 0.85 pg/L in VO respectively after 25 days and 340 days and 0.93 pg/L in XAD (Fig. 2.4.7).

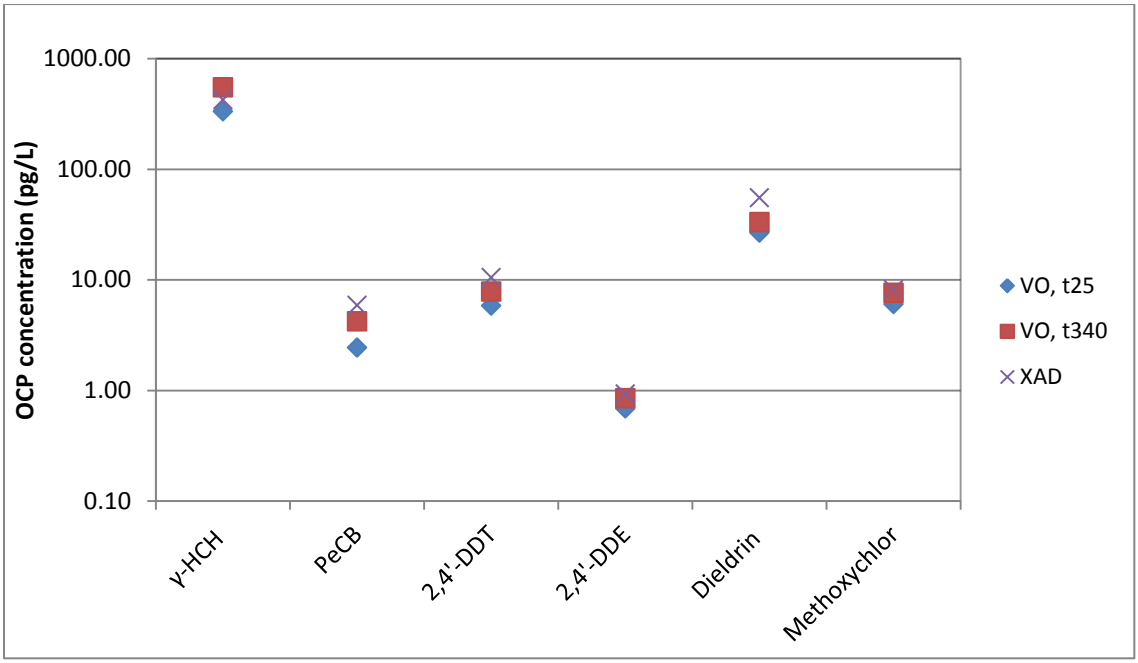

Fig. 2.4.7: Comparison of γ-HCH water concentration in VO and in XAD (Appendix table 11)

2.4.3 Specific conclusion

The release of PRC is not affected during a long period of VO deployment. XAD will provide accurate values of pollutant concentration in clean water after a purge. The sampler VO can predict the water concentration from XAD if the concentration efficiency is above the LOQ.

2.5 PCB and Dioxin behavior in VO exposed in a Stevenson screen box

Due to the semi-volatile character of PCDD/F, ambient air is the most important medium for their distribution and transport in the (atmospheric) environment (Alcock and Jones, 1996). Many studies have used the passive sampler SPMD for the investigation of persistent organic pollutants, although there are relatively few studies which have demonstrated the usefulness of these devices for measuring the dioxin compounds (Prest et al., 1992; Lebo et al., 1995; Ranthalainen et al., 1998; Lohmann et al., 1998 and 2001). Since the introduction of performance reference compounds (Booij et al., 1998; Huckins et al., 2002), scientist have used PCB as PRC to estimate dioxin concentration (Zhu et al., 2007; Coots and Friese, 2011; Roach et al., 2009). Levy et al. (2007) reveal that, in contrary to others compounds whose exchange rates decrease with increase log K_{ow}, the highest molecular weights *MW* in PCDD/F are released faster from SPMD than the lowest *MW* The photodegradation of dioxin was

proposed as a possible explanation of this paradox but more information regarding the behaviour of PCDD in VO is still needed.

The purpose of this present study was to investigate the VO exchange rate of PCDD/F and PCB compounds in air. Native PCDD/F and PCB loaded in VO were used as test analytes. The experiments were achieved in a containment called Stevenson screen box to minimize the effects of photo-degradation and air-flow turbulences on the compound mass transfer in VO.

2.5.1 Sampling sites and Experimental

VO was deployed into Stevenson screen boxes of untreated wood (50 cm x 50 cm x 40 cm) placed in an outside area at about 3 m from the laboratory building 24 at Helmholtz Centre Munich in spring time on 06.05.2008 to 19.05.2008 at 11°C to 18.5°C. The Stevenson devices hinder wet deposition and direct irradiation of sunlight, but allow air to flow through them. Inside each Stevenson screen box, four metal frames were disposed in parallel, where five VO were placed on each frame.

For the preparation of VO, 1.5 mL of a fly-ash extract that contained the PCDD/F and 15 µL of a standard mixture that contained all 209 PCB congeners (0.25 to 0.75 µg/mL), purchased from Wellington Laboratories (Canada), were reduced to 0.3 mL. 250 µL of this condensate was spiked to 10 g triolein. The loaded VO were stored in closely sealed aluminium heat cleaned 10 mL glass vials at -30°C and kept cool during transportation until deployment.

The compounds of interest in this work were the indicator PCB (PCB 28, 52, 101, 138, 153 and 180), dioxin-like PCB (PCB 77, 81, 105, 114, 118, 123, 126, 156, 157, 167, 169 and 189),7 PCDD (2,3,7,8-TCDD; 1,2,3,7,8-PCDD; 1,2,3,4,7,8-HxCDD; 1,2,3,6,7,8-HxCDD; 1,2,3,7,8,9-HxCDD; 1,2,3,4,6,7,8-HpCDD; OCDD) and 10 PCDF (2,3,7,8-TCDF; 1,2,3,7,8-PCDF; 2,3,4,7,8-PCDF; 1,2,3,4,7,8-HxCDF; 1,2,3,6,7,8-HxCDF; 1,2,3,7,8,9; HxCDF; 2,3,4,6,7,8-HxCDF; 1,2,3,4,6,7,8-HpCDF; 1,2,3,4,7,8,9-HpCDF; OCDF)

The VO samples were transported in the hermetic vials to the Stevenson screen box to avoid contamination. VO weights were controlled before and after the exposure in air as a quality control of possible triolein losses. A VO with more than 10% loss of weight was discarded and a new VO sample was analysed.

Three trials were carried out at different physical conditions and different exposure times. In the first trial, the samples were exposed directly in the air; in the second trial, the samples

were kept in the glasses and these exposed in the air; in the third trial, the samples were stored in the fridge from -30 °C to -80 °C (Table 2.5.1).

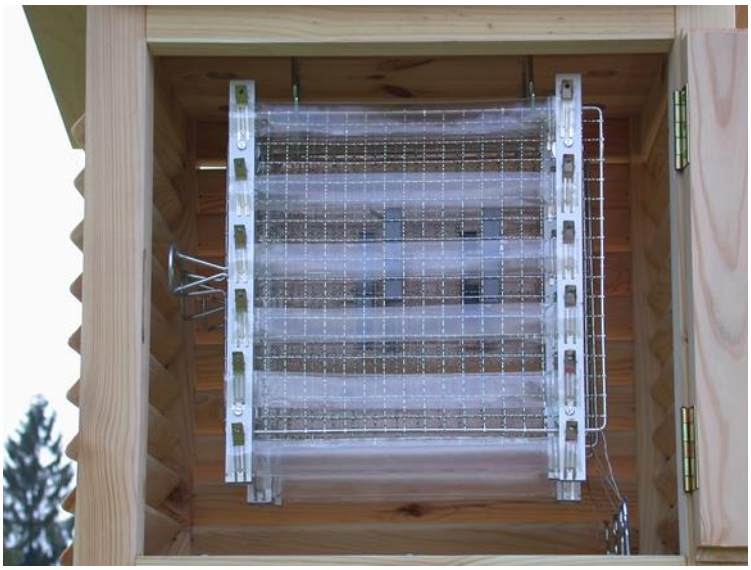

Fig.2.5.1: The VO expose into Stevenson screen box

Table 2.5.1: Experiment of PCDD/F and PCB in VO exposed in air: physical conditions and exposure times.

VO Elimination kinetics of PCDD/F and PCB Starting days: May 6th at about 9 am All VO samples were stored at -30°C until exposure								
Exposure time (h)	2	4	6	24	48	72	168	312
VO exposed	x	x	x	x	x	x	x	x
VO in vial				x			x	
VO from -30 °C to -80 °C				x			x	
All VO samples will be stored back to -80 °C until analysis								

2.5.2 Results and discussion

VO exposed in air

Results presented that a certain amount of PCDD/F was released in the VO exposed in air even though an uptake was expected. An explanation of this inconsistency may be due to the fact that the VO was overloaded with dioxin to equilibrium. The saturation limit of the device could have been reached for these compounds, leading to its dissipation from the VO to the atmosphere.

At the end of the exposure period, the amount of PCDD/F in the VO had decreased with increasing chlorination (Fig.2.5.2). Hence, TCDD and PeCDD showed a decrease of 15-35%, while the higher chlorinated HxCDD, HpCDD and OCDD presented a decrease of 45-75%. PCDF, the more volatile compound of PCDD/F, was predominantly available in the gas phase. The more chlorinated compounds OCDF, HpCDF, HxCDF and PeCDF showed a decrease of almost 99-97%, while the less chlorinated compounds TCDF presented a decrease of 80%. In general, the results show that the concentration of PCDD/F in the VO decreases as the chlorinated level increases.

PCDD/F was generated and could normally be adsorbed on aerosol or found in the gas phase during combustion processes. The emissions, the isomer distribution and the partitioning between gas and particulate phases could vary significantly, depending on the process, the input and the operating conditions. Studies reported OCDD to be the most abundant congener in the atmospheric pattern of dioxin (Morales et al., 2014). However, PCDD/F appeared to mainly be present in the aerosol phase and only 10% in the gas phase, in which 13% Cl_{4-5}-CDD/F and more than 70% Cl_{6-8}-CDD/F (Lohmann et al., 2000). Thus, the aerosol phase in the atmosphere was enriched with the lower *MW* PCDD congeners, such as TCDD and PeCDD. Meanwhile, the gas phase was enriched with the higher *MW*, such as HxCDD, HpCDD and OCDD. Lohmann and Jones (1998) reported that the kinetic exchange in VOs at equilibrium depends on the air concentration and physicochemical properties of the sampled compounds. Taking into account that the VO is able to sample mainly the compounds in the gas phase and nano-particulate phase (Lohmann et al., 2001), the availability of HxCDD/F, HpCDD/F and OCDD/F in gas phase have led to its releases in VO.

The behaviour of PCDD/F in VO does not agree with the other compounds such as PAH, whose uptake rate decreases with a high *MW* (See PAH behaviour in VO, chapter 2.2.). At ambient temperature, two-ring naphthalene almost entirely exited in the gas phase, whereas five-ring PAH and higher-rings PAH were predominantly absorbed on particles (Zielinska et al; 2004). Besides, the degree of chlorination increased with the octanol-air partition coefficient (K_{oa}) value. K_{oa} is equivalent to K_{ow}, used to indicate the compound affinity between air and a lipophilic phase. The VO was reported to sequestrate preferentially high K_{oa}.

For PCDD/F, particles in air partitioned with low *MW* are more abundant. Pennise and Kamens, 1996 demonstrated that the lower chlorinated congeners of PCDD/F were removed mainly from the vapour phase by reaction with OH radicals while dry gas deposition was

more important for higher chlorinated PCDD/F congeners. However, the fact that dioxins with high K_{oa} were released faster than their congeners with low K_{oa} in VO is still unclear.

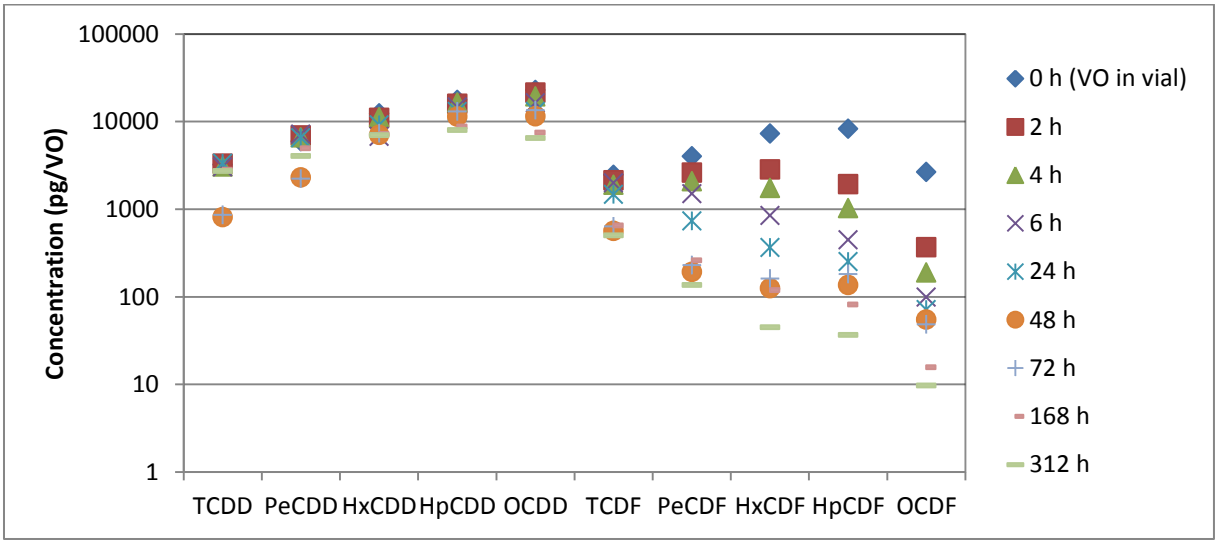

Fig.2.5.2: PCDD/F release after 2h, 4h, 6h, 24h, 48h, 72h, 168h and 312h in VO in air. The release increases with the degree of chlorination of PCDD/F compounds. TCDD: 2,3,7,8-Tetrachlorodibenzo-p-dioxin; PeCDD: 1,2,3,7,8-Pentachlorodibenzo-p-dioxin; HxCDD:1,2,3,4,7,8-Hexachlorodibenzo-p-dioxin, 1,2,3,6,7,8-Hexachlorodibenzo-p-dioxin and 1,2,3,7,8,9-Hexachlorodibenzo-p-dioxin; HpCDD: 1,2,3,4,6,7,8-Heptachlorodibenzo-p-dioxin. TCDF: 2,3,7,8-Tetrachlorodibenzofuran; PeCDF: 1,2,3,7,8-Pentachlorodibenzofuran and 2,3,4,7,8-Pentachlorodibenzofuran; HxCDF: 1,2,3,4,7,8-Hexachlorodibenzofuran, 1,2,3,6,7,8-Hexachlorodibenzofuran, 1,2,3,7,8,9-Hexachlorodibenzofuran and 2,3,4,6,7,8-Hexachlorodibenzofuran; HpCDF: 1,2,3,4,6,7,8-Heptachlorodibenzofuran and 1,2,3,4,7,8,9-Heptachlorodibenzofuran (Appendix Table1)

Counter to the atmospheric pattern of PCDD/F, an uptake of PCB into VO was observed (Fig.2.5.3). This absorption may be due to the fact that the PCB amounts spiked in the VO were not sufficient enough to reach the equilibrium as its accumulation capacity was not attained. At the end of the exposure period, the results reveal an uptake of PCB #28, PCB#52, exceeding six times the initial amount. Hence, after 312h of deployment, PCB#28 and PCB#52, sequestered in VO, ranged from 896 pg/sample to 2585 pg/sample and from 698 pg/sample to 4300 pg/sample respectively. PCB#101 followed, with an increased amount ranging from 1612 pg/sample to 2751pg/sample. The higher chlorinated compounds were more or less stable during this experiment. According to German study, PCB congeners with a low degree of chlorination were dominant in gas phase, whereas those with a high degree dominated in aerosols (WHO, 1993). This fact could explain the uptake amount of PCB#28, PCB #51 and PCB 101 in the VO during this experiment.

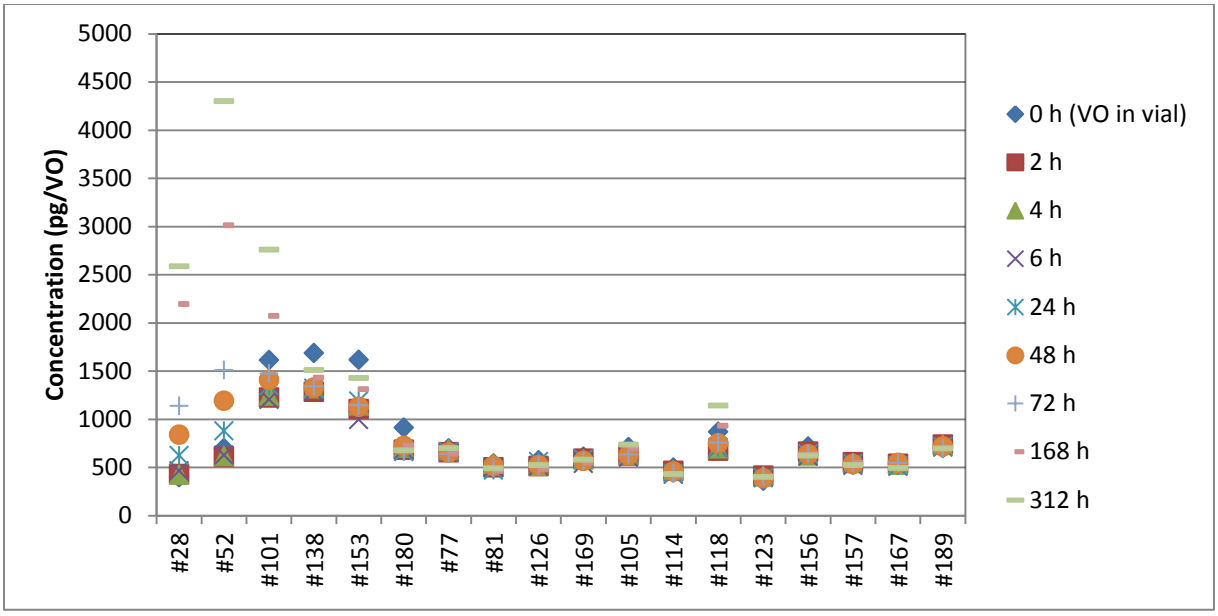

Fig.2.5.3: PCB uptake after 2h, 4h, 6h, 24h, 48h, 72h, 168h and 312h in VO in air. The uptake is detected for PCB#28, PCB#52 and PCB#101. The higher chlorinated compounds didn't present a significant uptake (Appendix Table 4)

VO inserted a glass vial and exposed in air

Similar to the VO in air, release of OCDD and PCDF are observed in a VO inserted in a glass vial and exposed to air (Fig.2.5.4). At the end of the exposure period, OCDD showed a decrease of 35% and PCDF up to 98 %. Possible explanations of this result could be that the glass vials were not hermitically sealed and so allowed an exchange between volatile pollutants in air and the VO. These samples are usually used as a field blank, a quality control step intended for detection of any potential contamination that could be introduced into the process through sample handling. It has been assumed that the VO loaded with PCDD/F has reached their saturation limit. Therefore, the exposure of the device in air sampled in the vial may have generated the release of OCDD and PCDF.

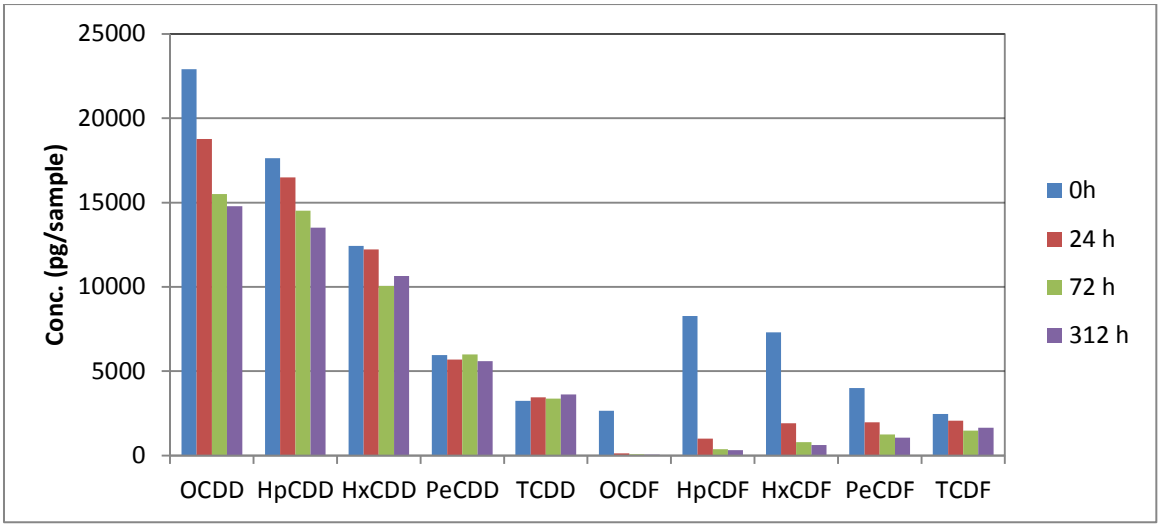

Fig.2.5.4: PCDD/F release after 2h, 24h, 72h and 312h in VO in a glass vial. The release in PCDD is significant for OCDD only, while in PCDF, steepest release is present for HpCDF, HxCDF and PeCDF (Appendix Table 2).

The experiment shows no uptake of PCB detected in the VO inserted in a glass vial (Fig.2.5.5). This settlement can be explained by the fact that the level of PCB in the air sampled in the vial was not significant enough to allow an uptake into the passive sampler. Surprisingly, a decrease of PCB after 24h of some PCB compounds was observed. This may probably be due to the high value of uncertainty during the estimation of PCB concentration.

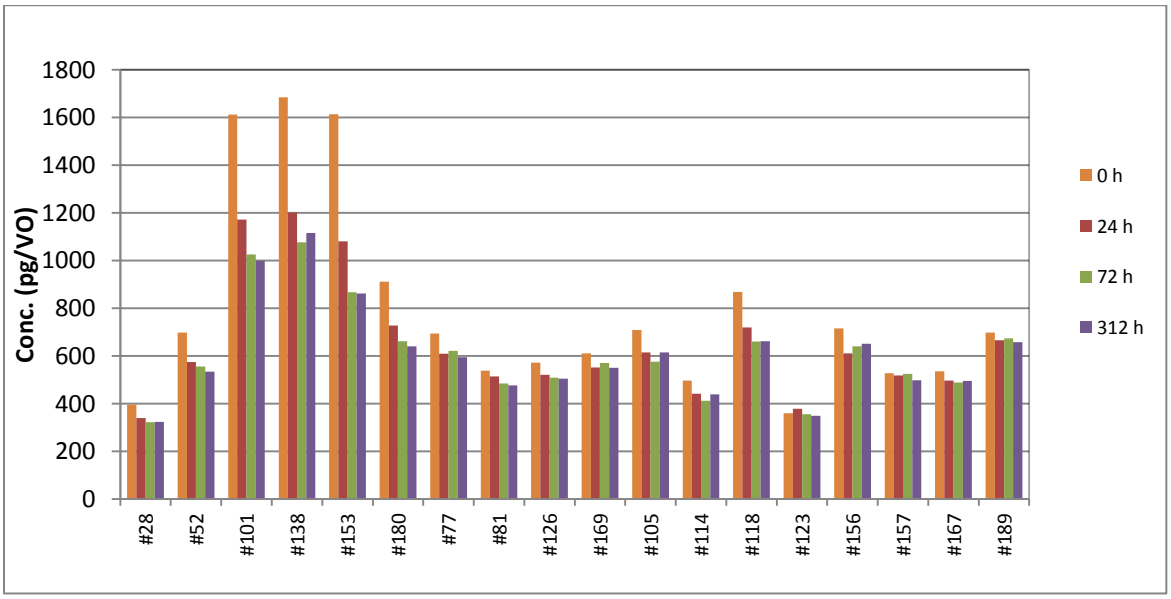

Fig.2.5.5: PCB uptake after 2h, 24h, 72h and 312h in VO in a glass vial. No uptake of PCB is detected during exposure period (Appendix Table 5)

VO frozen from -30 °C to -80 °C

Booij et al. (2003b) suggest that the sampling rate of VO decreases with temperature. The results observed in this study confirm this assessment. There is no detected PCDD/F release (Fig. 2.5.6) and no detected PCB uptake (Fig. 2.5.7) in VO frozen from -30 °C to -80 °C. At low temperatures, the fugacity capacity of the compounds was stabilized so that no significant exchanged amounts were detected. Moreover, there was a long period between the end of the trial and the laboratory analysis. During this storage period when the VO was frozen at -80 °C, the absorbed contaminant amounts were not affected.

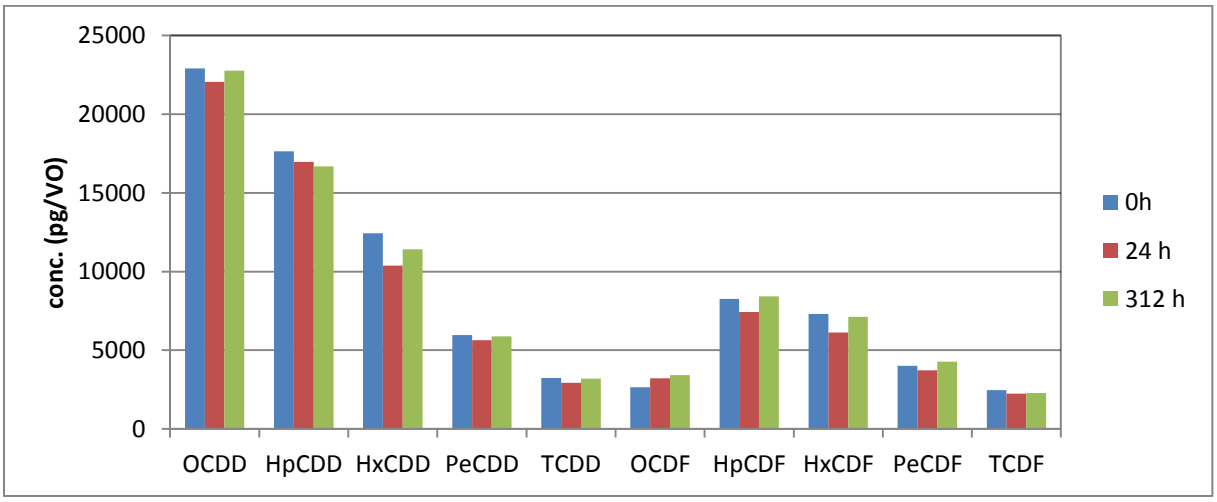

Fig. 2.5.6: Release of PCDD/F from loaded VO kept in the fridge and frozen from -30°c to -80°C during 0h, 24h and 312h. No release was detected (Appendix Table 3)

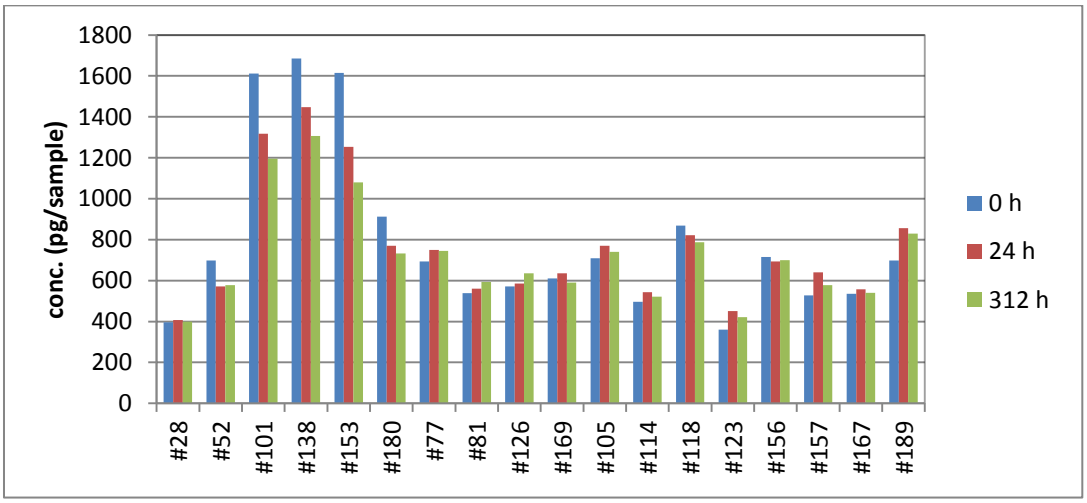

Fig. 2.5.7: Uptake of PCB from loaded VO, kept in the fridge and frozen from -30°c to -80°C during 0h, 24h and 312h. No uptake detected (Appendix Table 6)

2.5.3 Specific conclusion

The atmospheric pattern of PCDD/F in this study indicates the predominance of the higher chlorinated species in gas phase and the lower chlorinated ones in particle deposition. The PCDD/F compounds with low K_{oa} were sequestered preferentially in the VO. This contradicted the behaviour of other compounds such as PCB, where a lower K_{oa} mean higher uptake capacities in VO. The reason for this difference is still not clear. It should also be noted that the results of PCDD/F in VO exposed in air have been referred to as "release", although it is not known whether the compounds were truly released or remained associated with particles adhered to the VO's surface. However, the physico-chemical properties of PCDD/F and PCB differ widely between homologue groups and congeners, and are still quite uncertain due to difficulties in their determination (Mackay and Paterson, 1991) The use of PCB as PRC is clearly inappropriate for the estimation of PCDD/F concentration. Storage at -80°C stabilizes the organic pollutant compounds activities in VO.

2.6 Test of ^{14}C-OCDD in VO

An exposure experiment with ^{14}C-OCDD was performed to give us further information about the transport fate of a high chlorinated compound of the PCDD/F group, enclosed and exposed in VO to air. This trial is the supplementary of the PCB and dioxin experiment (cf 2.5.). OCDD despite its high *MW*, often decreased rapidly in concentration in VO when under outdoor conditions. The radioactive compound may give useful information as to whether OCDD is truly released to the atmosphere or disappears as a detectable chemical individual by other mechanisms, e.g. stocked in VO strongly associated with triolein or LPDE.

2.6.1 Sampling sites and experimental

On the initial day of exposure, the VO were taken out of the freezer and warmed up to room temperature inside their storage glasses. A number of VO were kept in the freezer as the t_0 controls and for every exposure time period, 3 VO were randomly and cautiously taken out of their glasses and mounted onto stainless steel frames specially designed for VO exposure to air. The frames were hung into the upper part of a fume hood (Fig.2.6.1). Another 3 VO for every exposure time period were kept inside their glasses and stored in the same hood as references for the same time period (Fig 2.6.2). The surface of the VO on the frames was regularly checked for released radioactivity, but with negative results. The sliding front window of the fume hood was closed to about three quarters of the maximum opening during exposure. At the time of sampling, the three corresponding VO were removed from the frame

and encased again in their original glasses which, together with the three samples which had been kept enclosed, were stored at -80°C until analysed.

Fig. 2.6.1: Close up view of SPMD on frames.

Fig. 2.6.2: Fume hood with exposed SPMD on frames and reference samples in glasses.

2.6.2 Results and discussions

The percentage of recovery of radioactivity was stable during 16 days of exposure time in both VO exposed in air and in a glass vial (Fig. 2.6.3). These results indicated that no losses of ^{14}C-OCDD to the atmosphere had occurred. The statement contradicts our previous studies,

where OCDD, the most chlorinated PCDD congener, quickly reduced in concentration while the lowest molecular weight PCB were stable in VO (cf. 2.5). Studies have demonstrated that the passive sampler was able to sample particles associated with vapour phase (Lohmann et al., 2001). The recovery of radioactivity alone, however, is not a proof of the chemical integrity of the labelled compound, although chemical interactions of OCDD with e.g. triolein, retaining the radioactive labelling in reaction products, seem to be very unlikely due to the very low reactivity of the mother compound.

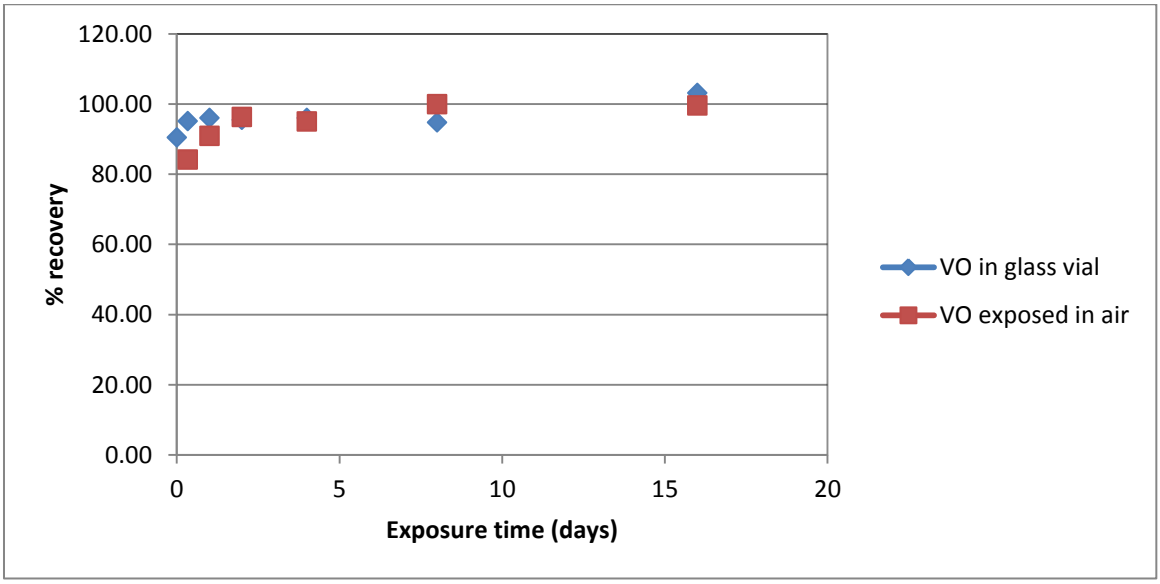

Fig. 2.6.3: Recovery of ^{14}C-OCDD in VO after 16 days of deployment

..

Table 2.6.1 Total ^{14}C OCDD radioactivity DPM measured in the scintillation counter, in GC/MS sample and in PCDD/F clean-up of the rest-sample with LPDE-tubing

Sample	Total measured DPM activity triolein + membrane (a)	Total activity measured in the scintillation counter (b)	Activity measured in GC/MS-sample (c)	Activity in the rest-sample stored in freezer (d)	Total activity measured in LPDE-tubing (e)	Residue in LPDE-tubing (f)	Activity measured in Eluate after first extraction (g)	Activity measured in Eluate from *Sc*+*Cc* (h)	Activity measured in eluate from *Cc* (i)	Activity measured in *Sc* and *Cc* (j)	Activity measured in Alox column (k)	Activity measured in the bulb (l)	Total activity from rest sample (m)	Total activity measured in VO (n)
907236	52552	26500	15403	10649	1009	842	4945	2386	22	2256	342		10793	52696
1107078	52319	29275	15631	7413	1776	1722	3487	455			41		5705	50611
1107068	55942	8253		47689	1031	782	47689						48471	56724
1107075	53802	25745	13183	14874	1232	663	4598	3891		2220	1095	157	12624	51552
1107076/1	50760	1523	1724	43958	1324	805	34201	4					35010	38257
1107076/2		1292	2263					430	28	491	1197		2146	5701
1107077	52665	1674	19489	31502	1300	1300	31502						32802	53965
1107069	28948	1062	11626	16260	1300	1300	16260						17560	30248
Total	346988	95324	79319	172345	8972	7414	142682							

***Sc*: Sandwich Column, *Cc*: Carbon Column**

m= f+g+h+i+j+k+l; d= a-(b+c); n=m+b-c

Some samples were used for the measure of ^{14}C-OCDD radioactivity in GC/MS analysis and in PCDD/F clean up, to check whether or not these processes could be the cause of OCDD degradation. The PCDD/F clean up procedure (see chapter 1.4.3) reveals neglected radioactivity value in the sandwich column, carbon column and Alox column after elution (Table 2.6.1). No radioactivity in eluate Ols F1 was detected. The total activity from the rest sample (m) and the deduced activity in the rest-sample (d) presented similar radioactivity values. Moreover, the total calculated activity in the VO (n) and the total measured activity in the VO (a) presented similar values. The similarities between (m) and (d) and between (n) and (a) confirm the reliability of the PCDD/F clean-up process. GC/MS analysis and PCDD/F clean up procedure supported the assumption that OCDD did not undergo chemical degradation depending on time during this experiment. So, compared with the Stevenson box experiment, different findings still remain unresolved.

Furthermore, previous studies have demonstrated that organic compounds in VO can also be accumulated in the membrane (Gale, 1998) The measure of ^{14}C radioactivity DPM in LPDE-tubing has revealed values from 1009 at 0 day to 1776 DPM (Appendix Table 14) at 16 days, which were low compared to the total values of around 30248-56724 DPM per VO (Table 2.6.1). Nevertheless, the results were consistent with Rantalainen et al. (2000) reporting that the molecule breadths of some PCDD/F can be larger than the maximal transient pore diameter in the VO membrane (< 10 Å) so that they may be impeded in transport through LPDE.

The results revealed the insufficiency of the VO to accumulate PCDD/F compounds, but so far, several studies have proved the performance of VO in monitoring dioxin in comparison with other passive samplers such as the spruce needles (Zhu et al., 2007).

The use of a VO for monitoring PCDD/F and their uses as PRC are still a big issue that needs to be elucidated in future researches. This clarification can open a new aspect concerning the theory of the isotropic exchange kinetic in VO.

2.6.3 Specific conclusion

VO may be able to sample PCDD/F from the atmosphere (Rantalainen et al., 2000; Lohmann et al., 2001) only if the uptake rate is calibrated for the compounds of interest. High chlorinated PCDD/F compounds can mainly be strongly bounded with triolein or LPDE in VO, causing the decrease in its concentration. However, the reason for losses of dioxins in the device in some experiment is still unclear and could not be clarified by the ^{14}C-OCDD

experiment. An abnormal decrease of high chlorinated PCDD/F compounds in VO may suggest that the device cannot be reliably used for the quantification of PCDD/F, but rather as an initial screening tool.

3 Chapter III: Theory for estimation of analyte water concentration in VO

SPMD are passive samplers used for integrative measurements of dissolved persistent organic pollutants POP and PAH in multiple media (Huckins et al., 1990; Petty et al., 1993; Söderström and Bergqvist, 2003). The sampling in SPMD is realized by physical absorption on the membrane, then diffusion through the membrane and absorption into the enclosed layer of the neutral lipid triolein. Hence, the uptake depends on the boundary layer at the exposed medium interface, on a biofilm at the exterior membrane surface and on the membrane. This polymeric membrane with a maximal passage dimension of approximatively 10Å restricts the passage of compounds with higher molecular dimensions. Previous studies have used SPMD for the investigations of polycyclic aromatic hydrocarbons PAH (Lebo J.A, 1992; Crunkilton and DeVita, 1997), polychlorinated biphenyls (PCB), dioxins (Prest et al., 1992; Rantalainen et al., 2000; Roach et al., 2009) organochlorine pesticides (OCP) (Verweij et al., 2004).

It has been demonstrated that environmental conditions affected the sampling rate of SPMD during the sampling procedure (Vrana and Schüürmann, 2002). Furthermore, Huckins et al, 1999 and Booij et al., 1998 suggested that the uptake rate of compounds with log K_{ow} > 4.4, such as PAH, OCP, PCB and chlorinated dioxins and furans is controlled by the water boundary layer only. The water boundary layer (WBL) is a thin hydrodynamically complex area between the passive sampler membrane and the water body, where molecular diffusion dominates mass transfer. The WBL resistance depends on the water flow rate. Temperature, biofouling, turbulence or wind-speed influence the thickness of this boundary layer and thereby affect the SPMD sampling rate. Augulyte and Bergqvist (2007) have investigated the monitoring of high hydrophobic compounds with SPMD and came to the conclusion that fouling, such as sludge particles, fat and salt particles can influence the thickness of the water boundary layer (WBL) on the surface of the SPMD membranes, which in turn can affect the uptake rate of high molecular weight compounds with high log $K_{ow.}$ Quantitative measurements with SPMD need the value of the sampling rate. However, the field sampling conditions can be difficult to replicate and maintain over extended periods, making it complicated to generate precalibrated sampling rate values that reflect the true sampling situation. Moreover, calibrating the SPMD prior to use require tests of many different sampling conditions for a number of compounds. Huckins et al. proposed the use of performance reference compounds, PRC, to calibrate the SPMD sampling rate in situ and thereby assess the actual water sampling situation by predicting the site effects of hydrodynamics, temperature, and biofouling (Huckins et al., 1993). PRC theory states that the

release rates of these compounds are related to the uptake rates of the native sampled compounds and PRC appear to be able to assess the difference between temperature and hydrodynamics during sampling period (Huckins et al., 2002a). The calculation method of Huckins consisted of an extrapolation of the sampling rate of analytes $Rs_{analyte}$ *(H)* with values derived from laboratory calibration studies and a chosen PRC limited to a criterion of arbitrary values from 20 to 80% losses to minimize propagation of errors from subtracting two large numbers. Liu et al. (2013) suggest that different mechanisms may occur during the exchange rate between the target analyte and PRC, thus leading to an inaccurate concentration value of the affected compound. Tomaszewski and Luthy (2008) referred to the Huckins method and used a single PRC to investigate a suite of PCB with a passive sampler Polyethylene (PE) in pore water, and came to the conclusion that after 28 days of deployment, this approach matched field-measured uptake rates for most congeners but tended to underestimate uptake rates for higher molecular weight compounds. Booij and Smedes (2010) used the nonlinear squares (NLS) methods to estimate sampling rates of all PRC compounds without discrimination, but the occurrence of matrix interferences can affect results in the NLS analysis, especially for very high hydrophobic compounds. Thus, a large number of PRC may need to be used to ensure that measured sampling rates are appropriate for the exchange rate, which is also influenced by the membrane and the boundary layer .In this work, an alternative method is presented using in situ data from sixteen ^{13}C-PAH-PRC with 3.4 > log K_{ow} < 6.5 and four PCB-PRC 5.9 > log K_{ow} < 7.2 to infer key mass transfer properties. The method was achieved by applying it to VO during sampling campaigns in the Yangtze River (China) 2011. Water concentrations of sixteens native PAH were deduced from the alternative method and compare with the results to concentrations measured from Huckins method.

3.1 Theories

Huckins et al. (2002b) and Booij et al. (2007b) provide different modelling approaches for water media, in which uptake rates of the target analyte in SPMD are governed by the aqueous boundary layer under low flow conditions for solutes in the log K_{ow} range from 4.4 to 8.0. The analyte sampling rate is then estimated using laboratory calibration data and PRC. The kinetic models developed in this study allow the estimation of analyte sampling rate, using only in situ PRC-based sampling rate and not taking uptake rate limiting into account.

3.1.1 Huckins theory

PRC method proposed by Huckins et al. (2006b) has been widely used for the quantification of hydrophobic organic contaminant in the freely dissolved phase in water (Gourlay-Francé et al., 2008). This method involves spiking of PRC, such as ^{13}C-PAH or PCB that are not found in the environment, into the receiving phases of SPMD before exposure. The release of these compounds follows the same mass transfer principles as the uptake of contaminants, and the passive sampler exhibit first order isotropic exchange kinetics. Both of these observations allow for the adjustment of observed differences in uptake between sampling sites and between field exposure and laboratory calibration studies. Thus, the field sampling rate $Rs_{,PRC}$ in VO calculation from Eqn.1.5 showed an increase of $Rs_{,PRC}$ values with increase log K_{ow}, while the empirical model suggested by Huckins presented Rs values as relatively constant (Fig. 3.1.1). Huckins assumes that the exchange kinetic is only controlled by the WBL and there is a lack of correlation between linear flow velocity and $Rs_{,PRC}$ values. An empirical model to extrapolate PRC-based sampling rates is then proposed using the Booij equation (Booij et al., 2003a; Booij et al., 2003b). This equation relies on theoretical considerations and on the observation that accounting for sorption to DOC may bridge the gap between theory and experimental sampling rates (Huckins et al., 2006a).

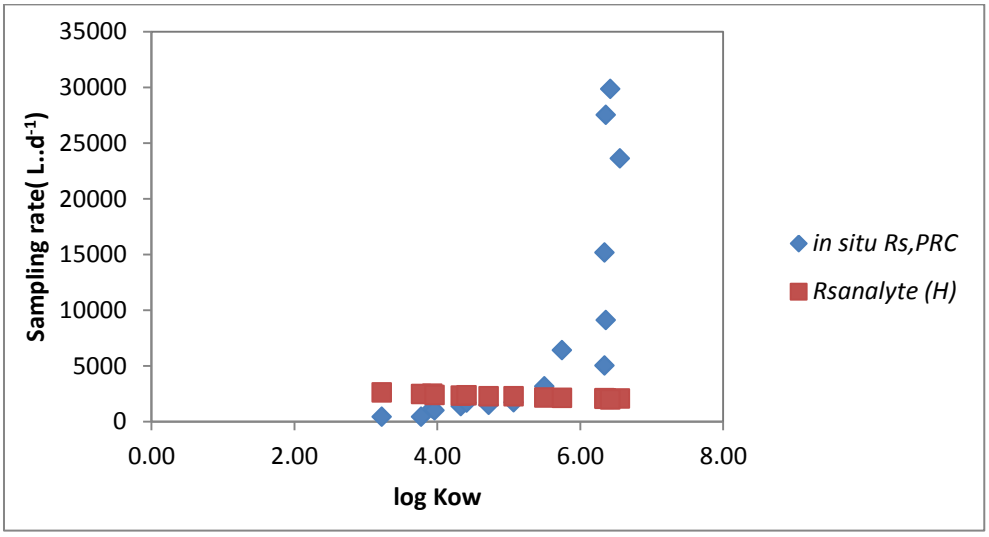

Fig 3.1.1: Comparison of in situ sampling rates $Rs_{,PRC}$ (Eqn.1.5) and Huckins sampling rate $Rs_{analyte}$ *(H)* (Eqn.3.1) in VO as a function of log K_{ow} at 15±4 °C. Both sampling rate were estimated using release values of PRC compounds from previous studies (see chapter 2.2) (Appendix Table 13).

The equation of analyte sampling rate $Rs_{analyte}$ *(H)* proposed by Huckins is applied when the exchange kinetic is under the WBL control and determined using experimental values as following:

$$Rs_{analyte}(H) = Rs,_{PRC} \cdot (\frac{Vm,_{PRC}}{Vm})^{0.39} \qquad \text{Eqn.3.1}$$

$Vm,_{PRC}$ is the LeBas molar volume of the selected PRC, *Vm* is the molar volume of the target analyte and $Rs,_{PRC}$ (L/day) is the in situ PRC-based sampling rate from Eqn.1.5

Analytes sequestered by the VO may be in the linear uptake (integrative) sampling, curvilinear, or equilibrium partitioning sampling phases. A model to calculate the water concentration was introduced regardless of whether the analyte's uptake was in a linear, curvilinear, or equilibrium phase, together in combination with $Rs_{analyte}$, K_{VO_W} and N_{VO}, the absorbed amount of organic compound after exposure time (Huckins et al. (2006b)

$$C_W = \frac{N_{VO}}{V_S \cdot K_{VO\_W}(1 - \exp(-\frac{R_{Sanalyte} \cdot t}{V_S \cdot K_{VO\_W}})} \qquad \text{Eqn.3.2}$$

3.1.2 Booij theory

To improve the estimation of $Rs_{analyte}$ *(H)*, Booij et al.2010 established the un-weighted non-linear least squares (NLS), a non-linear regression model where all PRC data can be used. Hence, by considering f as a continuous function of K_{VO_W} (L.kg^{-1}) with $Rs,_{PRC}$ as an adjustable parameter:

$$f = \exp(-\frac{Bt}{K_{VO\_W} M^{0.47} m}) \qquad \text{Eqn.3.3}$$

Where *B* is constant, t is the exposure time (days), *M* is the molecular weight (g.mol^{-1}) and *m* is the mass of the sampler (kg).

The estimation of Booij analyte sampling rate $Rs_{analyte}$ is given by:

$$Rs_{analyte} = \frac{B}{MW^{0.47}} \qquad \text{Eqn.3.4}$$

B can be used to estimate the analyte sampling rate Rs^{300} with molecular weight (*MW*) of 300 g/mol(Booij and Smedes, 2010)

The application of this method guarantees the estimation of sampling rates without criterion of selection, but some studies revealed the dependence of this model for PRC in the transition range.

3.2 New theory

The alternative method is based on the use of all in situ PRC data, including those whose remaining PRC concentration are close to the limit of detection LOD and those whose PRC are non-depleted. To allow this approach to proceed, uncertainties are modelled using blank PRC data. The Student-t distribution is used to obtain confidence limits for measurement uncertainty. Replicated VO-field blanks were measured to obtain a standard deviation that could be used directly as the standard analytical uncertainty. The uncertainty values were used to estimate the minimal sample rate R_{min}. Efforts to reduce bias and variability can be improved by increasing the number of blank samples. R_{min} was applied as the new values of PRC sampling rate $Rs,_{PRC}(N)$ if a direct measurement was not obtainable.

Twelve replicated VO-field blanks produced during sampling campaigns in 2011 together with the samples deployed in twelve different sampling sites along Three Gorges Reservoir (TGR) were used in this study. The VO-field blanks consisted of loaded samplers taken to and from the field with other VO but never removed from their airtight vials. These blanks were prepared and analysed simultaneously in the same manner as the deployed samplers to determine whether contamination or losses occurred during the VO loading, transport or analysis. A normal distribution for the results can be assumed because the PRC concentrations can be determined well in cases of minor or no losses.

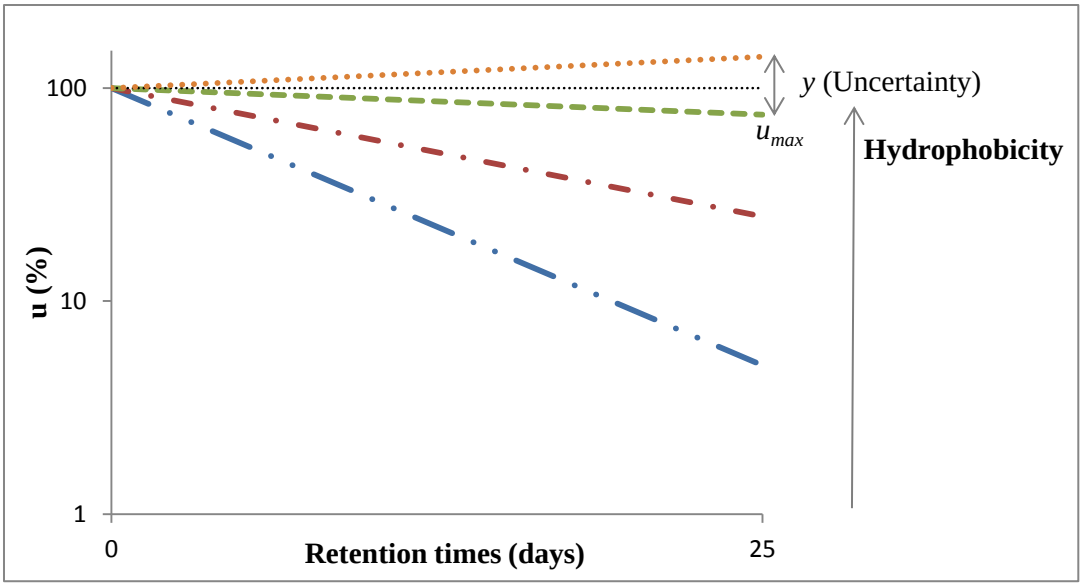

Fig.3.2.1: Schema representing uncertainty field of dissipated PRC values (u) during exposure times. u_{max} is the largest possible deviation from the average dissipation ū of a PRC which does not exhibit significant dissipation after a certain sampling period. u_{max} can be used to estimate the minimal possible sampling rate for such compounds.

For each PRC, the standard deviation was calculated from obtained retained PRC values of the blank samples. The obtained values u_o of a blank sample were first normalized in percentage *%u* according to the expected values u_w, following this equation (Fig.3.2.1):

$$\%u = \frac{u_o}{u_w} \cdot 100 \quad \% \qquad \text{Eqn.3.4}$$

Then the standard deviation *Sn*(%) was obtained by following the equation:

$$Sn(\%) = \sqrt{\frac{\sum_{i=1}^{n} (\%u_i - \%\bar{u})^2}{n-1}} \qquad \text{Eqn.3.5}$$

$\%u_i$, are the obtained values in percent for the blank sample *i; ū* is the sample mean of the obtained values and *n* is the number of blank samples used for the measurements.

The coefficient of variation *CV* (%) is calculated as following:

$$CV(\%) = \frac{S_n}{\%\bar{u}} \times 100 \qquad \text{Eqn.3.6}$$

The standard error S_{CV} of the coefficient of variation is calculated as:

$$S_{CV} = \frac{CV}{\sqrt{2n}} \qquad \text{Eqn.3.7}$$

The uncertainty (y) of the VO-field blanks is then:

$$y = CV \pm t_{\alpha,\nu} S_{CV} \qquad \text{Eqn.3.8}$$

Where $t_{\alpha,\nu}$ is the critical value of Student's t for the chosen α level and for ν= n-1 degrees of freedom. The analysis is based on the best measurement capability. The uncertainty value (y=CV-$t_{\alpha,\nu}$ S_{CV}) is used to obtain the maximal retained PRC concentration after exposure time:

$$u_{\max} = 100 - y, \qquad \text{Eqn.3.9}$$

u_{max} is used to determinate the maximum elimination rate ke_{max}

$$ke_{\max} = -\frac{\ln(u_{\max} / u_0)}{t} \qquad \text{Eqn.3.10}$$

The minimal expected sampling rate (Rs_{min}) is thereby deduced.

$$R_{S\min} = VsK_{VO\_W} ke_{\max} \qquad \text{Eqn.3.11}$$

Rs_{min} is used to adjust Rs_{PRC} (Eq.1.3) to $Rs_{,PRC}(N)$. The *in situ* sampling rate of PRC $Rs_{,PRC}(N)$ represents the *in situ* sampling rate of target compound $Rs_{analyte}$ (N) with similar physicochemical properties

A relation between $Rs_{,PRC}(N)$ and log K_{ow} was applied to estimate the sampling rate of various organic pollutants $Rs_{analyte}$ (N) and was presented as an exponential function form with a correlation coefficient R^2 > 0.75. The sampling rates among studies appeared shift by relatively constant factors *a* and *b*. A fitted model relation in this field condition was given as:

$$R_{Sanalyte}(N) = ae^{blogK_{ow}} \qquad \text{Eqn.3.12}$$

Where *a* and *b* are constants for a given exposure, but may vary among exposures according to differences in hydrodynamical conditions and sampler geometry.

3.2.1 New theory application

The method was tested by applying it to VO impregnated with the sixteen PAH-PRC and four PCB-PRC, which were inserted in twelves different sampling sites along the Three Gorges Reservoir (TGR) during sampling campaign in 2011. The information of the different sampling sites and the exposure time during sampling campaign in 2011 are presented in chapter II (2.2.1). The different sampling sites included: 1. Maoping (MP); 2. Guojiaba (GJ); 3. Badong I (BD1); 4. Badong II (BD2); 5. Daning I (DN1); 6.Daning II (DN2); 7. Fengxi (FJ); 8.Xiaojang I (XJ1); 9. Xiaojang II (XJ2); 10.Wanzhou (WZ); 11. Changshou (CS); 12. Chongqing (CQ).

Under the null hypothesis, which suggests that the blank sample values of biased estimate coefficient of variation were equal to zero, the calculation of T-criterion $t_{\alpha,v}$ was 4.9. This value is larger than the critical value of a student's t distribution k= 2.201 for α=0.05, ν=11 degrees of freedom and 95% confidence interval. Thus, the null hypothesis is rejected and the biased estimate of blank samples coefficient of variation is concluded larger than zero. Uncertainty values (Eq.3.8) of each individual PRC are given at 95% level of confidence interval. These values provide the maximum retained PRC in the blank VO sample ($u_{max)}$ that lead to a minimum sampling rate Rs_{min}. Rs_{min} of each sampling sites was estimated using Eq.3.11 (Table 3.2.1). The Rs_{min} values ranged from 0.004 L.d^{-1} for naphthalene to 24.75 L.d-1 for PCB#159 and were used to obtain the determinable value of $Rs_{,PRC(N)}$.(Appendix Table 15)

Table 3.2.1: Rs_{min} of ^{13}C-PRC-PAH and -PCB are estimated after a deployment time of 26 days in Maoping. The uncertainty (%) is used to obtain the maximal dissipation rate capacity ke_{max}. Log K_{ow} values of unlabeled PAH and PCB from Huckins et al. (2004).

PRC-PAH	**log Kow**	**Sn**	**ū**	**CV(%)**	**S_{CV}**	**$t\alpha,\nu\ S_{CV}$**	**CV- $t\alpha\nu S_{CV}$**	**u, max**	**ke,max**	**Rs,min**
	-	**%**	**%**	**%**	**%**	**%**	**%**	**%**	**d^{-1}**	**$L.d^{-1}$**
Naphthalene-$^{13}C_6$	3.38	6	96	6	1.32	2.90	3.56	96	0.001	0.004
Acenaphthylene-$^{13}C_6$	4.07	8	96	9	1.78	3.91	4.79	95	0.002	0.026
Acenaphthene-$^{13}C_6$	3.92	11	101	10	2.14	4.70	5.76	94	0.002	0.022
Fluorene-$^{13}C_6$	4.1	10	104	10	1.96	4.31	5.29	95	0.002	0.030
Phenanthrene-$^{13}C_6$	4.46	8	92	9	1.80	3.96	4.86	95	0.002	0.066
Anthracene-$^{13}C_6$	4.54	14	109	13	2.56	5.64	6.91	93	0.003	0.117
Fluoranthene-$^{13}C_6$	4.84	3	93	4	0.73	1.61	1.98	98	0.001	0.070
Pyrene-$^{13}C_3$	5.18	4	95	4	0.80	1.76	2.15	98	0.001	0.194
Benzo(a)anthracene- $^{13}C_6$	5.6	8	98	9	1.76	3.87	4.74	95	0.002	0.911
Chrysene-$^{13}C_6$	5.84	8	100	8	1.61	3.54	4.34	96	0.002	1.451
Benzo(b)fluoranthene-$^{13}C_6$	6.44	8	98	8	1.68	3.69	4.52	95	0.002	6.129
Benzo(k)fluoranthene-$^{13}C_6$	6.44	8	97	8	1.61	3.53	4.33	96	0.002	6.189
Benzo(a)pyrene-$^{13}C_4$	6.42	9	98	9	1.83	4.02	4.92	95	0.002	6.385
Indeno(1,2,3-cd)pyrene-$^{13}C_6$	6.42	8	91	8	1.68	3.70	4.53	95	0.002	6.015
Benzo(g,h,i)perylene-$^{13}C_{12}$	6.63	4	34	12	2.53	5.57	6.83	93	0.003	14.310
Dibenzo(a,h)anthracene-$^{13}C_6$	6.5	9	94	10	1.99	4.37	5.36	95	0.002	8.418
PRC-PCB										
$^{13}C_{12}$-PCB#37	5.83	37	96	38	10.96	28.16	9.80	90	0.004	1.159
$^{13}C_{12}$-PCB #60	6.11	26	58	44	12.77	32.81	11.41	89	0.005	3.012
$^{13}C_{12}$-PCB #127	6.95	17	61	28	8.10	20.81	7.24	93	0.003	25.982
$^{13}C_{12}$-PCB #159	7.24	11	52	21	6.15	15.80	5.50	95	0.002	46.779

The PRC sampling rate $Rs,_{PRC}(N)$ was deduced as native sampling rates $Rs,_{PAH}(N)$ and $Rs,_{PCB}(N)$ and the results were summarized in Table 3.2.2. Naphtalene presented the lowest $Rs,_{PAH}(N)$ with 0.67 L.d-1 and DahA, the highest with 151.52 L.d-1. The reason for this discrepancy could be the result of the difference of exposure conditions at the various sampling sites. The dissipation of most PRC-PCB was insignificant and so the value was replaced with $Rs_{min.}$ $Rs,_{PAH}(N)$ increment for high hydrophobic compounds was observed at each sampling site regardless of the physical conditions. The contrast of the exchange kinetic

between moderate and high hydrophobic PRC into VO may be caused by a potential perturbation during molecule transport or by dissimilarity affinities to the LPDE membrane between PRC and the target analyte, so that the resistance was controlled by the membrane instead of WBL, according to Huckins theory. This suggestion is consistent with a previous study (Luellen and Shea, 2002) seemingly disbelieving towards the assumption that the WBL checking for high hydrophobic compounds during transportation. Furthermore previous studies suggested that the membrane permeability limitation should be a factor for high hydrophobic PAH with a dimension ≥ 10 Å, which is more than the maximal pore diameter of the LPDE (Meadows et al., 1998; Rusina et al., 2010). The prediction of various compounds with high log K_{ow} would be then impossible with only one PRC, as some of these compounds can only pass through the pore diameter of LPDE in one of its dimensions.

Many chemical factors have a significant influence on the uptake kinetics of high log K_{ow} into VO. Lipophilic compounds are preferentially accumulated to DOC in water columns and the main chemical characteristic of these compounds that contributes to the association with DOC is their hydrophobicity. Therefore, the hydrophobicity conversely increases with the uptake rate of the compound into the VO (Meadows et al., 1998). This chemical aspect can strongly affect the resistance of the WBL to mass transfer. Furthermore, the salinity can also affect the uptake amounts of high hydrophobic compounds and can cause a bias of the result even if only one PRC compound is used. Brown and Weiss (1978) demonstrated that water quality variables, such as salinity can affect the dissolved concentrations of hydrophobic compounds in environmental waters, and studies have shown that the salinity in some places of the water resources areas in the Yangtze River, during periods in dry season, could exceed the standard (0.25‰) with a salinity value greater than 0.48‰ (Baodong et al., 1999; HSU et al., 1999; An et al., 2009).

A relationship between $Rs_{,PRC}(N)$ and log K_{ow} was established for each sampling site (Fig. 3.2.2) to allow the estimation of $Rs_{analyte}\ (N)$ of compounds with moderate and high hydrophobicity. Hence $Rs_{analyte}\ (N)$ can be calculated from the in situ PRC sampling rate independently from the resistance to the mass transfer across the VO membrane. A strong correlation (R^2>0.75) was found between log K_{ow} and $Rs_{PRC}(N)$

Table 3.2.2: The sampling rate of fifteen PAH $Rs_{,PAH}(N)$ values (L d^{-1}) and four PCB $Rs_{,PCB}(N)$ with log K_{ow} ranging from 3.38 to 7.24 at twelve different sites across the Three Gorges Reservoir using improved model refers to section 3.2. Estimated values of some compounds fail because their analogue PRC was having entirely dissipated during the 26 days of deployment. In situ sampling rates were replaced by the Rs_{min} if they presented negative values (red values).

PRC-PAs	Maoping	Guojiaba	Xiangxi I	Xiangxi II	Daning I	Daning II	Fendji	Xiaojiang I	Xiaojiang II	Wanzhou	Changshou	Chongqing
Naphthalene-13C6	0.67		0.73	0.73								0.73
Acenaphthylene-13C6	1.71	3.04	2.45	2.74			3.04	3.07	2.96	2.03	1.65	3.11
Acenaphthene-13C6	0.74	1.54	1.17	1.15		1.43				0.98	1.08	1.31
Fluorene-13C6	1.09	2.03	2.10	2.58	2.57	2.96	2.37	2.41	2.37	1.52	1.99	3.03
Phenanthrene-13C6	1.46	2.15	2.42	2.87	3.08	3.05	2.89	2.93	2.94	1.83	2.24	6.20
Anthracene-13C6	1.58	2.31	2.51	2.97	3.27	3.18	3.19	3.22	3.25	2.03	2.41	7.91
Fluoranthene-13C6	1.12	2.04	1.40	1.59	1.71	1.36	1.63	1.47	1.46	1.66	1.09	6.63
Pyrene-13C3	1.76	2.45	4.14	2.74	2.76	3.54	2.93	2.92	2.76	2.43	2.20	2.23
Benzo(a)anthracene- 13C6	4.57	3.02	3.25	2.75	3.25	5.92	4.06	4.91	4.92	4.95	4.95	11.30
Chrysene-13C6	8.85	8.01	7.07	4.82	9.59	10.46	8.47	8.84	8.47	8.51	8.51	38.58
Benzo(b)fluoranthene-13C6	33.75	12.24	27.00	16.54	6.17	16.17	16.21	16.13	16.19	6.36	7.84	109.62
Benzo(k)fluoranthene-13C6	32.12	19.41	22.29	17.75	6.23	16.23	19.49	16.19	16.25	6.42	10.07	41.97
Benzo(a)pyrene-13C4	30.89	33.97	25.26	8.23	9.43	18.21	17.08	16.38	12.66	6.62	100.44	74.64
Indeno(1,2,3-cd)pyrene-13C6	21.25	17.91	6.15	6.12	6.06	6.06	6.09	6.01	6.08	6.24	22.68	18.65
Benzo(g,h,i)perylene-13C12	57.91	127.07	69.53	53.73	10.83	43.24	28.77	14.31	14.46	14.84	63.28	116.98
Dibenzo(a,h)anthracene-13C6	29.83	11.57	22.26	14.77	8.48	9.45	8.53	8.42	8.51	8.73	28.53	151.52
13C12-PCB#37	1.16	1.16	1.49	8.27	1.16	5.92	5.00	1.16	33.27	1.16	6.60	12.39
13C12-PCB #60	14.64	14.64	20.03	6.68	4.63	4.66	7.30	3.01	10.64	3.01	3.01	26.26
13C12-PCB #127	25.98	25.98	25.98	25.98	25.98	25.98	25.98	25.98	25.98	25.98	25.98	61.13
13C12-PCB #159	46.78	46.78	46.78	46.78	46.78	46.78	46.78	46.78	46.78	46.78	46.78	83.66

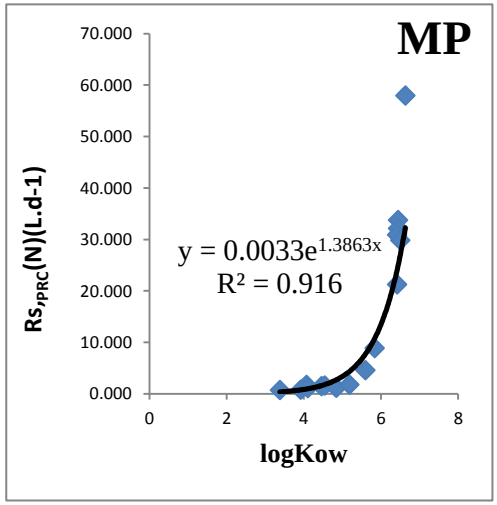
MP
y = 0.0033e1.3863x
R² = 0.916
RSPRC(N)(L.d-1)
logKow

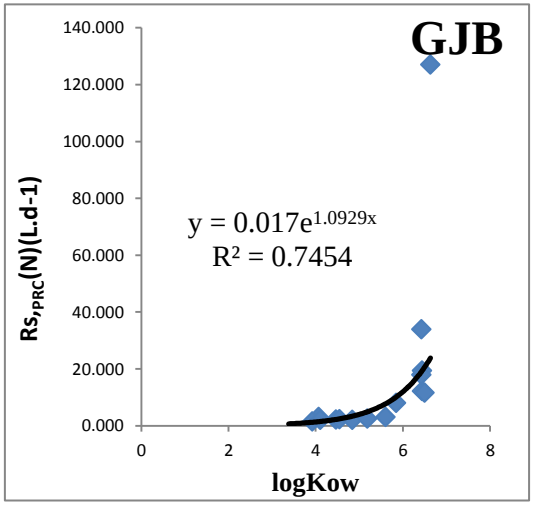
GJB
y = 0.017e1.0929x
R² = 0.7454
RSPRC(N)(L.d-1)
logKow

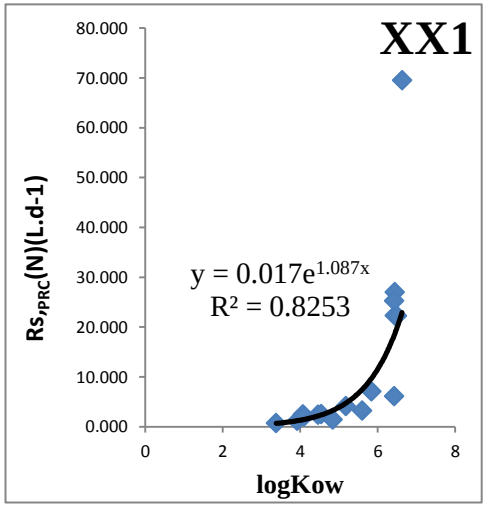
XX1
y = 0.017e1.087x
R² = 0.8253
RSPRC(N)(L.d-1)
logKow

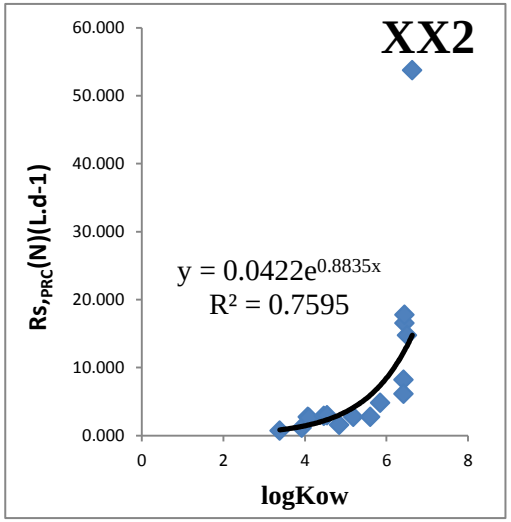
XX2
y = 0.0422e0.8835x
R² = 0.7595
RSPRC(N)(L.d-1)
logKow

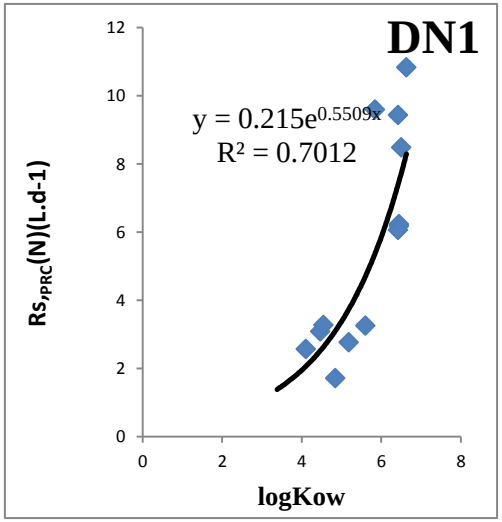
DN1
y = 0.215e0.5509x
R² = 0.7012
RSPRC(N)(L.d-1)
logKow

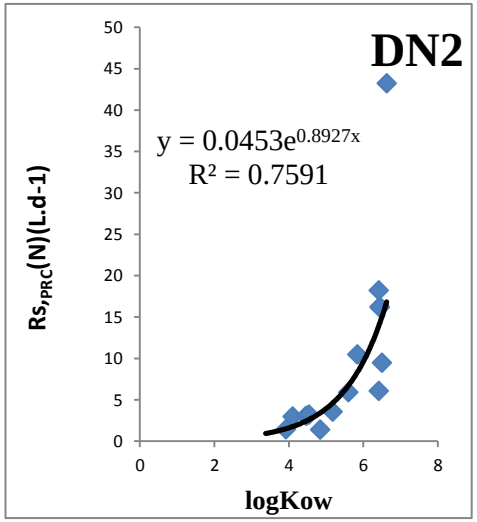
DN2
y = 0.0453e0.8927x
R² = 0.7591
RSPRC(N)(L.d-1)
logKow

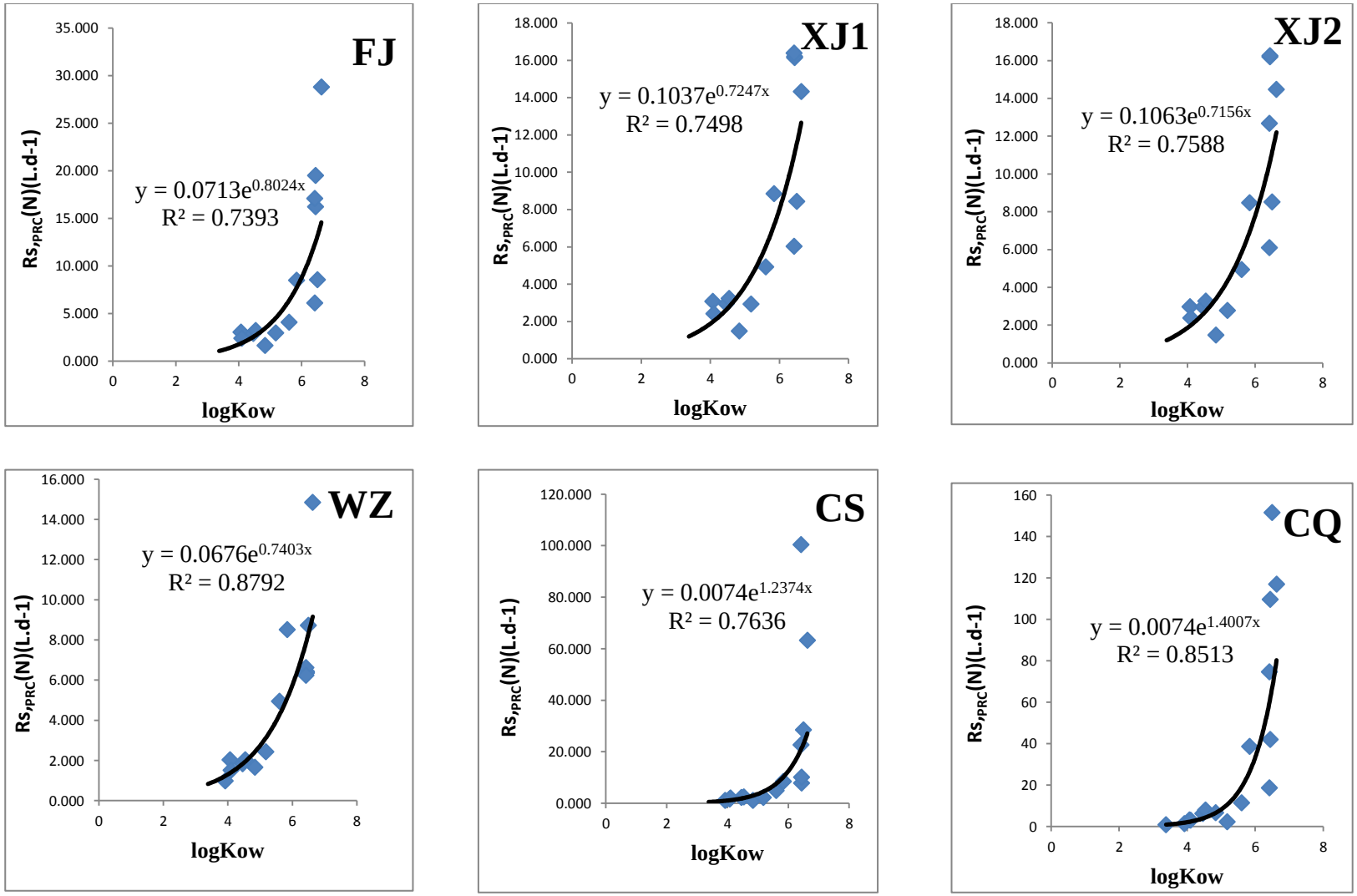

Fig.3.2.2: Relationship of PRC sampling rate $Rs_{,PRC}(N)$ (L.d^{-1}) and octanol water partition coefficient K_{ow} measured in each sampling site in TGR. Exponential function y is established with $R^2 > 0.75$ in twelves sites in TGR :Maoping(MP) ; Guojiaba (GJB); Xiangxi I (XX1); Xiangxi II (XX2); Daning I (DN1); Daning II(DN2); Fendji(FJ); Xiaojiang I(XJ1); Xiaojiang II(XJ2); Wanzhou(WZ); Changshou(CS); Chongqing(CQ)

3.3 Comparisons of Huckins and new theories

$Rs_{,PRC}(N)$ of the fifteen ^{13}C-PRC-PAH was used to estimate the native PAH sampling rates $Rs_{analyte}(N)$ with similar physicochemical properties and were compared with the experimental sampling rate $Rs_{analyte}(H)$ of Huckins (Eq.3.1). PRC-fluoranthene, with a loss between 20 to 80 percent, was selected (Huckins et al., 2002a). The result yields to a slight decrease of $Rs_{analyte}(H)$ at different log K_{ow} values ranging from 3.38 to 7.24.The diffusion is suggested to be controlled under WBL, so the VO acted as diffuse sampler. In contradiction to this, a significant deviation of $Rs_{analyte}(N)$ was observed for compounds with log K_{ow} values in the range of 5.18 to 7.24 (Fig.3.3.1). On the one hand, membrane diffusion could be an explanation of this observation. Under chemical conditions, as demonstrated above, rate control may have switched from WBL to membrane for certain high hydrophobic compounds. The VO acts, in this case, as a permeate sampler. On the other hand, the significant deviation corresponds with the theories from Vrana and Schüürmann (2002), Luellen and Shea (2002) and Booij et al. (2007a), suggesting that under water boundary layer control in SPMD, the sampling rate of compounds increases with increasing log K_{ow} and a maximum value in sampling rate is reached for compounds with log K_{ow} value at around six. $Rs_{,PRC}(H)$ and $Rs_{,PRC}(N)$ similarly increased for compounds with log K_{ow} ranging from 3.38 to 5.18, but for compounds with log K_{ow} ranging from 5.18 to 7.24, an increase of $Rs_{analyte}(N)$ may be due to the fact that his maximum value is reached for compounds with log K_{ow} higher than six with VO. This observation is likely due to the fact that the amount of triolein (44%) in this passive sampler VO is higher than the standard amount of Huckins (20%) in SPMD, consequently affecting the diffusion in such a way that after log $K_{ow} \geq 5.18$, instead of decreasing as expected, the diffusion coefficient increases with increasing molar mass. Thus, the WBL controlled uptake model may not be appropriate for compounds with log $K_{ow} \geq 5.18$, as kinetic exchange could switch from a WBL control to mass transfer control. The Huckins method has ignored the no flux boundary at the sampler's membrane, thus representing a situation in which the sampler is taken to be infinitely thick. The gap may be bridged when using PRC and target chemicals that exactly match in terms of partition coefficient and diffusivity, but the model would be inappropriate for measuring any target chemical which does not have a diffusion and sorption matching the PRC.

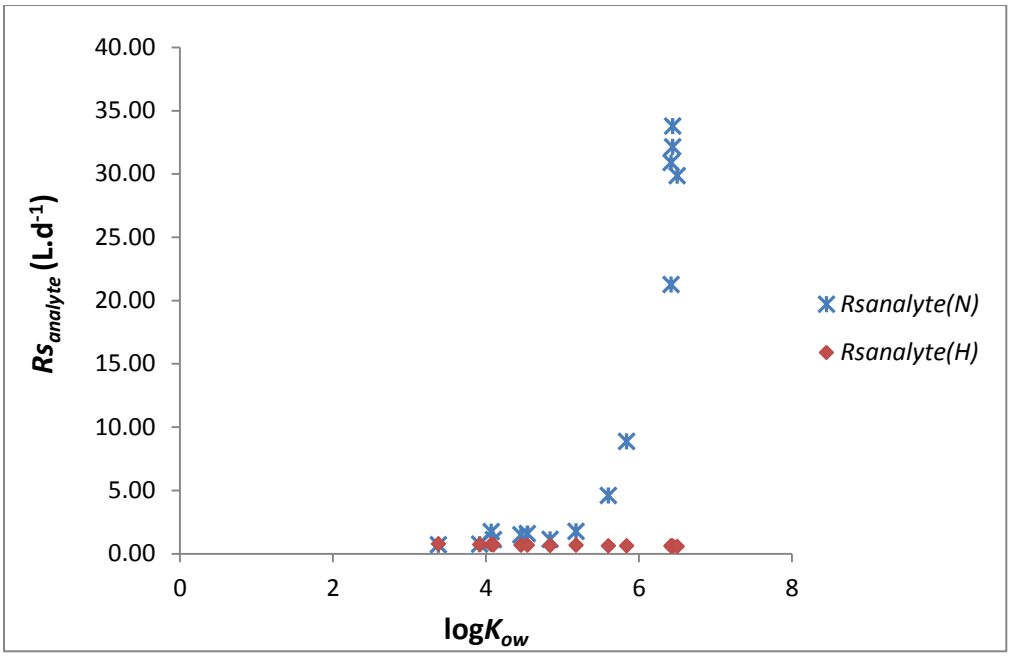

Fig.3.3.1: Comparison of $Rs_{analyte}$ *(N)* and $Rs_{analyte}$*(H)* (L.d^{-1}) as a function of log K_{ow} from ranging from 3.38 to 6.5 of sixteen 13C PRC-PAH. The sampling site was in Maoping (near the dam) at 14.1±4°C after 26 days of deployment. $Rs_{analyte}$*(H)* remains constant for compounds with log K_{ow} values range from 3.38 to 6.63 while $Rs_{analyte}$ *(N)* increases significantly for compounds with log K_{ow} values range from 5.18 to 6.63

3.3.1 Validation of $Rs_{analyte}$*(N)*

Acenaphtylene is expected to be in equilibrium stage after 26 days of exposure. In this case, Huckins et al. (2006b) demonstrated that the concentration in the water phase can be calculated with the partition coefficient K_{VO_W} (L.L^{-1}), the amount of analyte accumulated after a given exposure time *N* (mass) and the volume of the receiving phase V_S (L) as follows:

$$Cw_{(eq)} = \frac{N}{Vs\, K_{VO\_W}} \qquad \text{Eqn.3.13}$$

Or with $Rs_{analyte}$*(N)*(L.d^{-1}), giving as:

$$C_{W(Rs)} = \frac{N}{Rs_{analyte}(N)\, t} \qquad \text{Eqn.3.14}$$

To check $Rs_{analyte}$*(N)* values, both water concentration of acenaphtylene are made. $C_{W(Rs)}$ (mass/L) is expected to be equal to $C_{W(eq)}$ (mass/L) after 26 days.

Results show similar values for $C_{W(eq)}$ and $C_{W(Rs)}$ (Table 3.3.1). In some cases, the remained PRC was not determinable because acenaphtylene-PRC was completely released, making it impossible to calculate $C_{W(Rs)}$.

Table 3.3.1: Comparison of water concentration (ng/L) of acenaphtylene from K_{VO_W} ($C_{W(eq)}$) and from sampling rate $Rs_{analyte}(N)$ ($C_{W(Rs)}$)

	Maoping	Guojiaba	Xiangxi I	Xiangxi II	Daning I	Daning II	Fendji	Xiaojiang I	Xiaojiang II	Wanzhou	Changshou	Chongqing
$C_{W(eq)}$	39.11	139.67	38.24	67.70	77.44	42.65	94.57	48.91	52.90	37.65	37.65	1251.36
$C_{W(Rs)}$	40.89	142.44	38.73	68.20	_	_	94.97	49.09	53.15	39.88	39.84	1256.53

The alternative model (3.2) and the Huckins model were applied to estimate the water concentration of high hydrophobic compounds (log $K_{ow} \geq 5.18$) such as benzo(a)anthracene, chrysene, benzo(b)fluoranthene, benzo(k)fluoranthene, benzo(a)pyrene, indeno(1,2,3-c,d)pyrene and dibenzo(a,h)anthracene (Fig.3.3.2). The concentration of the ΣPAH in the TGR ranged from 248 pg/L for six-ring compounds to 182,292 pg/L for four-ring compounds with the alternative model, whereas using Huckins model ΣPAH was considerably higher, ranging from 5,323 pg/L for six-ring compounds to 305,624 pg/L for four-ring compounds. Both models presented a high percentage of four-rings PAH freely dissolved in water. The difference between $Rs_{PAH}\ (N)$ and $Rs_{PAH}(H)$ was obvious for higher molecular weight compounds. In the Huckins estimation, the six- and five-ring PAH portion were respectively 2% and 12%, versus 0.1% and 1% by using directly the measured in situ sampling rate. Hence, low log K_{ow} PRC-compounds referenced to high log K_{ow} analytes can lead to a substantial overestimation of the analyte's water concentrations by orders of magnitude.

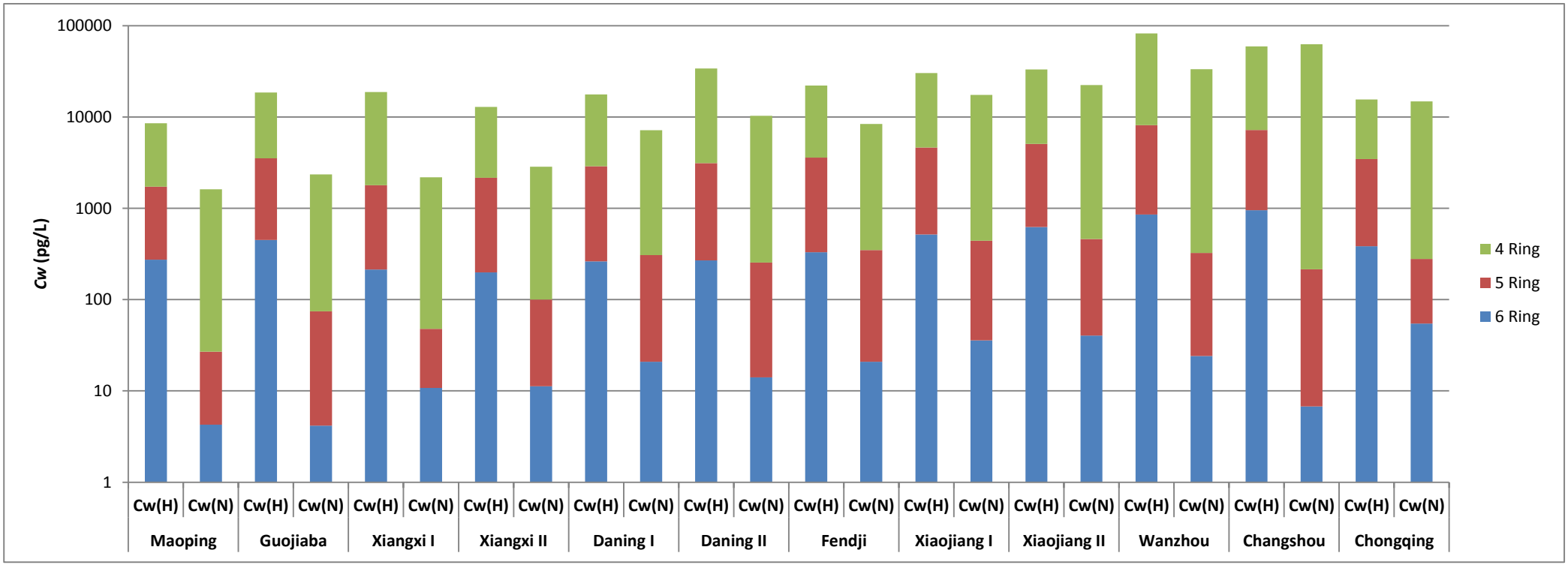

Fig.3.3.2: Comparison of water concentrations in ng/L, using Huckins method ($C_W(H)$) and the new procedure ($C_W(N)$), of four.-, five-, six-ring PAH with log K_{ow} range from 5.18 to 6.63 during 26 days of deployment (17.3°C - 23.9°C) at twelve different sampling sites along the Three Gorges Reservoir (Appendix Table 12)

3.4 Validation of the alternative method

VO samples were compared to XAD-cartridges for active sampling at the same period near TGD in Maoping. The concentration data evaluated by this type of sampling self-packed XAD cartridge have already been published to a large extent (Deyerling et al., 2014). Since only the freely dissolved form of a chemical is available to partition into the VO membrane, an estimation of total PAH concentration in crude water was established, also taking suspended particles and DOC into consideration (Appendix Table 16). For the simplification of the estimation of different masses constitutions, all densities δ were considered to be 1 kg/L. The Freundlich equation is used to estimate the contaminant release in suspended sediment, which was developed to model sorption from liquids to solids according to the approach of the United States Environmental Protection Agency EPA (EPA, 1996b):

$$C_{SP} = K_{OC} f_{OC} C_W \qquad \text{Eqn.3.15}$$

Where C_{SP} is the PAH concentration adsorbed on soil in ng/kg, *foc* is the fractional soil organic carbon content in g/g and *Koc* is the partition coefficient in L/kg between suspended particles and water normalized to the organic carbon content of the suspended particles and calculated from the octanol-water partition coefficient K_{ow} according to the following equation (EPA, 1996b):

$$\log K_{OC} = 0.0784 + (0.7919 \times \log K_{ow}) \qquad \text{Eqn.3.16}$$

The mass of PAH in water bound to suspended particles m_{SP} can then be estimated using the concentrations of suspended particles S_{SP} in kg/m^3, as follows:

$$m_{SP} = S_{SP} C_{SP} \qquad \text{Eqn.3.17}$$

The mean value of daily discharge of DOC S_{DOC} (1.6 mg C/L) in Yichang, determined by Müller et al. (2008), was used for the calculation. The mass of PAH in water bound to DOC m_{DOC} can then be estimated as follows:

$$m_{DOC} = K_{OC} S_{DOC} C_W \qquad \text{Eqn 3.18}$$

The total mass of PAH in water was given:

$$m_T = m_{SP} + m_{DOC} + m_W \qquad \text{Eqn 3.19}$$

Where m_w is the mass of PAH in its freely dissolved form.

The result of total PAH concentration found in the filter cartridge was 12.38 ng L^{-1} (Table 3.4.1) which was slightly lower than the concentration in VO from new method VO(N) with 21.48 ng/L and 3-fold lower than the concentration in VO from Huckins method VO(H) 44.89 ng/L. Although the sampling cartridge was generated within about 2 h on two consecutive days, the large sampling volume of about 400L helped to compensate this disadvantage and to generate representative average samples. Similarities in the concentration were observed between VO(N) and XAD-cartridge of 5 ring-PAH with a mean value of 2.12 ng/L and 2.82 ng/L respectively and of 6 ring-PAH with mean value of 1.10 ng/L and 1.57 ng/L respectively. VO(H) presented around 4-3 fold-higher concentration values for 5 ring-PAH(8.67 ng/L) and 6 ring-PAH(3.85ng/L). Consequently, the cartridge measurements further support the assumption that the new VO calculation method described in this study is more reliable than the Huckins method. Uptake rates of PAH begin to decrease in VOs when log K_{ow} ≥5.18 presumably due to a steric hindrance in the membrane. Hence the assumption that log K_{ow} ≥4.4 are generally under WBL as suggested by Huckins may not be true for PAH. This explains the discrepancy of high PAH concentration between VO(H) and VO(N).

Table 3.4.1: PAH water concentration in Maoping, determinates with new method calculation VO(N), with Huckins method VO(H) and from XAD-cartridge (ng/L)

Analytes	VO(H)	VO(N)	XAD
Naph	10.27	9.07	-
Acy	0.07	0.04	0.03
Ace	0.25	0.21	0.08
Fle	1.20	0.81	0.31
Fen	7.48	2.50	1.19
Ant	0.72	0.31	0.28
Flo	3.24	1.56	2.30
Pyr	5.50	1.69	1.68
BaA	0.96	0.91	0.90
Chr	2.69	1.16	1.23
BbF	3.93	1.19	1.38
BkF	1.61	0.23	0.40
BaP	1.69	0.61	0.87
InD	1.91	0.72	0.66
BghiP	1.94	0.38	0.91
DahA	1.44	0.09	0.17
Σ PAH	44.89	21.48	12.38

4 Chapter IV: Application of the new theory for quantitative Organochlorinated Pesticides analysis in VO

4.1 Sampling site and Experimental

Organochlorine pesticides (OCP) are one of the most important subgroups of persistent organic pollutants (POP) and have been of great concern around the world due to their chronic toxicity, persistence and bioaccumulation (Willett et al., 1998; Guo et al., 2008; Yu et al., 2010). Although the application of these chemicals has been banned or restricted in many countries especially the developed ones, some developing countries are still using these compounds because of their low cost and versatility in industry, agriculture and public health (Tanabe et al., 1994; Sarkar et al., 1997; Jeyakumar et al., 2014). As a major agricultural country, China is the second-largest producer and consumer of pesticides in the world. Consequently, former investigations have revealed a significant OCP content in the environment (Cai et al., 1996; Li et al., 2001; Jaward et al., 2005). The input pathways of OCP into the river environment include runoff from non-point sources, discharge of industrial wastewater and wet or dry deposition.

The Three Gorges Reservoir TGR region, covering an area of 59,900 km2 and a population of 16 million is greatly affected by the Three Gorges Project as this region is a rapidly developing area with serious non-point source pollution problems (Lu and Higgitt, 2001; Yang et al., 2002; Chen et al., 2008; Wang et al., 2008). However, in terms of persistent organic pollutants, most recent works have focused on estuarine and coastal areas (Yang et al., 2005; Guo et al., 2007; Zhang et al., 2009). There is limited relevant information of the TGR after the impounding in 2009 by the dam, with the water level rising from 145m to 172.5m. The Chongqing area suffers from severe environmental pollution because of agricultural production, commercial administration and finance, water and ground transportation activities, and heavy industries including power plants and several large steel and iron smelters. The objective of this present study is to apply the new method developed in Chapter III for the quantification of OCP in VO during the sampling campaigns in 2009 and 2011 in the whole TGR from Chongqing upstream to TGD downstream; to compare the results with the former study in 2008 (Wang et al., 2009), in which Huckins PRC method were used and to discuss their mass fluxes and possible sources and processes. The depth profile of the water column for OCP in 2012 in Maoping will be examined and compared with reports of 2009 and 2011.

4.1.1 Yangtze River in 2009, 2011 and 2012

The sampling campaign in 2011 is explained in detail in Chap II (2.2.1). The sampling campaigns in 2009 and 2011 covered a more than 600 km long distance from the upstream Chongqing to the great dam at Maoping and was realized during the water drawdown period of the reservoir (late April to early June). In 2009, the VOs were deployed for 14 days and 24 days in seven sampling sites: MP; GJ; BD1; BD2; WZ; CS and CQ. In April/May 2011, five sites were added (DN1, DN2, FJ, XJ1, and XJ2) before and after the mouth of the main tributary to allow the determination of their contribution to TGR pollution. CQ is one of the largest cities in TGR with a dense population of more than 6 million. WZ is the second largest city with 0.9 million people. CS is also an industrialized city with 0.4 million inhabitants and is located very close to CQ. The others sites are counties with a total population of 0.3 million (China National Bureau of Statistics). The VO was deployed in stainless steel cages and immerged into about 1 m depth water in Maoping near the dam, 10 m away from the riverbank. Other VO referred to as blanks, were kept inside their glasses and stored at the same sampling site. After the deployment period, the corresponding VO were removed from the cage and encased in their original glasses which, together with the blank samples, were then stored at -28°C until analysis.

The depth profile of the OCP water concentration was observed in a pattern ranging from 1 m to 61 m during the sampling campaign in August/September 2012. The VO was immerged into water at 1 m, 11 m, 21 m, 31 m, 41 m, 51 m, and 61 m depths. The sampling procedure was identical to the spatial deployment described above. The purpose of this second study was to analyze the OCP distribution between different water layers.

Average daily water runoffs were assessed at three different hydrological stations in Cantun, Wanzhou and Yichang depending on the sampling periods. These runoffs represent upstream and downstream flow boundaries for the TGR. The runoff in Wanzhou was available for a short sampling period from February 2004 to May 2007 only (afterwards only water level data was reported) and used as a reference for the runoff estimation. Average annual discharge data at the confluences or major control hydrological stations of major tributaries in the TGR were considered to estimate the mainstream runoff increase of the Yangtze River from upstream to downstream. This annual discharge data from the tributaries, together with upstream and

downstream flow boundaries based on averaged daily runoffs, allows the estimation of the total discharge of the Yangtze during the single sampling periods.

4.2 Results and Discussion

Equation to estimate OCP sampling rate $Rs_{,OCP}$ was established for each sampling site in 2009 and 2011 to evaluate the OCP water concentration(Table 4.2.1).. Eqn.1.5 was used to estimate Rs_{PRC}; Eqn.3.11 was used to estimate Rs_{min}, the corrector value of Rs_{PRC}.

Table 4.2.1: Relation between $Rs_{analyte}$ (y) from sixteen PAH-PRC and log K_{ow} (x) used to estimate water OCP concentration in TGR: after 25 days of deployment in twelve sites in 2011 and after 14 and 25 days of deployment in seven sites in 2009

Sampling sites	2009, 14d		2009, 25d		2011, 25d	
Maoping	$y = 16.678e^{1.0381x}$	$R^2 = 0.8754$	$y = 59.452e^{0.7309x}$	$R^2 = 0.907$	$y = 4.9812e^{1.34x}$	$R^2 = 0.9767$
Guojiaba	$y = 21.325e^{1.1089x}$	$R^2 = 0.8245$	$y = 53.414e^{0.8582x}$	$R^2 = 0.7735$	$y = 45.1e^{0.9225x}$	$R^2 = 0.9024$
Badong I	$y = 54.47e^{0.8604x}$	$R^2 = 0.8884$	$y = 125.57e^{0.6183x}$	$R^2 = 0.9798$	$y = 28.495e^{1.0051x}$	$R^2 = 0.9047$
Badong II	$y = 74.706e^{0.8168x}$	$R^2 = 0.8806$	$y = 136.86e^{0.6408x}$	$R^2 = 0.8797$	$y = 73.456e^{0.7927x}$	$R^2 = 0.8789$
Daning I					$y = 456.41e^{0.4271x}$	$R^2 = 0.8983$
Daning II					$y = 236.76e^{0.5542x}$	$R^2 = 0.7496$
Fendji					$y = 435.39e^{0.4387x}$	$R^2 = 0.9175$
Xiaojiang I					$y = 561.25e^{0.3818x}$	$R^2 = 0.9375$
Xiaojiang II					$y = 525.56e^{0.3946x}$	$R^2 = 0.9395$
Wanzhou	$y = 66.665e^{0.8121x}$	$R^2 = 0.9808$	$y = 86.433e^{0.7207x}$	$R^2 = 0.8552$	$y = 104.35e^{0.6493x}$	$R^2 = 0.9538$
Changshou	$y = 93.552e^{0.7918x}$	$R^2 = 0.8984$	$y = 13.15e^{1.1765x}$	$R^2 = 0.9068$	$y = 16.077e^{1.1199x}$	$R^2 = 0.7915$
Chongqing	$y = 299.42e^{0.5613x}$	$R^2 = 0.9707$	$y = 152.09e^{0.5986x}$	$R^2 = 0.8329$	$y = 9.9711e^{1.3667x}$	$R^2 = 0.9017$

4.2.1 Comparative estimation of OCP water concentrations

4.2.1.1 Sampling campaign in 2009

The total OCP in TGR for the sampling campaigns from April to June 2009 were estimated using the new model presented in this study and ranged from 1316 pg/L in Wanzhou to 515 pg/L at Maoping. The result shows clearly a substantial variation of OCP among samples, decreasing from upstream to downstream (Table 4.2.2). In the upstream with a high potential in the agriculture and industries, the total OCP level was twice as high as in the downstream. The agriculture was a significant industry sector in Chongqing (Wang et al., 2009) because of its favourable climate conditions, suitable for a wide range of agricultural products. Yet the share of agriculture has been decreasing while other manufacturing industries such as automotive, high-tech and IT have been continuing to expand, leading to an exodus of rural

migrants to urban areas nearby Chongqing, with similar climate conditions (e.g. Wanzhou). Thus this explains why there is a difference in concentration (Table 4.2.2).

The OCP were divided into groups of related compounds: ∑HCHs: α-HCH, β-HCH, γ-HCH, δ-HCH, ε-HCH; ∑chlorobenzene: PeCB, HCB, PeCA, OCS; ∑DDTs: 4,4'-DDT, 2,4'-DDT, 4,4'-DDD, 2,4'-DDD, 4,4'-DDE, 2,4'-DDE; ∑chlordane: trans-chlordane, cis-chlordane, oxy-chlordane, heptachlor, cis-heptachloroepoxide, trans-heptachloroepoxide; ∑drins: dieldrin, endrin; ∑endosulfan: endosulfan-I, endosulfan-II; methoxychlor and mirex. The main OCP components determined were α-, β-, γ-HCH, PeCB, HCB, PeCA and DDT (Table 4.2.3). The total HCH ranged from 331 to 766 pg/L and was the main contributor to OCP contaminants load in TGR. α-HCH made up 43% of the total HCH concentration in the TGR, followed by γ-HCH with 40% and β-HCH with 15%. An important spatial variation of the total HCH concentration can be observed between the Wanzhou River (506 pg/L) and the Badong River (330 pg/L) after 14 days of deployment. This result can also observed after 25 days with a total HCH water concentration dropping from 766 pg/L (Wanzhou) to 493 pg/L (Badong River).

Total DDT ranged from 28 to 137 pg/L and showed an important spatial variation between the Chongqing River (137 pg/L) and the Changshou River (29 pg/L). The major metabolites including the isomers 4, 4'-DDT, DDD and DDE presented a similar concentration in TGR and accounted for 71% of the total DDT. The other isomers 2, 4'-DDT, DDD and DDE were also of similar concentrations, but accounted for a minimum percentage of 29% of total DDT. Similarly to the distribution of HCH and DDT, total concentrations of the other metabolites chlorobenzenes (PeCB, HCB, PeCA and OCS) presented an important difference in TGR water ranging from 106 in Maoping to 535 pg/L in Chongqing, indicating their heterogeneous distribution in the whole reservoir. Discharge from tributaries between Chongqing and Badong could have led to a dilution of the mainstream, and thus a reduction of OCP concentration. Chlordane, heptachlor, dieldrin and endosulfan I and II, methoxychlor and mirex were detected in very low concentrations.

Table 4.2.2: Concentration of OCP in pg/L, estimated from new calculation theory, of two sampling program in late April-May 2009 for 14 days and May-June 2009 for 25 days in seven sites: MP (Maoping), GJB (Guojiaba), BD1 (Badong), BD2 (Badong), WZ (Wanzhou), CS (Changshou), and CQ (Chongqing)

	MP		GJB		BD1		BD2		WZ		CS		CQ	
Substances	**14d**	**25d**	**14d**	**25d**	**14d**	**25d**	**14d**	**25d**	**14d**	**25d**	**14d**	**25d**	**14d**	**25d**
α-HCH	110.90	207.72	109.51	230.03	117.01	224.32	109.54	230.80	206.67	339.55	194.41	271.11	241.29	261.85
β-HCH	39.79	72.88	36.51	77.77	38.21	76.99	38.71	72.39	81.65	130.91	58.23	105.09	55.02	83.80
γ-HCH	202.93	176.02	180.60	172.66	179.91	179.10	176.41	178.66	173.33	326.91	178.45	174.47	172.59	172.71
δ-HCH	3.07	8.18	3.15	8.34	3.24	9.17	3.49	7.94	9.98	11.69	7.49	13.58	9.21	11.31
ε-HCH	2.09	3.58	1.84	2.68	2.13	2.97	2.47	3.95	3.76	5.12	2.67	3.65	1.82	2.62
Pentachlorobenzene	44.88	35.33	70.91	50.46	101.33	62.09	84.41	51.32	50.20	167.09	62.89	58.79	135.93	93.52
Hexachlorobenzene	47.24	82.74	81.82	141.33	142.87	209.96	136.43	196.49	209.06	380.06	102.41	103.96	356.42	370.66
Pentachloroanisole	13.05	11.95	20.01	15.10	21.03	20.16	21.09	17.89	20.57	39.18	12.49	17.40	35.60	48.50
Octachlorostyrene	0.35	0.82	0.68	1.16	1.39	1.99	1.21	1.96	1.85	3.08	1.50	1.52	7.36	7.49
4,4'-DDT	11.66	10.00	7.03	11.55	11.67	17.81	14.54	16.47	13.99	21.57	8.36	9.15	58.41	39.51
2,4'-DDT	3.98	5.28	5.02	7.67	7.61	10.95	8.08	9.89	6.54	12.65	2.20	3.82	15.30	18.39
4,4'-DDD	4.06	8.60	7.54	14.62	13.47	21.19	14.54	19.52	19.62	33.40	8.02	13.12	26.04	29.32
2,4'-DDD	1.63	3.69	2.71	4.94	4.43	7.91	5.25	8.36	7.68	11.57	2.66	4.16	6.71	9.74
4,4'-DDE	3.78	7.53	6.61	11.71	12.26	20.97	12.66	17.62	13.66	27.01	5.55	7.64	21.98	27.21
2,4'-DDE	2.64	3.00	2.70	4.87	4.04	6.40	4.32	5.80	4.75	8.32	2.40	3.83	8.55	11.92
trans-Chlordane	1.02	1.09	1.38	1.91	1.93	2.55	1.71	2.32	2.21	4.69	1.38	2.38	5.75	7.41
cis-Chlordane	0.69	0.87	0.94	1.41	1.48	2.01	1.54	1.85	1.38	3.64	0.94	1.52	3.93	5.51
oxy-Chlordane	0.10	0.09	0.12	0.17	0.18	0.20	0.22	0.24	0.19	0.48	0.13	0.12	0.53	0.48
Heptachlor	0.03	0.03	0.03	0.03	0.10	0.11	0.06	0.05	0.09	0.13	0.07	0.03	0.19	0.17
cis-Heptachloroepoxide	0.87	0.61	0.51	0.85	0.69	0.89	0.69	0.76	0.81	1.90	0.64	1.05	1.27	1.72
trans-Heptachloroepoxide	1.00	0.75	0.67	0.56	0.96	0.83	0.55	0.47	1.01	1.26	0.75	0.64	10.75	10.42
Dieldrin	0.15	0.11	0.10	n.d.	n.d.	n.d.	n.d.	0.09	0.09	0.00	0.10	0.10	n.d.	n.d.
Endrin	4.86	3.64	3.26	2.72	3.78	3.22	3.51	2.89	2.98	3.85	3.31	2.60	3.13	2.99
Endosulfan-I	0.55	0.42	0.35	n.d.	0.43	n.d.	0.40	n.d.	0.33	n.d.	0.37	0.27	0.36	0.34
Endosulfan-II	8.82	10.14	2.38	3.19	2.16	2.69	3.02	2.89	6.45	11.33	12.50	20.77	35.37	40.45
Methoxychlor	3.79	2.92	2.40	2.02	2.98	2.56	2.76	2.24	2.31	3.06	2.58	1.83	2.52	2.37
Mirex	0.57	0.79	0.27	0.36	0.61	0.84	0.61	0.65	0.59	0.71	0.58	0.15	0.94	0.79
∑OCP	515	659	549	768	676	888	648	854	842	1549	673	823	1217	1261

n.d.=no detection

Table 4.2.3: Percentage of distribution of HCH, DDT and Chlorobenzene derivatives in 2009 during 14 and 25 days of deployment in seven cities along Three Gorges Reservoir from upstream Chongqing to downstream Maoping.

	MP		GJB		BD1		BD2		WZ		CS		CQ		Average	Pourcentage
Substances	14d	25d	14d	25d	14d	25d	14d	25d	14d	25d	14d	25d	14d	25d		
α-HCH	110.9	207.7	109.5	230.0	117.0	224.3	109.5	230.8	206.7	339.5	194.4	271.1	241.3	261.8	**203.9**	43%
β-HCH	39.8	72.9	36.5	77.8	38.2	77.0	38.7	72.4	81.6	130.9	58.2	105.1	55.0	83.8	**69.1**	15%
γ-HCH	202.9	176.0	180.6	172.7	179.9	179.1	176.4	178.7	173.3	326.9	178.4	174.5	172.6	172.7	**188.9**	40%
δ-HCH	3.1	8.2	3.1	8.3	3.2	9.2	3.5	7.9	10.0	11.7	7.5	13.6	9.2	11.3	**7.8**	2%
ε-HCH	2.1	3.6	1.8	2.7	2.1	3.0	2.5	3.9	3.8	5.1	2.7	3.6	1.8	2.6	3.0	1%
															472.8	
Average	**358.8**	**468.4**	**331.6**	**491.5**	**340.5**	**492.5**	**330.6**	**493.7**	**475.4**	**814.2**	**441.3**	**567.9**	**479.9**	**532.3**	6618.6	
Pourcentage	5%	7%	5%	7%	5%	7%	5%	7%	7%	12%	7%	9%	7%	8%		
4,4'-DDT	11.7	10.0	7.0	11.6	11.7	17.8	14.5	16.5	14.0	21.6	8.4	9.1	58.4	39.5	**18.0**	26%
2,4'-DDT	4.0	5.3	5.0	7.7	7.6	11.0	8.1	9.9	6.5	12.6	2.2	3.8	15.3	18.4	**8.4**	12%
4,4'-DDD	4.1	8.6	7.5	14.6	13.5	21.2	14.5	19.5	19.6	33.4	8.0	13.1	26.0	29.3	**16.6**	24%
2,4'-DDD	1.6	3.7	2.7	4.9	4.4	7.9	5.3	8.4	7.7	11.6	2.7	4.2	6.7	9.7	**5.8**	9%
4,4'-DDE	3.8	7.5	6.6	11.7	12.3	21.0	12.7	17.6	13.7	27.0	5.6	7.6	22.0	27.2	**14.0**	21%
2,4'-DDE	2.6	3.0	2.7	4.9	4.0	6.4	4.3	5.8	4.7	8.3	2.4	3.8	8.5	11.9	**5.3**	8%
															68.1	
	27.7	**38.1**	**31.6**	**55.4**	**53.5**	**85.2**	**59.4**	**77.7**	**66.2**	**114.5**	**29.2**	**41.7**	**137.0**	**136.1**	953.3	
	3%	4%	3%	6%	6%	9%	6%	8%	7%	12%	3%	4%	14%	14%		
Pentachlorobenzene	44.9	35.3	70.9	50.5	101.3	62.1	84.4	51.3	50.2	167.1	62.9	58.8	135.9	93.5	**76.4**	27%
Hexachlorobenzene	47.2	82.7	81.8	141.3	142.9	210.0	136.4	196.5	209.1	380.1	102.4	104.0	356.4	370.7	**183.0**	64%
Pentachloroanisole	13.1	12.0	20.0	15.1	21.0	20.2	21.1	17.9	20.6	39.2	12.5	17.4	35.6	48.5	**22.4**	8%
Octachlorostyrene	0.4	0.8	0.7	1.2	1.4	2.0	1.2	2.0	1.8	3.1	1.5	1.5	7.4	7.5	**2.3**	1%
															284.1	
	105.5	**130.8**	**173.4**	**208.1**	**266.6**	**294.2**	**243.1**	**267.7**	**281.7**	**589.4**	**179.3**	**181.7**	**535.3**	**520.2**	3977.0	
	3%	3%	4%	5%	7%	7%	6%	7%	7%	15%	5%	5%	13%	13%		

Pourcentage of OCP components in the whole reservoir

Average concentration of OCP components in the whole reservoir

Pourcentage of OCP components in each site at 14d and 25d

Summe of OCP concentration for each group

4.2.1.2 Sampling campaign in 2011

The sampling campaign from April to May 2011 is summarized in Table 4.2.5. The investigation extended to 25 days and endosulfan sulfate was included into the OCP analysis. The total OCP concentration in water, estimated from the new calculation theory, decreases from upstream in Wanzhou (1418 pg/L) to downstream in Maoping (410 pg/L). The main OCP compositions were α-, β-, γ-HCH, PeCB, HCB, PeCA, DDT and endosulfan (Table 4.2.4). The mean concentration of HCH ranged from 215 to 504 pg/L. α-HCH made up 68% of total HCH concentration in TGR, β-HCH followed with 19%. The γ-HCH concentration dropped by 10%. The application of lindane (γ-HCH), a compound widely used as insecticide in China (Wu et al., 1997), had considerably reduced from 2009 (40% γ-HCH) to 2011. The total DDT ranged from 19 to 157 pg/L. The para-position of the isomers 4, 4'-DDT, DDD and DDE was in a higher percentage in TGR water with 78%. The ortho-position of the isomers 2, 4'-DDT, DDD and DDE accounted for a minimum percentage of 22% of total DDT. The total concentrations of the other Chlorobenzene derivatives (PeCB, HCB, PeCA and OCS) ranged from 149 to 744 pg/L and became the main contributor to OCP contaminants in the TGR. The endosulfan distribution ranged from 15 to 50 pg/L. Endosulfan sulfate was in a higher percentage with 51% followed by endolsulfan I with 40%. The heterogeneous distribution of HCH, Chlorobenzenes derivatives and endosulfan could be observed in the whole reservoir. The concentrations of the total OCP in Hubei area were characterized as homogenous in comparison with the most urbanized Chongqing area. In the two years, ∑OCP concentration remained constant from upstream to downstream and had decreased in CQ following the decline of the agricultural sector in this area. A higher concentration of PeCB, OCS and PeCA was expected in the most urbanized city CQ as these components were most important as a byproduct of incomplete combustion (Bailey, 2007; Yang et al., 2011). However, a high load of PeCB, OCS and PeCA in WZ, a district of Chongqing with a high potential in agriculture, may suggest that pesticides such as pentachlorophenol used against schistosomiasis (Bao et al., 1995; Zheng et al., 2012), may also be taken into consideration as an important source of these contaminants, especially PeCA in China.

Table 4.2.4: Percentage of distribution of HCH, DDT, endosulfan and chlorobenzene derivatives in 2011 during 25 days of deployment in twelve cities along Three Gorge Reservoir from upstream Chongqing to downstream Maoping.

	MP	GJB	BD1	BD2	DN2	DN1	FJ	XJ2	XJ1	WZ	Cs	CQ	Average	Pourcentage
α-HCH	141.7	174.5	173.6	174.0	230.1	212.5	257.0	347.4	353.1	339.4	308.4	221.4	**244.4**	68%
β-HCH	35.7	46.9	40.3	42.5	51.3	53.3	72.1	89.3	89.9	77.9	104.5	108.7	**67.7**	19%
γ-HCH	30.6	29.8	27.3	33.8	29.4	27.8	31.2	54.1	38.4	48.0	44.8	32.1	**35.6**	10%
δ-HCH	4.8	6.3	6.1	6.5	7.5	6.0	8.9	10.6	9.2	9.6	14.7	19.4	**9.1**	3%
ε-HCH	2.4	2.3	2.2	2.4	2.3	2.1	3.7	2.4	3.3	2.4	3.2	2.8	**2.6**	1%
													359.5	
Sum HCH	**215.1**	**259.9**	**249.5**	**259.1**	**320.7**	**301.8**	**372.9**	**503.8**	**493.9**	**477.4**	**475.7**	**384.4**	4314.2	
Pourcentage of HCH	5%	6%	6%	6%	7%	7%	9%	12%	11%	11%	11%	9%		
4,4'-DDT	5.6	10.1	11.5	15.9	19.7	22.5	16.3	19.3	20.2	30.4	7.2	28.4	**17.3**	19%
2,4'-DDT	2.1	4.1	4.3	6.9	7.7	9.1	6.8	7.8	8.4	11.5	2.1	8.2	**6.6**	7%
4,4'-DDD	5.6	13.6	18.2	26.8	40.2	51.9	46.3	68.3	61.4	67.7	20.9	13.6	**36.2**	40%
2,4'-DDD	1.4	3.7	4.5	7.4	11.2	14.0	12.9	18.3	16.6	15.6	4.0	3.2	**9.4**	10%
4,4'-DDE	3.1	8.3	10.0	17.5	20.0	31.0	22.4	23.4	24.7	26.1	7.2	9.6	**16.9**	19%
2,4'-DDE	1.2	2.6	2.5	3.6	3.9	5.3	4.0	4.4	4.2	5.3	1.9	3.4	**3.5**	4%
													89.9	
Sum DDT	**18.9**	**42.4**	**51.1**	**78.1**	**102.8**	**133.9**	**108.9**	**141.5**	**135.6**	**156.5**	**43.1**	**66.4**	1079.1	
Percentage	2%	4%	5%	7%	10%	12%	10%	13%	13%	15%	4%	6%		
Pentachlorobenzene	53.6	85.3	93.1	115.9	126.9	144.3	135.0	149.5	151.0	180.4	302.8	124.7	**138.5**	28%
Hexachlorobenzene	81.8	180.1	205.8	302.1	331.9	439.7	334.2	391.0	418.0	479.4	194.7	362.9	**310.1**	62%
Pentachloroanisole	13.6	27.7	36.9	48.9	59.4	71.3	59.8	66.5	69.8	80.0	26.9	32.8	**49.5**	10%
Octachl.	0.3	0.9	1.3	2.4	2.7	4.5	3.3	4.9	4.9	3.9	0.0	4.3	**2.8**	1%
													500.9	
Sum PeCB	**149.4**	**294.1**	**337.2**	**469.3**	**520.9**	**659.9**	**532.3**	**611.8**	**643.8**	**743.7**	**524.4**	**524.6**	6011.3	
Percentage	2%	5%	6%	8%	9%	11%	9%	10%	11%	12%	9%	9%		
Endosulfan-I	11.1	7.3	5.0	5.6	5.3	5.7	5.9	5.5	7.3	5.4	16.5	34.1	**9.6**	40%
Endosulfan-II	2.2	2.1	2.1	1.3	2.2	2.1	2.1	2.1	2.1	2.7	2.1	2.3	**2.1**	9%
Endosulfan-sulfat	7.4	9.0	8.0	7.8	9.8	9.7	9.6	14.4	14.8	18.5	31.6	6.0	**12.2**	51%
													23.9	
Sum Endo	**20.7**	**18.4**	**15.0**	**14.8**	**17.4**	**17.5**	**17.6**	**22.0**	**24.2**	**26.6**	**50.2**	**42.5**	286.9	
	7%	6%	5%	5%	6%	6%	6%	8%	8%	9%	18%	15%		

Pourcentage of OCP components in the whole reservoir

Pourcentage of OCP components in each site

Average concentration of OCP components in the whole reservoir

Summe of OCP concentration for each group

Table 4.2.5: Concentration of OCP in pg/L (new calculation theory) of sampling program in late May-June 2011 for 25 days in twelve sites: MP (Maoping), GJB (Guojiaba), BD1 (Badong), BD2 (Badong), DN1 (Wushan), DN2 (Wushan), FJ (Fengjie), XJ1 (Yunyang), XJ2 (Yunyang), WZ (Wanzhou), CS (Changshou), and CQ (Chongqing)

Substances	MP	GJB	BD1	BD2	DN2	DN1	FJ	XJ2	XJ1	WZ	CS	CQ
α-HCH	141.65	174.50	173.55	173.98	230.14	212.54	256.99	347.38	353.07	339.38	308.44	221.40
β-HCH	35.71	46.95	40.34	42.53	51.29	53.29	72.07	89.33	89.94	77.94	104.54	108.68
γ-HCH	30.55	29.85	27.34	33.82	29.42	27.79	31.16	54.05	38.39	48.04	44.78	32.14
δ-HCH	4.81	6.31	6.05	6.46	7.54	6.01	8.93	10.64	9.17	9.57	14.71	19.36
ε-HCH	2.39	2.34	2.20	2.35	2.28	2.14	3.72	2.44	3.28	2.45	3.24	2.84
Pentachlorobenzene	53.62	85.35	93.09	115.86	126.90	144.25	135.04	149.52	151.04	180.41	302.77	124.66
Hexachlorobenzene	81.82	180.11	205.84	302.08	331.92	439.74	334.19	390.97	418.01	479.40	194.69	362.87
Pentachloroanisole	13.62	27.75	36.92	48.89	59.38	71.34	59.80	66.46	69.83	79.95	26.90	32.82
Octachlorostyrene	0.35	0.92	1.31	2.43	2.67	4.53	3.25	4.89	4.95	3.94	0.02	4.29
4,4'-DDT	5.57	10.14	11.49	15.92	19.69	22.55	16.34	19.30	20.25	30.43	7.16	28.38
2,4'-DDT	2.14	4.09	4.31	6.91	7.69	9.08	6.83	7.85	8.40	11.47	2.07	8.15
4,4'-DDD	5.57	13.59	18.23	26.80	40.25	51.95	46.32	68.31	61.41	67.71	20.85	13.61
2,4'-DDD	1.35	3.71	4.51	7.39	11.18	14.00	12.95	18.28	16.58	15.56	3.95	3.24
4,4'-DDE	3.10	8.28	10.02	17.46	20.04	31.03	22.39	23.36	24.69	26.06	7.19	9.64
2,4'-DDE	1.16	2.56	2.53	3.64	3.93	5.31	4.05	4.37	4.24	5.25	1.89	3.35
trans-Chlordane	0.50	1.06	1.80	2.24	2.28	2.40	2.31	3.33	3.13	2.91	2.23	5.38
cis-Chlordane	0.40	0.49	0.88	1.17	1.13	1.96	1.26	1.67	2.13	1.77	1.53	2.97
oxy-Chlordane	0.06	0.08	0.18	0.10	0.24	0.29	0.12	0.11	0.33	0.85	0.19	1.73
Heptachlor	0.02	0.02	0.05	0.04	0.05	0.06	0.06	0.05	0.07	0.12	0.03	0.04
cis-Heptachloroepoxide	0.66	0.45	0.71	0.56	0.80	0.68	1.07	1.13	1.02	0.85	1.08	1.77
trans-Heptachloroepoxide	0.62	0.55	0.70	0.46	0.77	0.55	0.58	0.44	0.56	1.09	0.64	8.47
Aldrin	0.02	0.03	0.03	0.08	0.08	0.07	0.08	0.09	0.09	0.44	0.03	0.07
Dieldrin	2.77	2.62	2.58	2.79	2.72	2.58	2.59	2.66	2.62	3.36	2.66	2.08
Endrin	0.76	0.73	0.74	0.64	1.11	0.79	0.68	0.97	0.90	1.17	0.94	2.35
Endosulfan-I	11.07	7.28	5.01	5.65	5.35	5.69	5.87	5.47	7.26	5.42	16.48	34.15
Endosulfan-II	2.22	2.10	2.07	1.32	2.20	2.09	2.09	2.15	2.12	2.72	2.14	2.27
Endosulfan-sulfate	7.42	9.03	7.96	7.84	9.81	9.68	9.62	14.37	14.85	18.49	31.60	6.04
Methoxychlor	0.22	2.66	0.29	0.31	0.38	4.82	5.07	0.36	0.31	1.33	0.35	2.83
Mirex	0.01	0.02	0.02	0.04	0.05	0.10	0.12	0.11	0.07	0.11	0.04	0.03
∑OCP	410	449	661	830	971	1127	1046	1290	1309	1418	1103	1046

∑OCP concentration in the TGR estimated in 2008 with Huckins method (Wang et al., 2009) after 7 days of deployment ranged from 4299 to 8612 pg/L and after 24 days of deployment ranged from 8327 to 19661 pg/L (Table 4.2.6). VOs in CQ and BD2 were lost or broken by high water flow and turbulence. A comparison of OCP in 2008, 2009, 2011 and in 1m depth of depth profile data collected during the sampling campaign in Maoping in 2012 was also carried out. Results showed a decrease in ∑OCP concentration in water from the TGR from 2008 to 2011. Floods and precipitation may render the soil more vulnerable to erosion and affect the growth conditions of plants and agricultural practices, altering land-use management strategies (Scholz et al., 2008). These phenomena may partly have caused a reduction in ∑OCP concentration. The sampling campaign in 2012 was performed in September during a hot and rainy period. This can explain why the OCP concentration was higher compared to 2009 and 2011. The main factor that may account for the variation includes the use of two different PRC methods; Huckins method in 2008 and the new calculation method (cf. 3.2.) from 2009, to estimate OCP water concentrations in the TGR.

Table 4.2.6: ∑OCP concentration in water (pg/L) from upstream Chongqing (CQ) to Maoping (MP) near the dam in 2008 and in 2011

	CQ	CS	WZ	BD2	BD1	GJB	MP
May 2008	8612	631632	5035	5702	5414	4857	4299
May-June 2008		19661	14445		11213	8327	9890
April-May 2009	1217	673	842	648	676	549	515
May-June 2009	1261	823	1549	854	888	768	659
April-May 2011	1046	1103	1418	830	661	449	410
Sept. 2012							1117

4.2.1.3 Sampling campaign in 2012 (depth profiles)

The depth profile analysis of 29 OCP congeners was performed in 2012 at Maoping to approve homogeneity of the water body as a basis for mass flux estimations. The results show a homogeneous distribution of OCP concentration from 1m to 61 m ranging from 1012 pg/L in 31 m depth to 1143 pg/L in 61 m depth (Table 4.2.7). These results agree with Sawford (1983) suggesting that fluctuations in concentration due to an instantaneous cloud source ultimately are negligible compared with the mean-field concentration. HCH were the most abundant compounds with a mean concentration of 483 pg/L from which α-HCH represented 64%. Cl-Benzenes follow with a mean concentration of 470 pg/L whose 62% HCB, then DDT and endosulfan with a mean concentration of 104 pg/L and 36 pg/L respectively. Since 2010, the water level in the Three Gorges Reservoir has followed an annual cycle peaking at 175m for

power generation and navigation during winter months from November to February, then gradually declining to 170–150m for downstream irrigation and navigation in spring from March to May, and finally reaching its lowest constraining level of ~145m for flood control during the monsoon season from June to August(Wang et al., 2013b). The sampling campaign in 2012 was executed during the monsoon season. This could be a reason why a high value of OCP concentration can be observed. Since the concentrations are very similar, the 1m data are suitable as a basis of mass flux calculations.

Table 4.2.7 OCP depth profile and OCP concentration (pg/L) (new calculation theory) at Maoping during sampling campaign in August/September 2012 for 21 days of deployment from 1m to 61m water depth

Substances	Depth profile						
	1 m	11 m	21 m	31 m	41 m	51 m	61 m
α-HCH	313.0	346.1	332.4	279.6	302.1	280.4	314.3
β-HCH	138.2	136.5	142.5	98.4	129.0	109.6	124.6
γ-HCH	39.0	32.3	32.3	32.4	32.9	32.2	32.5
δ-HCH	8.4	8.9	6.3	5.3	5.7	5.3	6.6
ε-HCH	8.1	8.1	8.1	8.1	8.2	8.0	8.1
Pentachlorobenzene	110.9	110.0	108.7	106.7	111.9	106.0	113.0
Hexachlorobenzene	280.4	277.3	295.4	277.2	294.1	296.8	322.2
Pentachloroanisole	56.0	60.6	55.4	54.4	63.6	55.4	62.7
Octachlorostyrene	8.3	9.7	9.8	8.6	12.3	8.1	10.7
4,4'-DDT	34.9	30.7	31.8	32.2	35.5	29.1	30.7
2,4'-DDT	11.4	11.1	10.9	10.9	12.0	9.6	10.9
4,4'-DDD	29.5	31.8	28.9	30.2	39.1	28.6	33.5
2,4'-DDD	8.6	9.3	8.6	7.7	12.2	7.8	9.6
4,4'-DDE	12.5	12.8	13.0	11.6	14.3	11.1	14.4
2,4'-DDE	4.7	5.0	4.8	4.6	5.2	4.4	4.7
trans-Chlordane	3.3	3.1	3.3	3.3	3.7	2.7	4.0
cis-Chlordane	2.7	2.0	2.1	2.3	2.1	1.7	2.8
oxy-Chlordane	0.1	0.1	0.0	0.1	0.1	0.1	0.0
Heptachlor	0.0	0.0	0.0	0.0	0.0	0.0	0.0
cis-Heptachloroepoxide	1.2	1.1	1.0	1.2	1.0	0.8	1.1
trans-Heptachloroepoxide	0.0	0.0	0.0	0.0	0.0	0.0	0.0
Aldrin	0.0	0.0	0.0	0.0	0.0	0.0	0.0
Dieldrin	0.3	0.4	0.7	0.4	1.0	0.3	0.6
Endrin	0.1	0.0	0.0	0.3	0.0	0.0	0.0
Endosulfan-I	6.4	5.0	4.4	4.1	4.5	3.9	4.6
Endosulfan-II	2.2	2.2	2.2	2.3	2.3	2.2	2.2
Endosulfan-sulfate	36.3	35.3	34.5	30.2	30.6	27.7	28.7
Methoxychlor	0.5	0.4	0.4	0.5	0.5	0.5	0.4
Mirex	0.0	0.0	0.0	0.0	0.0	0.0	0.0
∑OCP (pg/L)	1117	1140	1138	1012	1124	1032	1143

4.2.2 OCP source analysis

The dominant isomer α-HCH in sampling campaign 2009, 2011 and 2012 indicated an input of HCH into TGR water. HCH concentrations in the TGR tended to decrease from upstream

Chongqing to downstream Maoping. The ratio α-HCH/γ-HCH was used to give information about the pollution source of HCH. This is because most of HCHs in the environment come from the use of technical HCHs (α-HCH/γ-HCH> 3.0) or lindane (α-HCH/γ-HCH ≈0). The ratios of α-HCH/γ-HCH in this study ranged from 0.5 to 1.6 (mean value of 1.1) in 2009, 4.6 to 9.2 (mean value of 6.9) in 2011 and 8.0 to 10.7 (mean value of 9.3) in 2012 (Table 4.2.8). It can be concluded from these results that the input of HCH into TGR could be mainly related with the application of lindane in 2009 and with the industrial and agricultural activities in 2011 and 2012. The application of lindane (γ-HCH), widely used as an insecticide in china (Wu et al., 1997), decreased from 2009 to 2011.

DDT was found in high concentration in TGR, as China is still producing it for export for malaria control and for domestic use in dicofol production. DDT can be gradually degraded into the stable metabolites DDE. Hence, the ratio *p.p'*-DDT/*p,p'*-DDE is used to give information about source and history of DDT in the environment, whether DDT is new (*p.p'*-DDT/*p,p'*-DDE > 1) or aged (*p.p'*-DDT/*p,p'*-DDE < 1)(Strandberg et al., 1998). This ratio from 2009 ranged from 0.8 to 3.1 for 4,4'-DDT/ 4,4'-DDE and from 0.9 to 1.9 for 2,4'-DDT/2,4'-DDE. Ratio values lower than 1 in BD1, BD2 and WZ indicated aged input of DDT. In 2011, the ratio value ranged from 0.7 to 2.9 and from 1.1 to 2.4 respectively for 4,4'-DDT/4,4'-DDE and 2,4'-DDT/2,4'-DDE. Values, lower than 1, were revealed in BD2, DN1, FJ, XJ1 and XJ2. MP presented a fresh input of DDT from 2009 to 2012, where 4,4'-DDT/4,4'-DDE ranged from 2,1 to 2,8 and 2,4'-DDT/2,4'-DDE ranged from 2.2 to 2.4. TGR water regularly received a fresh input of DDT but also an aged input of DDT coming from smaller cities where industries were not as developed. The ratio of *o.p'*-DDT/*p,p'*-DDT can provide us with further information about DDT sources. When this ratio is around 0.2, DDT originated from industries and when this ratio is around 7, DDT originated from the application of DDT-containing dicofol (Qiu et al., 2005). In this study, the ratio mean value of 2,4'-DDT/4,4'-DDT was 0.5 in 2009, 0,4 in 2011 and 0.3 in 2012. The main sources of DDT could then be from the re-emissions of industrial DDT residues from historic uses because the industrial DDT has been banned in China since 1983 (Zhang et al., 2003). Besides, dicofol used in China is mainly in downstream of Yangtze River, in contrast to TGR.

The dominant Chlorobenzene compounds in TGR water was HCB and PeCB. HCB was initiated as a byproduct in municipal waste combustion and cheap insecticide in China. PeCB is

a metabolite of HCB. The high concentration levels of HCB determined in this study indicate that this molecule is still being used as an insecticide in the TGR.

Table 4.2.8: HCH, DDT and chlorobenzene source analysis in TGR in 2009, 2011 and 2012

2009	MP		GJB		BD1		BD2		WZ		CS		CQ	
	14d	25d	14d	25d	14d	25d	14d	25d	14d	25d	14d	25d	14d	25d
α-HCH/γ-HCH	0.5	1.2	0.6	1.3	0.7	1.3	0.6	1.3	1.2	1.0	1.1	1.6	1.4	1.5
4,4'-DDT/4,4'-DDE	3.1	1.3	1.1	1.0	1.0	0.8	1.1	0.9	1.0	0.8	1.5	1.2	2.7	1.5
2,4'-DDT/2,4'-DDE	1.5	1.8	1.9	1.6	1.9	1.7	1.9	1.7	1.4	1.5	0.9	1.0	1.8	1.5
2,4'-DDT/4,4'-DDT	0.3	0.5	0.7	0.7	0.7	0.6	0.6	0.6	0.5	0.6	0.3	0.4	0.3	0.5

2011	MP	GJB	BD1	BD2	DN2	DN1	FJ	XJ2	XJ1	WZ	CS	CQ
α-HCH/γ-HCH	4.6	5.8	6.3	5.1	7.8	7.6	8.2	6.4	9.2	7.1	6.9	6.9
4,4'-DDT/4,4'-DDE	1.8	1.2	1.1	0.9	1.0	0.7	0.7	0.8	0.8	1.2	1.0	2.9
2,4'-DDT/2,4'-DDE	1.8	1.6	1.7	1.9	2.0	1.7	1.7	1.8	2.0	2.2	1.1	2.4
2,4'-DDT/4,4'-DDT	0.4	0.4	0.4	0.4	0.4	0.4	0.4	0.4	0.4	0.4	0.3	0.3

2012, MP	1m depth	11m depth	21m depth	31m depth	41m depth	51m depth	61m depth
α-HCH/γ-HCH	8.0	10.7	10.3	8.6	9.2	8.7	9.7
4,4'-DDT/4,4'-DDE	2.8	2.4	2.4	2.8	2.5	2.6	2.1
2,4'-DDT/2,4'-DDE	2.4	2.2	2.3	2.4	2.3	2.2	2.3
2,4'-DDT/4,4'-DDT	0.3	0.4	0.3	0.3	0.3	0.3	0.4

4.2.3 OCP freights

4.2.3.1 OCP freights calculation

For the estimation of OCP mass fluxes MF_{OCP}, the need of the water concentration and the flow data in the TGR was necessary in the application of the following equation:

$$MF_{OCP} = C_W \times D(x,t) \qquad \text{Eqn.4.1}$$

where MF_{OCP} is the OCP mass flux in mg/s, C_W is OCP concentration in water determined by VO in pg/L and $D(x,t)$ is the discharge of the Yangtze dependent on the location x and time t in m^3s^{-1}(Deyerling et al., 2014). Between two locations the discharge of the tributaries D_{tr} was estimated with the following equation:

$$D_{tr} = D(x,t) - D(x+1,t) \qquad \text{Eqn.4.2}$$

Where *D(x,t)* is the discharge upstream and *D(x+1,t)* is the discharge downstream of the tributaries, both in m^3s^{-1}. The mass fluxes difference from upstream to downstream ΔMF_{OCP} are given by

$$\Delta MF_{OCP} = MF_{OCP}(downstr.) - MF_{OCP}(upstr.) \quad \text{Eqn.4.3}$$

$\Delta MF_{OCP} > 0$, when the OCP water concentration between two sampling sites from upstream to downstream increases. The increase is then assumed in this present study to be due to contamination provided from tributaries. Therefore the calculation of a minimum concentration of OCP of a tributary that is necessary to increase the OCP flux within the TGR is developed as

$$C_{\min\_tr} = \frac{\Delta MF_{OCP}}{D_{tr}} \quad \text{Eqn.4.4}$$

$\Delta MF_{OCP} < 0$ may correspond to dilution, adsorption to suspended particles, evaporation into the air or photolytic and biological degradation.

Positive values of the sum of OCP mass flux difference $\Sigma\Delta MF_{OCP}$ correspond to an increasing total amount of OCP in TGR and negative values to a decreasing amount. OCP mass flux gives information on whether the total OCP amount in the TGR has increased ($\Sigma\Delta MF_{OCP} > 0$) or decreased ($\Sigma\Delta MF_{OCP} < 0$). The calculation of OCP concentrations that were absorbed onto suspended particles is performed to evaluate whether absorption is one origin of OCP discharge process in water.

The total OCP concentration in water C_t is then giving, using Eqn 3.17 as following:

$$C_t = C_W(1 + S_{SP}K_{OC}f_{OC}) \quad \text{Eqn.4.8}$$

4.2.3.2 OCP freights from Chongqing to Maoping

OCP mass fluxes MF_{OCP} decreased in all three sampling campaigns from upstream to downstream. The major source of OCP in the TGR was in the metropolitan area Chongqing in 2009 ranging from 4.58 to 8.07 mg/s in April/May 2009, from 5.59 to 9.6 mg/s in May/June 2009 and from 2.97 to 7.8 mg/s in 2011 and in 2011. The main total OCP mass flux issued at Chongqing ranged from 2.97 to 7.8 mg/s in 2011. The mean contributors to the total OCP load were HCH, DDT, Chlorobenzene derivatives and endosulfan which caused 75-80% of the total

OCP mass flux. The mass balance indicates that the amount of OCP that was introduced to the reservoir downstream Chongqing is nearly two to three times lower than the disappearing OCP amount. This discrepancy may come from the highest OCP concentration in Wanzhou, then leading to a potential source of OCP in the TGR as Changshou presents a lower OCP input.

Table 4.2.9 shows a reduction of total OCP input into the TGR from 2008 to 2011 by 0.41 Mga^{-1} to 0.07 Mga^{-1}. The major OCP input were α-HCH, PeCB, HCB and Endosulfan I with respectively 0.738 Mga^{-1}, 0.371 Mga^{-1}, 0.991 Mga^{-1} and 0.762 $Mga^{-}1$. This input was generated at Chongqing area and was compensated by more than 100% of OCP output at Maoping.

Table 4.2.9: OCP mass fluxes MF_{OCP} balance (Mga^{-1}) from upstream Chongqing to downstream Maoping in TGR in 2008, 2009 and 2011

	2011, 26d		2009 , 14d		2009, 25d		2008, 7d		Total	
	in	out	in	out	in	out	in	out	in	out
α-HCH	0.030	-0.022	0.063	-0.026	0.083	-0.014	0.562	-0.157	0.738	-0.220
β-HCH	0.003	-0.009	0.021	-0.008	0.034	-0.010	0.110	-0.039	0.168	-0.066
γ-HCH	0.007	-0.006	0.066	0.000	0.081	-0.024	<LOQ	<LOQ	0.155	-0.030
t-HCH	0.000	-0.002	0.003	-0.002	0.003	-0.001	0.015	-0.002	0.022	-0.007
e-HCH	0.001	-0.001	0.001	-0.0003	0.001	0.000	0.009	-0.007	0.012	-0.008
PeCB	0.031	-0.021	0.046	-0.031	0.039	-0.028	0.255	-0.131	0.371	-0.212
HCB	0.075	-0.043	0.105	-0.089	0.127	-0.100	0.685	-0.284	0.991	-0.516
PACB	0.012	-0.003	0.011	-0.007	0.014	-0.010	0.096	-0.043	0.133	-0.063
OCS	0.001	-0.001	0.002	-0.002	0.002	-0.002	0.015	-0.011	0.020	-0.016
4,4'-DDT	0.005	-0.005	0.016	-0.012	0.011	-0.008	0.081	-0.030	0.114	-0.056
2,4'-DDT	0.002	-0.002	0.005	-0.004	0.006	-0.004	0.020	-0.007	0.034	-0.017
4,4'-DDD	0.013	-0.004	0.008	-0.007	0.010	-0.007	0.064	-0.023	0.095	-0.041
2,4'-DDD	0.003	-0.001	0.003	-0.002	0.003	-0.002	0.036	-0.013	0.045	-0.018
4,4'-DDE	0.005	-0.001	0.007	-0.006	0.010	-0.008	0.048	-0.027	0.070	-0.041
2,4'-DDE	0.001	0.000	0.002	-0.002	0.004	-0.003	0.018	-0.007	0.025	-0.012
Endo.I	0.0005	-0.005	0.0002	-0.0001	0.0003	-0.0002	0.761	-0.600	0.762	-0.604
Endo.I	0.0002	-0.0001	0.007	-0.005	0.013	-0.009	<LOQ	<LOQ	0.020	-0.015
Endo.sulfate	0.004	-0.003							0.004	-0.003
Σ OCP	0.11	-0.18	0.15	-0.20	0.07	-0.15	0.41	-0.81		

Henry's law constant H describes the rate at which a substance evaporates from water. As H increases, it becomes more likely that a chemical will move from water to air. An evaluation of a potential OCP evaporation process in the TGR during the sampling campaign in 2011 of some compounds was carried out. In this evaluation, reduction was observed, revealing that there is a lack of correlation between a percentage of OCP reduction and their respective Henry's law constants (Fig.4.2.1) Although evaporation to the air is a dominant mechanism of release, this contribution in the OCP water remediation is meaningless. Biodegradation or photolysis may also be other factors that have to be taken into account. Studies show that the presence of microorganisms or algae accelerates photochemical reactions due to the fact that these components are capable of absorbing sunlight (Dabrowska et al., 2004). Zheng et al. (2009) reveal that the highest values of algal density in TGR are 1 427 times greater than the normal values. Biodegradation processes can naturally clean up the environments. It expected to be the major mechanism of reduction for most persistent chemical compounds (Dabrowska et al., 2004; Varsha et al., 2011).

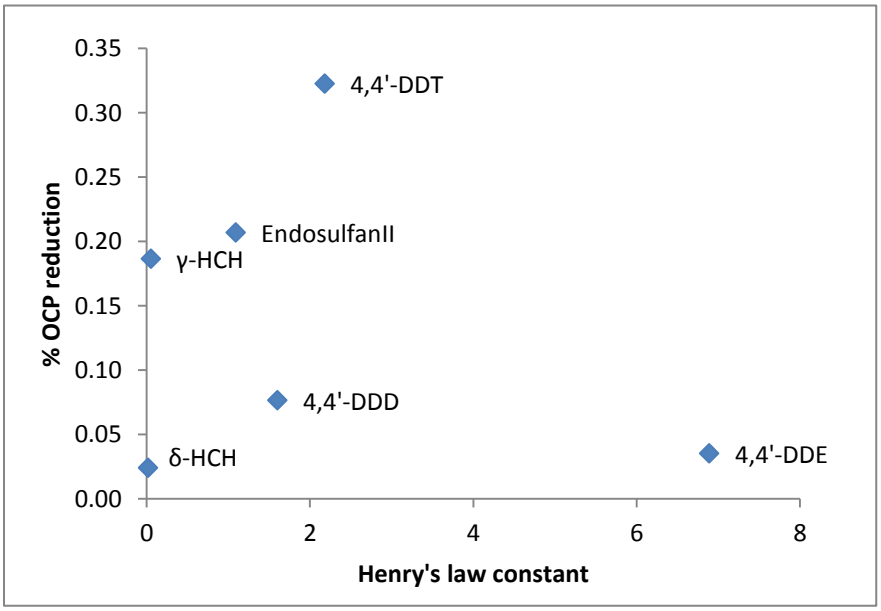

Fig.4.2.1: The Henry's law constant of OCP components, where reduction was observed, doesn't show any correlation with the percentage of OCP reduction in TGR during sampling campaign in 2011. It can be deduced from this observation that the evaporation process is not pronounced in the OCP remediation in TGR

Tributaries input of OCP concentration in the TGR was investigated (Table. 4.2.10). Eqn.4.4 was used to estimate $C_{min,\ tr}$, with a presumption that the tributaries were the only OCP source between the two sampling sites. Due to their weak self-purification and water exchange, concentrations of OCP in the tributaries were higher than those in the mainstream. Shennongxi River (between BD1/BD2), Daning River (between DN1/DN2) and the Xiaojiang River (Between XJ1/XJ2) presented a very low OCP concentration from 1635 pg/L in Mai/June 2009 to undetectable in April/May 2011. This low concentration could have contributed to the OCP disappearance in the mainstream. The Daxi River, tributary flowing between FJ and DN1 with a HCB concentration of 13528 pg/L in 2011, revealed a significant effect on the main stream, where HCB increased from 334 in FJ to 440 pg/L in DN1

Table 4.2.10: Contribution of tributaries in the input of the dominant OCP compounds PeCB, HCB, α-HCH and 4,4'-DDT in the main stream TGR (concentration in pg/L)

Main	May-June 2008					April-May 2009					May-June 2009					April-May 2011				
stream	PeCB	HCB	α-HCH	4,4-DDT	Σ_{28}OCP	PeCB	HCB	α-HCH	4,4-DDT	Σ_{28}OCP	PeCB	HCB	α-HCH	4,4-DDT	Σ_{28}OCP	PeCB	HCB	α-HCH	4,4-DDT	Σ_{28}OCP
CQ	734	2047	1184	228	8612	136	356	241	58	1217	94	371	262	40	1261	125	363	221	28	1046
CS	845	1432	1158	192	6316	63	102	194	8	673	59	104	271	9	823	303	195	308	7	1103
WZ	352	1420	845	219	5035	50	209	207	14	842	124	284	312	16	1316	180	479	339	30	1418
XJ1																151	418	353	20	1309
XJ2																150	391	347	19	1290
FJ																135	334	257	16	1046
DN1																144	440	213	23	1127
DN2																127	332	230	20	971
BD2	528	2047	1391	195	5702	84	136	110	15	648	51	196	231	16	854	116	302	174	16	830
BD1	520	1876	1467	160	5414	101	143	117	12	676	62	210	224	18	888	93	206	174	11	661
GJB	370	1344	1582	207	4857	71	82	110	7	549	50	141	230	12	768	85	180	175	10	449
MP	377	1225	1236	154	4299	45	47	111	12	515	35	83	208	10	659	54	82	142	6	410
Triburaties																				
CQ													632							
CS	5174		144										874			7398		3775		3395
WZ		1257		586			1659	373	91	3135	1015	2728		110	8018		2804	592	220	3991
XJ1																		1106		
XJ2																107		188		767
FJ																				
DN1																1287	13528		792	11263
DN2																		964		
BD2	1446	5316	4238	70	9180	263			17				83	19						
BD1	346		3120			469	283	279		1278	296	503	280	47	1635			160		
GJB			2579	614	30			45										196		
MP	732							181	247											

Table 4.2.11: Mass flux (mg/s) of the dominant OCP compounds PeCB, HCB, α-HCH and 4,4'-DDT in TGR water in seven sampling sites in 2008, 2009 and in twelves sampling sites in 2011 from upstream Chongqing to downstream Maoping.

Sampling	May 2008					April-May 2009					May-June 2009					2011				
sites	PeCB	HCB	α-HCB	4,4-DDT	ΣOCP	PeCB	HCB	α-HCB	4,4-DDT	Σ_{28}OCP	PeCB	HCB	α-HCB	4,4-DDT	Σ_{28}OCP	PeCB	HCB	α-HCH	4,4-DDT	Σ_{28}OCP
CQ	4.87	13.57	7.85	1.51	57.10	0.90	2.36	1.60	0.39	8.07	0.62	2.46	1.74	0.26	8.36	0.60	1.73	1.06	0.14	5.00
CS	5.75	9.74	7.87	1.31	42.95	0.43	0.70	1.32	0.06	4.58	0.40	0.71	1.84	0.06	5.59	1.48	0.95	1.51	0.04	5.41
WZ	2.57	10.37	6.17	1.60	36.76	0.37	1.53	1.51	0.10	6.14	0.91	2.07	2.28	0.12	9.60	0.99	2.64	1.87	0.17	7.80
XJ1																0.85	2.34	1.98	0.11	7.33
XJ2																0.87	2.27	2.01	0.11	7.48
FJ																0.84	2.07	1.59	0.10	6.48
DN1																0.90	2.75	1.33	0.14	7.05
DN2																0.81	2.12	1.47	0.13	6.22
DB2	4.59	17.81	12.10	1.70	49.61	0.73	1.19	0.95	0.13	5.64	0.45	1.71	2.01	0.14	7.43	0.76	1.99	1.15	0.11	5.48
DB1	4.73	17.07	13.35	1.46	49.27	0.92	1.30	1.06	0.11	6.15	0.57	1.91	2.04	0.16	8.08	0.63	1.40	1.18	0.08	4.49
GJB	3.76	13.64	16.06	2.10	49.30	0.72	0.83	1.11	0.07	5.57	0.51	1.43	2.33	0.12	7.80	0.61	1.28	1.24	0.07	3.19
MP	3.90	12.68	12.79	1.59	44.49	0.46	0.49	1.15	0.12	5.33	0.37	0.86	2.15	0.10	6.82	0.39	0.59	1.03	0.04	2.97

The OCP load has considerably declined from 2008 to 2011 (Table 4.2.11). The major OCP mass flux during these years was PeCB, HCB, α-HCH and 4,4'-DD. Hence, the PeCB load ranged from 4.87 mg/s in CQ in 2008 to 0.37 mg/s in MP in May-June 2009. HCB load ranged from 17.81 mg/s in DB2 in 2008 to 0.49 mg/s in MP in April-May 2009. α-HCH ranged from 16.06 mg/s in GJB in 2008 to 0.95 mg/s in DB2 in April-May 2009. 4,4'-DDT load ranged from 2.10 mg/s in GJB in 2008 to 0.04 mg/s in MP in 2011. HCB mass flux in 2011 increased from 2.07 mg/s in FJ to 2.75 mg/s in DN1 due to its high load coming from the Daxi River. The development of agriculture activities in WZ may have had an influence on the OCP concentration and load. The reason for the OCP mass flux reduction could be, as invocated above for the concentration, the water impounding but also the use of different estimation methods for water concentration from VO content. Furthermore, since the Stockholm convention on POP became effective in China, the government has taken many actions for the reduction of these persistent compounds in the environment.

4.2.4 Total water concentration in TGR

From previous studies, the high hydrophobic compounds (log K_{ow} > 4.5) are more commonly sorbed in suspended particles of matter in water columns (Chiou et al., 1979; Clansky, 1992; Zhou and Rowland, 1997; WHO, 2014). Since OCP are highly insoluble in water, theoretically they would accumulate through the water column directly to the sediment. However, due to OCP's high partitioning affinity to DOC, it can be transported effectively in the water column. The availability of OCP trace pollutants adsorbed on suspended sediments has been previously investigated (Wu et al., 2005) and results have been reported as consistent. Hence, the determination of the OCP concentration on suspended sediment in this study has been taken into account as a possible sub-compartment. The calculation was done for available data in 2009, 2011 and the 1m data of the OCP depth profile measured in 2012 at Maoping. The mean value of 1.16% of organic carbon content for suspended particles within the TGR, determined by Wu et al. (2007), was used for the calculation. The concentration of OCP bound on suspended sediment was obtained from Eqn.3.17 and allowed the estimation of the total OCP concentration in both water and suspended sediment (Eqn.4.8). Results showed a slight variation between the OCP concentration dissolved in water and the total concentration (Table 4.2.12). The OCP concentration bound to suspended particles ranged from 0.36 pg/L in 2011 to 13.9 pg/L in 2012. As expected, the value of C_{sp} was much higher, ranging from 63.9 ng/kg in

2011 to 232.61 ng/kg in 2012. During the dry season in 2012, the concentration of sediment is higher because of the water column reduction.

Table.4.2.12: Comparison of OCP concentration dissolved in water C_W and total OCP concentration *Ct* (water and suspended particles) in TGR in 2009, 2011 and 2012

Period, deployment days	2009, 25d		2011, 25d		2012, 21d	
	Cw	*Ct*	*Cw*	*Ct*	*Cw*	*Ct*
	pg/l	ng/L	pg/l	pg/l	pg/l	pg/l
α-HCH	207.72	207.75	141.65	141.67	309.70	310.04
β-HCH	72.88	72.89	35.71	35.71	125.56	125.67
γ-HCH	176.02	176.03	30.55	30.55	33.38	33.40
δ-HCH	8.18	8.18	4.81	4.81	6.64	6.66
ε-HCH	3.58	3.58	2.39	2.39	8.10	8.11
Pentachlorobenzene	35.33	35.38	53.62	53.67	109.60	110.78
Hexachlorobenzene	82.74	83.01	81.82	82.01	291.91	299.01
Pentachloroanisole	11.95	11.98	13.62	13.64	58.31	59.37
Octachlorostyrene	0.82	0.82	0.35	0.35	9.64	10.29
4,4'-DDT	10.00	10.03	5.57	5.58	32.12	32.69
2,4'-DDT	5.28	5.30	2.14	2.14	10.98	11.22
4,4'-DDD	8.60	8.64	5.57	5.58	31.67	32.62
2,4'-DDD	3.69	3.71	1.35	1.36	9.11	9.61
4,4'-DDE	7.53	7.59	3.10	3.12	12.82	13.60
2,4'-DDE	3.00	3.01	1.16	1.17	4.77	4.87
trans-Chlordane	1.09	1.09	0.50	0.50	3.34	3.39
cis-Chlordane	0.87	0.88	0.40	0.40	2.25	2.28
oxy-Chlordane	0.09	0.09	0.06	0.07	0.07	0.07
Heptachlor	0.03	0.03	0.02	0.02	n.d.	n.d.
cis-Heptachloroepoxide	0.61	0.61	0.66	0.66	1.06	1.06
trans-Heptachloroepoxide	0.75	0.75	0.62	0.62	n.d.	n.d.
Aldrin	n.d.	n.d.	0.02	0.02	0.02	0.02
Dieldrin	0.11	0.11	2.77	2.78	0.51	0.52
Endrin	3.64	3.64	0.76	0.76	0.05	0.05
Endosulfan-I	0.42	0.42	11.07	11.07	4.69	4.72
Endosulfan-II	10.14	10.15	2.22	2.23	2.22	2.23
Endosulfan-sulfate	n.d.	n.d.	7.42	7.43	31.90	32.07
Methoxychlor	2.92	2.92	0.22	0.22	0.45	0.45
Mirex	0.79	0.79	0.01	0.01	n.d.	n.d.
∑OCP (pg/L)	659	659	410	411	1101	1115

Conclusion

The calculation of analyte concentration in water with VO involves several steps. Firstly, the water sampling rates must be calculated from the PRC fractions (PRC amounts at the end and beginning of exposure) that are retained. The retained PRC fraction is inversely proportional to the sampling rates used for the calculation of analyte concentration. The PRC field data are screened prior to calculating sampling rates. Detection limits for PRC may depend on the amounts of the other compounds present in the extract. Therefore, all PRC responses should be carefully inspected for possible interferences from other analytes, particularly if the PRC concentration in the extract is low. The new procedure presented herein can be used to estimate in situ $Rs_{analyte}(N)$ of hydrophobic organic compounds with a wide range of K_{ow}, using sixteen PAH-PRC and four PCB-PRC with log K_{ow} range from 3.38 to 7.24, in order to improve the accuracy of the estimated water concentration.

Under water boundary WBL control, $Rs_{analyte}(N)$ values were expected to gradually decline due to a small reduction in diffusion coefficient Dw (Rusina et al, 2010; Vrana et al 2007) following the mass transfer coefficient model from Huckins et al (2006). Field application of VO revealed that diffusion of PRC compounds like Naph-$^{13}C_6$, Ace-$^{13}C_6$, Acy-$^{13}C_6$, with a slight variation of $Rs_{analyte}(N)$, are under WBL control while diffusion of highly hydrophobic compounds(log $K_{ow} \geq 5.18$) like Benzo(a)anthracene, Chrysene, Benzo(b)fluoranthene, Benzo(k)fluoranthene, Benzo(a)pyrene, Indeno(1,2,3-c,d)pyrene, Benzo(g,h,i)perylene and Dibenzo(a,h)anthracene, PCB #37, PCB#60, PCB#127, PCB#159 with increasing $Rs_{analyte}(N)$ can be either under membrane control or under WBL control.

The uniformity between contaminant water concentration of PAH and OCP in VO and in XAD-2 during the sampling campaign in the outdoor well had confirmed the accuracy of the new method developed in this study.

Investigation of the OCP concentration in water in TGR with VO showed evidence of spatial variations in the reservoir. The contaminants tended to be higher in Chongqing area. The consequence of the expansion of agricultural sector in Wanzhou has led to an increase in the OCP concentration in water column. The OCP disappearance from upstream to downstream could also be due to dilution from discharge of the tributaries when the OCP concentration and load of the tributaries are lower than in the mainstream, or because of dilution from rainfall. The main OCP components were HCB, DDT, Cl-benzenes derivatives and endosulfan. A decrease in OCP concentration was observed after 175m water impoundment in the TGR. The sampling campaign in 2008 showed values of OCP water concentration approximatively 20-

fold higher than in 2011(Wang et al., 2009). Although several factors might explain the reduction of the OCP water concentration in the TGR, the main reason is the use in this study of field data for the calculation of sampling volume. Hence, the previous application of Huckin's method for determining the total OCP may have been leading to a substantial overestimation of the water concentration.

The OCP mass flux in the TGR varies in accordance to the OCP concentration. Spatial concentration data decreased from the upstream Chongqing area to the less urbanized Hubei area.

References

Alcock, R.E., Jones, K.C., 1996. Dioxins in the environment: a review of trend data. Environmental science & technology 30, 3133-3143.

An, Q., Wu, Y., Taylor, S., Zhao, B., 2009. Influence of the Three Gorges Project on saltwater intrusion in the Yangtze River Estuary. Environmental geology 56, 1679-1686.

Anyakora, C., Coker, H., Arbabi, M., 2011. Application of polynuclear aromatic hydrocarbons in chemical fingerprinting: the niger delta case study. Iranian Journal of Environmental Health Science & Engineering 8, 75-84.

Augulyte, L., Bergqvist, P.-A., 2007. Estimation of water sampling rates and concentrations of PAHs in a municipal sewage treatment plant using SPMDs with performance reference compounds. Environmental science & technology 41, 5044-5049.

Bailey, R.E., 2007. Pentachlorobenzene–Sources, environmental fate and risk characterization. Science dossier, Euro Chlor, 44 pages.

Ballschmiter, K., Buchert, H., Niemczyk, R., Munder, A., Swerev, M., 1986. Automobile exhausts versus municipal-waste incineration as sources of the polychloro-dibenzodioxins (PCDD) and-furans (PCDF) found in the environment. Chemosphere 15, 901-915.

Bank, H.S.D., 2009. Toxnet from the US National Library of Medicine.

Bao, Z., Wang, K., Kang, J., Zhao, L., 1995. Analysis of polychlorinated dibenzo-p-dioxins and polychlorinated dibenzofurans in pentachlorophenol and sodium pentachlorophenate. Environ. Chem 14, 317-321.

Baodong, W., Feng, L., Guiyun, W., 1999. Horizontal distributions and seasonal variations of dissolved oxygen in the southern Huanghai Sea [J]. ACTA OCEANOLOGICA SINICA 4, 006.

Bartkow, M.E., Huckins, J.N., Müller, J.F., 2004. Field-based evaluation of semipermeable membrane devices (SPMDs) as passive air samplers of polyaromatic hydrocarbons (PAHs). Atmospheric Environment 38, 5983-5990.

Baumard, P., Budzinski, H., Garrigues, P., Narbonne, J., Burgeot, T., Michel, X., Bellocq, J., 1999. Polycyclic aromatic hydrocarbon (PAH) burden of mussels (Mytilus sp.) in different marine environments in relation with sediment PAH contamination, and bioavailability. Marine Environmental Research 47, 415-439.

Beck, H., Droβ, A., Eckart, K., Mathar, W., Wittkowski, R., 1989. PCDDs, PCDFs and related compounds in paper products. Chemosphere 19, 655-660.

Berdowski, J., Baas, J., Bloos, J., Visschedijk, A., Zandveld, P., 1997. The European Inventory of Heavy Metals and Persistent Organic Pollutants for 1990, TNO Institute of Environmental Sciences. Energy Research and Process Innovation (MEP), Berlin, 239 pages.

Bergmann, A., Bi, Y., Chen, L., Floehr, T., Henkelmann, B., Holbach, A., Hollert, H., Hu, W., Kranzioch, I., Klumpp, E., 2012. The Yangtze-Hydro Project: a Chinese–German environmental program. Environmental Science and Pollution Research 19, 1341-1344.

Booij, K., Hoedemaker, J.R., Bakker, J.F., 2003a. Dissolved PCBs, PAHs, and HCB in pore waters and overlying waters of contaminated harbor sediments. Environmental science & technology 37, 4213-4220.

Booij, K., Hofmans, H.E., Fischer, C.V., Van Weerlee, E.M., 2003b. Temperature-dependent uptake rates of nonpolar organic compounds by semipermeable membrane devices and low-density polyethylene membranes. Environmental science & technology 37, 361-366.

Booij, K., Sleiderink, H.M., Smedes, F., 1998. Calibrating the uptake kinetics of semipermeable membrane devices using exposure standards. Environ Toxicol Chem 17, 1236-1245.

Booij, K., Smedes, F., 2010. An improved method for estimating in situ sampling rates of nonpolar passive samplers. Environmental science & technology 44, 6789-6794.

Booij, K., Smedes, F., Van Weerlee, E.M., 2002. Spiking of performance reference compounds in low density polyethylene and silicone passive water samplers. Chemosphere 46, 1157-1161.

Booij, K., van Bommel, R., Jones, K.C., Barber, J.L., 2007a. Air–water distribution of hexachlorobenzene and 4, 4′-DDE along a North–South Atlantic transect. Marine pollution bulletin 54, 814-819.

Booij, K., Van Bommel, R., Mets, A., Dekker, R., 2006. Little effect of excessive biofouling on the uptake of organic contaminants by semipermeable membrane devices. Chemosphere 65, 2485-2492.

Booij, K., Vrana, B., Huckins, J.N., 2007b. Theory, modelling and calibration of passive samplers used in water monitoring. Passive sampling techniques in environmental monitoring 48, 141-169.

Brown, R.A., Weiss, F.T., 1978. Fate and effects of polynuclear aromatic hydrocarbons (PNA) in the aquatic environment. Am. Pet. Inst., Publ.;(United States) 4297, 23 pages.

Cai, D., Sun, L., Ke, J., Tang, G., 1996. Pesticide usage in China, prepared for Environment Canada. Environment Canada.

Cai, Q., Hu, Z., 2006. Studies on eutrophication problem and control strategy in the Three Gorges Reservoir. Acta hydrobiologica sinica/Shuisheng Shengwu Xuebao 30, 7-11.

Carrera, G., Fernández, P., Vilanova, R.M., Grimalt, J.O., 2001. Persistent organic pollutants in snow from European high mountain areas. Atmospheric environment 35, 245-254.

Charlestra, L., Courtemanch, D.L., Amirbahman, A., Patterson, H., 2008. Semipermeable membrane device (SPMD) for monitoring PCDD and PCDF levels from a paper mill effluent in the Androscoggin River, Maine, USA. Chemosphere 72, 1171-1180.

Chen, X., Yan, Y., Fu, R., Dou, X., Zhang, E., 2008. Sediment transport from the Yangtze River, China, into the sea over the Post-Three Gorge Dam Period: A discussion. Quaternary International 186, 55-64.

Chiou, C.T., 1985. Partition coefficients of organic compounds in lipid-water systems and correlations with fish bioconcentration factors. Environmental science & technology 19, 57-62.

Chiou, C.T., Peters, L.J., Freed, V.H., 1979. A physical concept of soil-water equilibria for nonionic organic compounds. Science 206, 831-832.

Clansky, K., 1992. Suspect Chemicals Sourcebook, 1992-2 Editions. Roytech Publications, Bethesda, Maryland.

Crunkilton, R.L., DeVita, W.M., 1997. Determination of aqueous concentrations of polycyclic aromatic hydrocarbons (PAHs) in an urban stream. Chemosphere 35, 1447-1463.

Czuczwa, J.M., Hites, R.A., 1986. Sources and fate of PCDD and PCDF. Chemosphere 15, 1417-1420.

Dabrowska, D., Kot-Wasik, A., Namieoenik, J., 2004. The importance of degradation in the fate of selected organic compounds in the environment. Part II. Photodegradation and biodegradation. Pol. J. Environ. Stud 13.

De Maagd, P., ten Hulscher, D.T.E., van den Heuvel, H., Opperhuizen, A., Sijm, D.T., 1998. Physicochemical properties of polycyclic aromatic hydrocarbons: Aqueous solubilities, n-octanol/water partition coefficients, and Henry's law constants. Environ Toxicol Chem 17, 251-257.

Deyerling, D., Wang, J., Hu, W., Westrich, B., Peng, C., Bi, Y., Henkelmann, B., Schramm, K.-W., 2014. PAH distribution and mass fluxes in the Three Gorges Reservoir after impoundment of the Three Gorges Dam. Science of The Total Environment 491, 123-130.

Dorsey, A., 2005. Toxicological Profile for Alpha-, Beta-, Gamma-, and Delta-Hexachlorocyclohexane. US Department of Health & Human Services, Public Health Service, Agency for Toxic Substances and Disease Registry.

Dreyer, A., Weinberg, I., Temme, C., Ebinghaus, R., 2009. Polyfluorinated compounds in the atmosphere of the Atlantic and Southern Oceans: evidence for a global distribution. Environmental science & technology 43, 6507-6514.

Dunn, R.J.K., Teasdale, P., Warnken, J., Jordan, M., Arthur, J., 2007. Evaluation of the in situ, time-integrated DGT technique by monitoring changes in heavy metal concentrations in estuarine waters. Environmental Pollution 148, 213-220.

Dunnivant, F.M., Elzerman, A.W., Jurs, P.C., Hasan, M.N., 1992. Quantitative structure-property relationships for aqueous solubilities and Henry's law constants of polychlorinated biphenyls. Environmental science & technology 26, 1567-1573.

EPA, 1996b. Technical Background Document part 5. Soil Screening

EPA, D., 2009. Integrated science assessment for particulate matter. US Environmental Protection Agency Washington, DC.

EPA, U., 1994. Estimating Exposure to Dioxin-like compounds, Vols 1-3. Office of Health and Environmental Assessment, Office of Research and Development. EPA/6006-88/005, Washington, USA.

Erickson, M.D., Kaley II, R.G., 2011. Applications of polychlorinated biphenyls. Environmental Science and Pollution Research 18, 135-151.

Eriksson, G., Jensen, S., Kylin, H., Strachan, W., 1989. The pine needle as a monitor of atmospheric pollution. Nature 341, 42-44.

Fetzer, J.C., 2007. The chemistry and analysis of large PAHs. Polycyclic Aromatic Compounds 27, 143-162.

Fiedler, H., 2003. Dioxins and furans (PCDD/PCDF). Persistent Organic Pollutants. Springer, pp. 123-201.

Gale, R.W., 1998. Three-compartment model for contaminant accumulation by semipermeable membrane devices. Environmental science & technology 32, 2292-2300.

Garofalo, E., Ceradini, S., Winter, M., 2004. The Use of Diffusive Gradients in Thin-Film (DGT) Passive Samplers for the Measurement of Bioavailable Metals in River Water. Annali di chimica 94, 515-520.

Geyer, H.J., Rimkus, G.G., Scheunert, I., Kaune, A., Schramm, K.-W., Kettrup, A., Zeeman, M., Muir, D.C., Hansen, L.G., Mackay, D., 2000. Bioaccumulation and occurrence of endocrine-disrupting chemicals (EDCs), persistent organic pollutants (POPs), and other organic compounds in fish and other organisms including humans. Bioaccumulation–New Aspects and Developments. Springer, pp. 1-166.

Geyer, H.J., Schramm, K.-W., Feicht, E.A., Behechti, A., Steinberg, C., Brüggemann, R., Poiger, H., Henkelmann, B., Kettrup, A., 2002. Half-lives of tetra-, penta-, hexa-, hepta-, and octachlorodibenzo-p-dioxin in rats, monkeys, and humans—a critical review. Chemosphere 48, 631-644.

Gilman, A., Newhook, R., Birmingham, B., 1991. An updated assessment of the exposure of Canadians to dioxins and furans. Chemosphere 23, 1661-1667.

Gourlay-Francé, C., Lorgeoux, C., Tusseau-Vuillemin, M.-H., 2008. Polycyclic aromatic hydrocarbon sampling in wastewaters using semipermeable membrane devices: accuracy of time-weighted average concentration estimations of truly dissolved compounds. Chemosphere 73, 1194-1200.

Guo, L., Qiu, Y., Zhang, G., Zheng, G.J., Lam, P.K., Li, X., 2008. Levels and bioaccumulation of organochlorine pesticides (OCPs) and polybrominated diphenyl ethers (PBDEs) in fishes from the Pearl River estuary and Daya Bay, South China. Environmental Pollution 152, 604-611.

Guo, Z., Lin, T., Zhang, G., Zheng, M., Zhang, Z., Hao, Y., Fang, M., 2007. The sedimentary fluxes of polycyclic aromatic hydrocarbons in the Yangtze River Estuary coastal sea for the past century. Science of the total environment 386, 33-41.

Güsten, H., Horvatić, D., Sabljić, A., 1991. Modelling n-octanol/water partition coefficients by molecular topology: polycyclic aromatic hydrocarbons and their alkyl derivatives. Chemosphere 23, 199-213.

Hansen, B.G., Paya-Perez, A.B., Rahman, M., Larsen, B.R., 1999. QSARs for K ow and K oc of PCB congeners: a critical examination of data, assumptions and statistical approaches. Chemosphere 39, 2209-2228.

Harman, C., Bøyum, O., Tollefsen, K.E., Thomas, K., Grung, M., 2008. Uptake of some selected aquatic pollutants in semipermeable membrane devices (SPMDs) and the polar organic chemical integrative sampler (POCIS). Journal of Environmental Monitoring 10, 239-247.

Hawker, D.W., Connell, D.W., 1988. Octanol-water partition coefficients of polychlorinated biphenyl congeners. Environmental science & technology 22, 382-387.

HSU, M.-H., KUO, A.Y.-S., LIU, W.-C., KUO, J.-T., 1999. Numerical simulation of circulation and salinity distribution in the Tanshui Estuary. Proceeding of the National Science Council ROC (A) 23, 259-273.

Huckins, J., Petty, J., Lebo, J., Orazio, C., Prest, H., Tillitt, D., Ellis, G., Johnson, B., Manuweera, G., 1996. Semipermeable membrane devices (SPMDs) for the concentration and assessment of bioavailable organic contaminants in aquatic environments. CRC Press: Boca Raton, FL, pp. 625-655.

Huckins, J.N., Booij, K., Petty, J.D., 2006a. Fundamentals of SPMDs. Monitors of Organic Chemicals in the Environment. Springer, pp. 29-43.

Huckins, J.N., Manuweera, G.K., Petty, J.D., Mackay, D., Lebo, J.A., 1993. Lipid-containing semipermeable membrane devices for monitoring organic contaminants in water. Environmental science & technology 27, 2489-2496.

Huckins, J.N., Petty, J.D., Booij, K., 2006b. Monitors of organic chemicals in the environment: semipermeable membrane devices. Springer Science & Business Media.

Huckins, J.N., Petty, J.D., Lebo, J.A., Almeida, F.V., Booij, K., Alvarez, D.A., Cranor, W.L., Clark, R.C., Mogensen, B.B., 2002a. Development of the permeability/performance reference compound approach for in situ calibration of semipermeable membrane devices. Environmental science & technology 36, 85-91.

Huckins, J.N., Petty, J.D., Orazio, C.E., Lebo, J.A., Clark, R.C., Gibson, V.L., Gala, W.R., Echols, K.R., 1999. Determination of uptake kinetics (Sampling rates) by lipid-containing semipermeable membrane devices (SPMDs) for polycyclic aromatic hydrocarbons (PAHs) in water. Environmental science & technology 33, 3918-3923.

Huckins, J.N., Petty, J.D., Prest, H.F., Clark, R., Alvarez, D., Orazio, C., Lebo, J., Cranor, W., Johnson, B., 2002b. A guide for the use of semipermeable membrane devices (SPMDs) as samplers of waterborne hydrophobic organic contaminants. API publication 4690, 1-192.

Huckins, J.N., Prest, H.F., Petty, J.D., Lebo, J.A., Hodgins, M.M., Clark, R.C., Alvarez, D.A., Gala, W.R., Steen, A., Gale, R., 2004. Overview and comparison of lipid-containing semipermeable membrane devices and oysters (Crassostrea gigas) for assessing organic chemical exposure. Environ Toxicol Chem 23, 1617-1628.

Huckins, J.N., Tubergen, M.W., Manuweera, G.K., 1990. Semipermeable membrane devices containing model lipid: A new approach to monitoring the bioavaiiability of lipophilic contaminants and estimating their bioconcentration potential. Chemosphere 20, 533-552.

Jaward, F.M., Zhang, G., Nam, J.J., Sweetman, A.J., Obbard, J.P., Kobara, Y., Jones, K.C., 2005. Passive air sampling of polychlorinated biphenyls, organochlorine compounds, and polybrominated diphenyl ethers across Asia. Environmental science & technology 39, 8638-8645.

Jensen, S., Eriksson, G., Kylin, H., Strachan, W., 1992. Atmospheric pollution by persistent organic compoumds: Monitoring with pine needles. Chemosphere 24, 229-245.

Jeyakumar, T., Kalaiarasi, I., Rajavel, A., Anbu, M., 2014. Levels of organochlorine pesticide residues in water and sediment from selected agricultural sectors of Kanyakumari District, Tamil Nadu, India. International Journal of Environmental Research 8, 493-500.

Karacık, B., Okay, O., Henkelmann, B., Pfister, G., Schramm, K.-W., 2013. Water concentrations of PAH, PCB and OCP by using semipermeable membrane devices and sediments. Marine pollution bulletin 70, 258-265.

Koning, J., Sein, A., Troost, L., Bremmer, H., 1993. Sources of dioxin emissions in the Netherlands. Organohalogen Compounds 14, 315-318.

Lebo J.A, Z.J.L., Huckins J.N., Petty J.D., Peterman P.H. , 1992. Use of semipermeable membrane devices for in situ monitoring of polycyclic aromatic hydrocarbons in aquatic environments. Chemosphere 25, 697-718.

Levy, W., Henkelmann, B., Pfister, G., Kirchner, M., Jakobi, G., Niklaus, A., Kotalik, J., Bernhöft, S., Fischer, N., Schramm, K.-W., 2007. Monitoring of PCDD/Fs in a mountain forest by means of active and passive sampling. Environmental research 105, 300-306.

Li, N., Wania, F., Lei, Y.D., Daly, G.L., 2003. A comprehensive and critical compilation, evaluation, and selection of physical–chemical property data for selected polychlorinated biphenyls. Journal of physical and chemical reference data 32, 1545-1590.

Li, S., Xu, Z., Cheng, X., Zhang, Q., 2008. Dissolved trace elements and heavy metals in the Danjiangkou Reservoir, China. Environmental Geology 55, 977-983.

Li, Y., Cai, D., Shan, Z., Zhu, Z., 2001. Gridded usage inventories of technical hexachlorocyclohexane and lindane for China with 1/6 latitude by 1/4 longitude resolution. Archives of Environmental Contamination and Toxicology 41, 261-266.

Liu, H.-H., Wong, C.S., Zeng, E.Y., 2013. Recognizing the limitations of performance reference compound (PRC)-calibration technique in passive water sampling. Environmental science & technology 47, 10104-10105.

Lohmann, R., Corrigan, B.P., Howsam, M., Jones, K.C., Ockenden, W.A., 2001. Further developments in the use of semipermeable membrane devices (SPMDs) as passive air samplers for persistent organic pollutants: field application in a spatial survey of PCDD/Fs and PAHs. Environmental science & technology 35, 2576-2582.

Lohmann, R., Lee, R.G., Green, N.J., Jones, K.C., 2000. Gas-particle partitioning of PCDD/Fs in daily air samples. Atmospheric Environment 34, 2529-2537.

Lu, X., Higgitt, D., 2001. Sediment delivery to the Three Gorges: 2: Local response. Geomorphology 41, 157-169.

Lubick, N., 2010. Endosulfan's exit: US EPA pesticide review leads to a ban. Science 328, 1466.

Luellen, D.R., Shea, D., 2002. Calibration and field verification of semipermeable membrane devices for measuring polycyclic aromatic hydrocarbons in water. Environmental science & technology 36, 1791-1797.

Mackay, D., Paterson, S., 1991. Evaluating the multimedia fate of organic chemicals: a level III fugacity model. Environmental science & technology 25, 427-436.

Mackay, D., Shiu, W.Y., Ma, K.C., 1992. Illustrated handbook of physical-chemical properties and environmental fate for organic chemicals. Volume II: polynuclear aromatic hydrocarbons, polychlorinated dioxins, and dibenzofurans. Lewis Publishers, Boca Raton, FL. 1992. 597.

Manz, M., Wenzel, K.-D., Dietze, U., Schüürmann, G., 2001. Persistent organic pollutants in agricultural soils of central Germany. Science of the Total Environment 277, 187-198.

Meador, J., Stein, J., Reichert, W., Varanasi, U., 1995. Bioaccumulation of polycyclic aromatic hydrocarbons by marine organisms. Reviews of environmental contamination and toxicology. Springer, pp. 79-165.

Meadows, J., Tillitt, D., Huckins, J., Schroeder, D., 1993. Large-scale dialysis of sample lipids using a semipermeable membrane device. Chemosphere 26.

Meadows, J.C., Echols, K.R., Huckins, J.N., Borsuk, F.A., Carline, R.F., Tillitt, D.E., 1998. Estimation of uptake rate constants for PCB congeners accumulated by semipermeable membrane devices and brown trout (Salmo trutta). Environmental science & technology 32, 1847-1852.

Meijer, S., Ockenden, W., Steinnes, E., Corrigan, B., Jones, K., 2003. Spatial and temporal trends of POPs in Norwegian and UK background air: Implications for global cycling. Environmental science & technology 37, 454-461.

Messinger, T., 2004. Polycyclic Aromatic Hydrocarbons in Bottom Sediment and Bioavailability in Streams in the New River Gorge National River and Gauley River National Recreation Area, West Virginia, 2002. US Department of the Interior, US Geological Survey.

Moeckel, C., Nizzetto, L., Guardo, A.D., Steinnes, E., Freppaz, M., Filippa, G., Camporini, P., Benner, J., Jones, K.C., 2008. Persistent organic pollutants in boreal and montane soil profiles: distribution, evidence of processes and implications for global cycling. Environmental science & technology 42, 8374-8380.

Monteyne, E., Roose, P., Janssen, C.R., 2013. Application of a silicone rubber passive sampling technique for monitoring PAHs and PCBs at three Belgian coastal harbours. Chemosphere 91, 390-398.

Moore, J.W., Ramamoorthy, S., 2012. Organic chemicals in natural waters: applied monitoring and impact assessment. Springer Science & Business Media.

Morrison, G., 1987. Bioavailable metal uptake rate determination in polluted waters by dialysis with receiving resins. Environmental Technology 8, 393-402.

Müller, B., Berg, M., Yao, Z.P., Zhang, X.F., Wang, D., Pfluger, A., 2008. How polluted is the Yangtze river? Water quality downstream from the Three Gorges Dam. Science of the total environment 402, 232-247.

Neff, J., 1979. Polycyclic Aromatic Hydrocarbons in the Aquatic Environment: Sources, Fates, and Biological Effects. . Applied Science Publishers, London (UK), 152-195.

Neff, J., 1985. Polycyclic aromatic hydrocarbons. In: Rand, G.M., Petrocelli, S.R. (Eds.), Fundamentals of Aquatic Toxicology, Methods and Applications. Hemisphere, New York, NY, 416-454.

Öberg, L., Andersson, R., Rappe, C., 1992. De novo formation of hepta-and octachlorodibenzo-p-dioxins from pentachlorophenol in municipal sewage sludge. Organohalogen Compounds 9, 351-354.

Öberg, L., Wagman, N., Andersson, R., Rappe, C., 1993. De novo formation of PCDD/Fs in compost and sewage sludge–a status report. Organohalogen compounds 11, 297-302.

Parliament, E., 2008. Directive 2008/105/EC of the European Parliament and of the Council of 16 December 2008 on environmental quality standards in the field of water policy, amending and subsequently repealing. Official Journal of the European Union, L 348, 84-97.

Pessah, I.N., Cherednichenko, G., Lein, P.J., 2010. Minding the calcium store: ryanodine receptor activation as a convergent mechanism of PCB toxicity. Pharmacology & therapeutics 125, 260-285.

Petty, J.D., 2000. Development of Monitors for Assessing Exposure of Military Personnel to Toxic Chemicals. DTIC Document.

Petty, J.D., Huckins, J.N., Zajicek, J.L., 1993. Application of semipermeable membrane devices (SPMDs) as passive air samplers. Chemosphere 27, 1609-1624.

Prest, H., Jarman, W., Burns, S., Weismüller, T., Martin, M., Huckins, J., 1992. Passive water sampling via semipermfable membrane devices (SPMDS) in concert with bivalves in the Sacramento/San Joaquin River Delta. Chemosphere 25, 1811-1823.

Qiu, X., Zhu, T., Yao, B., Hu, J., Hu, S., 2005. Contribution of dicofol to the current DDT pollution in China. Environmental science & technology 39, 4385-4390.

Rantalainen, A.L., Cretney, W.J., Ikonomou, M.G., 2000. Uptake rates of semipermeable membrane devices (SPMDs) for PCDDs, PCDFs and PCBs in water and sediment. Chemosphere 40, 147-158.

Rappe, C., Kjeller, L.-O., Kulp, S.-E., de Wit, C., Hasselsten, I., Palm, O., 1991. Levels, profile and pattern of PCDDs and PCDFs in samples related to the production and use of chlorine. Chemosphere 23, 1629-1636.

Reid, B.J., Jones, K.C., Semple, K.T., 2000. Bioavailability of persistent organic pollutants in soils and sediments—a perspective on mechanisms, consequences and assessment. Environmental Pollution 108, 103-112.

Roach, A.C., Muller, R., Komarova, T., Symons, R., Stevenson, G.J., Mueller, J.F., 2009. Using SPMDs to monitor water column concentrations of PCDDs, PCDFs and dioxin-like PCBs in Port Jackson (Sydney Harbour), Australia. Chemosphere 75, 1243-1251.

Roegge, C.S., Wang, V.C., Powers, B.E., Klintsova, A.Y., Villareal, S., Greenough, W.T., Schantz, S.L., 2004. Motor impairment in rats exposed to PCBs and methylmercury during early development. Toxicological Sciences 77, 315-324.

Rojo-Nieto, E., Sales, D., Perales, J.A., 2013. Sources, transport and fate of PAHs in sediments and superficial water of a chronically polluted semi-enclosed body of seawater: linking of compartments. Environmental Science: Processes & Impacts 15, 986-995.

Rood, D., 1999. practical guide to the care, maintenance, and troubleshooting of capillary gas chromatographic systems. Wiley-VCH.

Rusina, T.P., Smedes, F., Klanova, J., 2010. Diffusion coefficients of polychlorinated biphenyls and polycyclic aromatic hydrocarbons in polydimethylsiloxane and low-density polyethylene polymers. Journal of applied polymer science 116, 1803-1810.

Sarkar, A., Nagarajan, R., Chaphadkar, S., Pal, S., Singbal, S., 1997. Contamination of organochlorine pesticides in sediments from the Arabian Sea along the west coast of India. Water Research 31, 195-200.

Sawford, B., 1983. The effect of Gaussian particle-pair distribution functions in the statistical theory of concentration fluctuations in homogeneous turbulence. Quarterly Journal of the Royal Meteorological Society 109, 339-354.

Scholz, G., Quinton, J.N., Strauss, P., 2008. Soil erosion from sugar beet in Central Europe in response to climate change induced seasonal precipitation variations. Catena 72, 91-105.

Schramm, K.-W., Wang, J., Bi, Y., Temoka, C., Pfister, G., Henkelmann, B., Scherb, H., 2013. Chemical-and effect-oriented exposomics: Three Gorges Reservoir (TGR). Environmental Science and Pollution Research 20, 7057-7062.

Shoven, H.A., 2001. Monitoring dioxin levels in Maine rivers with semipermeable membrane devices. Electronic Theses and Dissertations. University of Maine, p. 399.

Söderström, H.S., Bergqvist, P.-A., 2003. Polycyclic aromatic hydrocarbons in a semiaquatic plant and semipermeable membrane devices exposed to air in Thailand. Environmental science & technology 37, 47-52.

Strandberg, B., van Bavel, B., Bergqvist, P.-A., Broman, D., Ishaq, R., Näf, C., Pettersen, H., Rappe, C., 1998. Occurrence, sedimentation, and spatial variations of organochlorine contaminants in settling particulate matter and sediments in the northern part of the Baltic Sea. Environmental science & technology 32, 1754-1759.

Stuer-Lauridsen, F., 2005. Review of passive accumulation devices for monitoring organic micropollutants in the aquatic environment. Environmental Pollution 136, 503-524.

Tanabe, S., Iwata, H., Tatsukawa, R., 1994. Global contamination by persistent organochlorines and their ecotoxicological impact on marine mammals. Science of the total environment 154, 163-177.

Tomaszewski, J.E., Luthy, R.G., 2008. Field deployment of polyethylene devices to measure PCB concentrations in pore water of contaminated sediment. Environmental science & technology 42, 6086-6091.

UNEP, U.N.E.P., 2005. Standardized Toolkit for identification and quantification of dioxin and furan releases. UNEP Chemicals Geneva, Switzerland.

USEPA, A., 1998. Guidelines for ecological risk assessment. EPA/630/R-95.

Varsha, Y., Naga Deepthi, C., Chenna, S., 2011. An emphasis on xenobiotic degradation in environmental cleanup. J Bioremed Biodegrad S 11, 1-10.

Verweij, F., Booij, K., Satumalay, K., van der Molen, N., van der Oost, R., 2004. Assessment of bioavailable PAH, PCB and OCP concentrations in water, using semipermeable membrane devices (SPMDs), sediments and caged carp. Chemosphere 54, 1675-1689.

Vrana, B., Schüürmann, G., 2002. Calibrating the uptake kinetics of semipermeable membrane devices in water: impact of hydrodynamics. Environmental science & technology 36, 290-296.

Wang, H., Yang, Z., Wang, Y., Saito, Y., Liu, J.P., 2008. Reconstruction of sediment flux from the Changjiang (Yangtze River) to the sea since the 1860s. Journal of Hydrology 349, 318-332.

Wang, J., Bi, Y., Pfister, G., Henkelmann, B., Zhu, K., Schramm, K.-W., 2009. Determination of PAH, PCB, and OCP in water from the Three Gorges Reservoir accumulated by semipermeable membrane devices (SPMD). Chemosphere 75, 1119-1127.

Wang, J., Henkelmann, B., Bi, Y., Zhu, K., Pfister, G., Hu, W., Temoka, C., Westrich, B., Schramm, K.-W., 2013a. Temporal variation and spatial distribution of PAH in water of Three Gorges Reservoir during the complete impoundment period. Environmental Science and Pollution Research 20, 7071-7079.

Wang, X., Chen, Y., Song, L., Chen, X., Xie, H., Liu, L., 2013b. Analysis of lengths, water areas and volumes of the Three Gorges Reservoir at different water levels using Landsat images and SRTM DEM data. Quaternary International 304, 115-125.

Whitefield, P.D., Hagen, D.E., 1995. Particulates and Aerosol Sampling From Combustor Rigs Using the UMR Mobile Aerosol Sampling System (MASS). 33rd Aerospace Sciences Meeting & Exhibit, Paper No. AIAA, pp. 95-0111.

WHO, 1993. Polychlorinated biphenyls and terphenyls. In: Dobson S, 1361 van Esch GJ (eds) Environ Heal Criteria 140, 2nd edn. World 1362 Health Organization (WHO), Geneva

WHO, 2014. IARC monographs on the evaluation of carcinogenic risks to humans. International Agency for Research on Cancer. 18-2-2014 28-2-2014]; Available from: http://monographs.iarc.fr/ENG/Classification/

Wiberg, K., Lundström, K., Glas, B., Rappe, C., 1989. PCDDs and PCDFs in consumers' paper products. Chemosphere 19, 735-740.

Willett, K.L., Ulrich, E.M., Hites, R.A., 1998. Differential toxicity and environmental fates of hexachlorocyclohexane isomers. Environmental science & technology 32, 2197-2207.

Wong, J.W., Hennessy, M.K., Hayward, D.G., Krynitsky, A.J., Cassias, I., Schenck, F.J., 2007. Analysis of organophosphorus pesticides in dried ground ginseng root by capillary gas chromatography-mass spectrometry and-flame photometric detection. Journal of agricultural and food chemistry 55, 1117-1128.

Wu, J., Huang, J., Han, X., Gao, X., He, F., Jiang, M., Jiang, Z., Primack, R.B., Shen, Z., 2004. The three gorges dam: an ecological perspective. Frontiers in Ecology and the Environment 2, 241-248.

Wu, S.-P., Tao, S., Zhang, Z.-H., Lan, T., Zuo, Q., 2005. Distribution of particle-phase hydrocarbons, PAHs and OCPs in Tianjin, China. Atmospheric Environment 39, 7420-7432.

Wu, W., Xu, Y., Schramm, K.-W., Kettrup, A., 1997. Study of sorption, biodegradation and isomerization of HCH in stimulated sediment/water system. Chemosphere 35, 1887-1894.

Wu, Y., Zhang, J., Liu, S., Zhang, Z., Yao, Q., Hong, G., Cooper, L., 2007. Sources and distribution of carbon within the Yangtze River system. Estuarine, Coastal and Shelf Science 71, 13-25.

Yang, R.-q., Jiang, G.-b., Zhou, Q.-f., Yuan, C.-g., Shi, J.-b., 2005. Occurrence and distribution of organochlorine pesticides (HCH and DDT) in sediments collected from East China Sea. Environment international 31, 799-804.

Yang, S.-l., Zhao, Q.-y., Belkin, I.M., 2002. Temporal variation in the sediment load of the Yangtze River and the influences of human activities. Journal of Hydrology 263, 56-71.

Yang, Z.-Z., Li, Y.-F., Li, Z.-C., Gu, Y.-M., Zhu, Y., Zhang, Z.-J., 2011. Distribution and characterization of higher chlorinated benzenes in outdoor dust collected from a fast developing city in North China. Bulletin of environmental contamination and toxicology 86, 38-42.

Yu, H.Y., Guo, Y., Zeng, E.Y., 2010. Dietary intake of persistent organic pollutants and potential health risks via consumption of global aquatic products. Environ Toxicol Chem 29, 2135-2142.

Zhang, H., Luo, Y., Li, Q., 2009. Burden and depth distribution of organochlorine pesticides in the soil profiles of Yangtze River Delta Region, China: Implication for sources and vertical transportation. Geoderma 153, 69-75.

Zhang, Z., Hong, H., Zhou, J., Huang, J., Yu, G., 2003. Fate and assessment of persistent organic pollutants in water and sediment from Minjiang River Estuary, Southeast China. Chemosphere 52, 1423-1430.

Zheng, B., Cao, C., Zhang, J., Huang, M., Chen, Z., 2009. [Analysis of algal blooms in Da-Ning River of Three Gorges Reservoir]. Environmental Sciences 30, 3218-3226.

Zheng, W., Yu, H., Wang, X., Qu, W., 2012. Systematic review of pentachlorophenol occurrence in the environment and in humans in China: not a negligible health risk due to the re-emergence of schistosomiasis. Environment international 42, 105-116.

Zhou, J.L., Rowland, S.J., 1997. Evaluation of the interactions between hydrophobic organic pollutants and suspended particles in estuarine waters. Water Research 31, 1708-1718.

Zhu, X., Pfister, G., Henkelmann, B., Kotalik, J., Fiedler, S., Schramm, K.-W., 2007. Simultaneous monitoring of PCDD/Fs and PCBs in contaminated air with semipermeable membrane devices and fresh spruce needles. Chemosphere 68, 1623-1629.

Appendix

Appendix Table 1: PCDD/F in VO exposed in air in pg/sample (Chapter 2.5)

all values in pg/sample		c0805007 0 h (SPMD in glass)	c0805001 2 h	c0805002 4 h	c0805003 6 h	c0805004 24 h	c0805005 48 h	c0805006 72 h	c0805008 168 h	c0805009 312 h
Sum Tetrachlorodibenzo-p-dioxins		3238	3308	3067	3050	3340	812	859	2818	2720
Sum Pentachlorodibenzo-p-dioxins		5958	6934	6612	7170	6575	2307	2238	4966	4040
Sum Hexachlorodibenzo-p-dioxins		12438	11041	11226	6796	9138	7090	7361	7263	7003
Sum Heptachlorodibenzo-p-dioxins		17637	15958	16583	14649	13038	11383	13056	8787	7995
Octachlorodibenzo-p-dioxin		22903	21511	19311	16329	13056	11492	13493	7472	6519
Sum Tetra- to Octachlorodibenzo-p-dioxins		62174	58752	56799	47994	45147	33084	37007	31306	28277
2,3,7,8-Tetrachlorodibenzo-p-dioxin	TCDD	170	150	139	127	105	88.1	108	62.4	46.6
1,2,3,7,8-Pentachlorodibenzo-p-dioxin	PeCDD	641	709	638	600	538	467	507	342	242
1,2,3,4,7,8-Hexachlorodibenzo-p-dioxin	HxCDD	640	627	599	344	471	444	470	319	230
1,2,3,6,7,8-Hexachlorodibenzo-p-dioxin	HxCDD	1107	1090	1021	884	723	606	711	380	278
1,2,3,7,8,9-Hexachlorodibenzo-p-dioxin	HxCDD	1052	908	834	480	547	678	814	340	256
1,2,3,4,6,7,8-Heptachlorodibenzo-p-dioxin	HpCDD	9420	8965	8770	7529	6095	5259	6197	3613	2888
Sum Tetrachlorodibenzofurans		2464	2147	1901	2006	1478	564	637	655	502
Sum Pentachlorodibenzofurans		4009	2623	2086	1498	733	193	230	260	137
Sum Hexachlorodibenzofurans		7297	2854	1754	849	364	125	161	119	45
Sum Heptachlorodibenzofurans		8267	1939	1030	448	253	137	181	81.7	36.6
Octachlorodibenzofuran		2659	369	190	98.9	71.2	54.8	48.7	15.7	9.7
Sum Tetra- to Octachlorodibenzofurans		24696	9932	6961	4900	2899	1074	1258	1131	730
2,3,7,8-Tetrachlorodibenzofuran	TCDF	84	92.8	82.1	62.9	56.7	45.4	59	27.6	14.5
1,2,3,7,8-Pentachlorodibenzofuran	PeCDF	231	208	168	139	72.4	47.5	60.1	26.6	15
2,3,4,7,8-Pentachlorodibenzofuran	PeCDF	389	206	132	67.2	18.6	14.4	18.5	3.9	8.8
1,2,3,4,7,8-Hexachlorodibenzofuran	HxCDF	661	259.0	137.0	129.0	26.9	18.8	22.4	8.6	2.8
1,2,3,6,7,8-Hexachlorodibenzofuran	HxCDF	807	375	219	98.7	48.2	30.9	48.2	19.6	8.4
1,2,3,7,8,9-Hexachlorodibenzofuran	HxCDF	197	45.3	20.3	n.d.	n.d.	4.3	n.d.	n.d.	n.d.
2,3,4,6,7,8-Hexachlorodibenzofuran	HxCDF	1042	403	215	65.9	27.8	18	25	11.7	4.3
1,2,3,4,6,7,8-Heptachlorodibenzofuran	HpCDF	5567	1540	788	340	171	131	191	68	30.5
1,2,3,4,7,8,9-Heptachlorodibenzofuran	HpCDF	434	54.7	33.7	14.4	9.5	8.8	10	n.d.	n.d.
Total sum PCDD and PCDF (Tetra to Octa)		86870	68684	63760	52894	48046	34158	38265	32437	29007
TEQ (NATO/CCMS)		1436	1125	961	770	653	581	667	391	288
TEQ (WHO 1998, Humans)		1734	1460	1263	1055	910	804	908	556	403

Appendix Table 2: PCDD/F in VO exposed in glass vial in pg/sample

all values in pg/sample		c0805007 0 h (SPMD in glass)	c0805010 24 h (SPMD in glass)	c0805012 72 h (SPMD in glass)	c0805013 312 h (SPMD in glass)
Sum Tetrachlorodibenzo-p-dioxins		3238	3447	3369	3621
Sum Pentachlorodibenzo-p-dioxins		5958	5700	6004	5591
Sum Hexachlorodibenzo-p-dioxins		12438	12216	10060	10642
Sum Heptachlorodibenzo-p-dioxins		17637	16495	14519	13517
Octachlorodibenzo-p-dioxin		22903	18766	15502	14779
Sum Tetra- to Octachlorodibenzo-p-dioxins		62174	56624	49454	48150
2,3,7,8-Tetrachlorodibenzo-p-dioxin	TCDD	170	167	134	139
1,2,3,7,8-Pentachlorodibenzo-p-dioxin	PeCDD	641	594	562	511
1,2,3,4,7,8-Hexachlorodibenzo-p-dioxin	HxCDD	640	596	517	510
1,2,3,6,7,8-Hexachlorodibenzo-p-dioxin	HxCDD	1107	989	806	844
1,2,3,7,8,9-Hexachlorodibenzo-p-dioxin	HxCDD	1052	856	728	730
1,2,3,4,6,7,8-Heptachlorodibenzo-p-dioxin	HpCDD	9420	8417	7422	6725
Sum Tetrachlorodibenzofurans		2464	2063	1473	1648
Sum Pentachlorodibenzofurans		4009	1976	1244	1057
Sum Hexachlorodibenzofurans		7297	1918	796	633
Sum Heptachlorodibenzofurans		8267	1003	388	315
Octachlorodibenzofuran		2659	131	71.7	51.8
Sum Tetra- to Octachlorodibenzofurans		24696	7091	3973	3705
2,3,7,8-Tetrachlorodibenzofuran	TCDF	84	85.8	63.1	68.6
1,2,3,7,8-Pentachlorodibenzofuran	PeCDF	231	153	106	96.3
2,3,4,7,8-Pentachlorodibenzofuran	PeCDF	389	145	56.4	40.9
1,2,3,4,7,8-Hexachlorodibenzofuran	HxCDF	661.0	131.0	46.8	38.0
1,2,3,6,7,8-Hexachlorodibenzofuran	HxCDF	807	223	99.4	83
1,2,3,7,8,9-Hexachlorodibenzofuran	HxCDF	197	20.5	n.d.	n.d.
2,3,4,6,7,8-Hexachlorodibenzofuran	HxCDF	1042	237	85	65.1
1,2,3,4,6,7,8-Heptachlorodibenzofuran	HpCDF	5567	795	285	235
1,2,3,4,7,8,9-Heptachlorodibenzofuran	HpCDF	434	27.2	13.7	8.4
Total sum PCDD and PCDF (Tetra to Octa)		86870	63715	53427	51855
TEQ (NATO/CCMS)		1436	970	776	738
TEQ (WHO 1998, Humans)		1734	1250	1043	980

Appendix Table 3: PCDD/F in VO frozen from -30 °C to -80 °C in pg/sample

all values in pg/sample		c0805007 0 h (SPMD in glass)	c0805011 24 h (SPMD in glass, from -30 to -80°C)	c0805014 312 h (SPMD in glass, from -30 to -80°C)
Sum Tetrachlorodibenzo-p-dioxins		3238	2945	3197
Sum Pentachlorodibenzo-p-dioxins		5958	5647	5894
Sum Hexachlorodibenzo-p-dioxins		12438	10367	11403
Sum Heptachlorodibenzo-p-dioxins		17637	16971	16673
Octachlorodibenzo-p-dioxin		22903	22052	22752
Sum Tetra- to Octachlorodibenzo-p-dioxins		62174	57982	59919
2,3,7,8-Tetrachlorodibenzo-p-dioxin	TCDD	170	166	197
1,2,3,7,8-Pentachlorodibenzo-p-dioxin	PeCDD	641	619	617
1,2,3,4,7,8-Hexachlorodibenzo-p-dioxin	HxCDD	640	610	632
1,2,3,6,7,8-Hexachlorodibenzo-p-dioxin	HxCDD	1107	1072	1097
1,2,3,7,8,9-Hexachlorodibenzo-p-dioxin	HxCDD	1052	1051	1102
1,2,3,4,6,7,8-Heptachlorodibenzo-p-dioxin	HpCDD	9420	9274	9442
Sum Tetrachlorodibenzofurans		2464	2247	2296
Sum Pentachlorodibenzofurans		4009	3725	4270
Sum Hexachlorodibenzofurans		7297	6131	7134
Sum Heptachlorodibenzofurans		8267	7430	8431
Octachlorodibenzofuran		2659	3229	3423
Sum Tetra- to Octachlorodibenzofurans		24696	22762	25554
2,3,7,8-Tetrachlorodibenzofuran	TCDF	84	89	97.7
1,2,3,7,8-Pentachlorodibenzofuran	PeCDF	231	234	250
2,3,4,7,8-Pentachlorodibenzofuran	PeCDF	389	355	364
1,2,3,4,7,8-Hexachlorodibenzofuran	HxCDF	661.0	648.0	701.0
1,2,3,6,7,8-Hexachlorodibenzofuran	HxCDF	807	740	795
1,2,3,7,8,9-Hexachlorodibenzofuran	HxCDF	197	206	203
2,3,4,6,7,8-Hexachlorodibenzofuran	HxCDF	1042	988	1066
1,2,3,4,6,7,8-Heptachlorodibenzofuran	HpCDF	5567	5305	5639
1,2,3,4,7,8,9-Heptachlorodibenzofuran	HpCDF	434	463	493
Total sum PCDD and PCDF (Tetra to Octa)		86870	80744	85473
TEQ (NATO/CCMS)		1436	1380	1451
TEQ (WHO 1998, Humans)		1734	1667	1736

Appendix Table 4: PCB in VO exposed in air in pg/sample(Chapter 2.5)

all values in pg/sample		p0805007 0 h (SPMD in glass)	p0805001 2 h	p0805002 4 h	p0805003 6 h	p0805004 24 h	p0805005 48 h	p0805006 72 h	p0805008 168 h	p0805009 312 h
Indikator PCB:										
2,4,4'/2,5,4'-Trichlorobiphenyl	PCB #28	396	430	424	462	622	837	1136	2195	2585
2,2',5,5'-Tetrachlorobiphenyl	PCB #52	698	608	616	627	878	1189	1511	3011	4300
2,2',4,5,5'-Pentachlorobiphenyl	PCB #101	1612	1224	1242	1205	1348	1408	1472	2071	2757
2,2',3,4,4',5'-Hexachlorobiphenyl	PCB #138	1685	1284	1319	1287	1321	1328	1339	1431	1511
2,2',4,4',5,5'-Hexachlorobiphenyl	PCB #153	1614	1103	1141	996	1186	1129	1144	1311	1425
2,2',3,4,4',5,5'-Heptachlorobiphenyl	PCB #180	912	684	701	681	664	721	664	725	676
Non-ortho PCB:										
3,3',4,4'-Tetrachlorobiphenyl	PCB #77	694	655	683	661	663	653	640	641	699
3,4,4',5-Tetrachlorobiphenyl	PCB #81	538	499	537	497	469	513	498	464	490
3,3',4,4',5-Pentachlorobiphenyl	PCB #126	572	514	513	512	559	523	516	481	522
3,3',4,4',5,5'-Hexachlorobiphenyl	PCB #169	610	590	580	539	585	567	566	550	581
Mono-ortho PCB:										
2,3,3',4,4'-Pentachlorobiphenyl	PCB #105	709	623	628	604	646	625	632	694	736
2,3,4,4',5-Pentachlorobiphenyl	PCB #114	496	462	469	427	436	455	437	418	431
2,3',4,4',5-Pentachlorobiphenyl	PCB #118	868	674	695	702	704	748	757	933	1140
2',3,4,4',5-Pentachlorobiphenyl	PCB #123	360	413	408	397	390	387	405	404	401
2,3,3',4,4',5-Hexachlorobiphenyl	PCB #156	715	662	621	617	638	637	641	636	622
2,3,3',4,4',5'-Hexachlorobiphenyl	PCB #157	527	554	542	520	541	532	546	546	522
2,3',4,4',5,5'-Hexachlorobiphenyl	PCB #167	535	536	526	510	516	546	547	489	494
2,3,3',4,4',5,5'-Heptachlorobiphenyl	PCB #189	698	736	733	708	714	714	696	701	694
TEQ (WHO 1998, Humans)		64.5	58.5	58.3	57.7	62.9	59.2	58.4	54.8	59.2

Appendix Table 5: PCB in VO exposed in glass vial in pg/sample (Chapter 2.5)

all values in pg/sample		p0805007 0 h (SPMD in glass)	p0805010 24 h (SPMD in glass)	p0805012 72 h (SPMD in glass)	p0805013 312 h (SPMD in glass)
Indikator PCB:					
2,4,4'/2,5,4'-Trichlorobiphenyl		396	340	322	323
2,2',5,5'-Tetrachlorobiphenyl	PCB #28	698	575	555	534
2,2',4,5,5'-Pentachlorobiphenyl	PCB #52	1612	1172	1025	999
2,2',3,4,4',5'-Hexachlorobiphenyl	PCB #101	1685	1202	1077	1116
2,2',4,4',5,5'-Hexachlorobiphenyl	PCB #138	1614	1081	867	862
2,2',3,4,4',5,5'-Heptachlorobiphenyl	PCB #153	912	727	661	640
	PCB #180				
Non-ortho PCB:					
3,3',4,4'-Tetrachlorobiphenyl		694	609	622	594
3,4,4',5-Tetrachlorobiphenyl	PCB #77	538	514	485	476
3,3',4,4',5-Pentachlorobiphenyl	PCB #81	572	520	509	505
3,3',4,4',5,5'-Hexachlorobiphenyl	PCB #126	610	551	570	550
	PCB #169				
Mono-ortho PCB:					
2,3,3',4,4'-Pentachlorobiphenyl		709	614	576	615
2,3,4,4',5-Pentachlorobiphenyl	PCB #105	496	442	412	439
2,3',4,4',5-Pentachlorobiphenyl	PCB #114	868	720	660	662
2',3,4,4',5-Pentachlorobiphenyl	PCB #118	360	378	356	349
2,3,3',4,4',5-Hexachlorobiphenyl	PCB #123	715	610	640	651
2,3,3',4,4',5'-Hexachlorobiphenyl	PCB #156	527	518	524	498
2,3',4,4',5,5'-Hexachlorobiphenyl	PCB #157	535	497	488	495
2,3,3',4,4',5,5'-Heptachlorobiphenyl	PCB #167	698	666	674	658
	PCB #189				
TEQ (WHO 1998, Humans)		64.5	58.6	57.7	57.1

Appendix Table 6: PCB in VO frozen from -30 °C to -80 °C in pg/sample

all values in pg/sample		p0805007 0 h (SPMD in glass)	p0805011 24 h (SPMD in glass, from -30 to -80°C)	p0805014 312 h (SPMD in glass, from -30 to -80°C)
Indikator PCB:				
2,4,4'/2,5,4'-Trichlorobiphenyl	PCB #28	396	407	400
2,2',5,5'-Tetrachlorobiphenyl	PCB #52	698	571	578
2,2',4,5,5'-Pentachlorobiphenyl	PCB #101	1612	1317	1195
2,2',3,4,4',5'-Hexachlorobiphenyl	PCB #138	1685	1448	1307
2,2',4,4',5,5'-Hexachlorobiphenyl	PCB #153	1614	1253	1080
2,2',3,4,4',5,5'-Heptachlorobiphenyl	PCB #180	912	770	732
Non-ortho PCB:				
3,3',4,4'-Tetrachlorobiphenyl	PCB #77	694	750	745
3,4,4',5-Tetrachlorobiphenyl	PCB #81	538	561	593
3,3',4,4',5-Pentachlorobiphenyl	PCB #126	572	585	636
3,3',4,4',5,5'-Hexachlorobiphenyl	PCB #169	610	635	591
Mono-ortho PCB:				
2,3,3',4,4'-Pentachlorobiphenyl	PCB #105	709	770	740
2,3,4,4',5-Pentachlorobiphenyl	PCB #114	496	543	521
2,3',4,4',5-Pentachlorobiphenyl	PCB #118	868	822	788
2',3,4,4',5-Pentachlorobiphenyl	PCB #123	360	451	421
2,3,3',4,4',5-Hexachlorobiphenyl	PCB #156	715	693	699
2,3,3',4,4',5'-Hexachlorobiphenyl	PCB #157	527	641	578
2,3',4,4',5,5'-Hexachlorobiphenyl	PCB #167	535	558	540
2,3,3',4,4',5,5'-Heptachlorobiphenyl	PCB #189	698	856	830
TEQ (WHO 1998, Humans)		64.5	66.2	70.8

Appendix Table 7: Data during XAD deployment in well (Chapter 2.4)

Date	Time	Reference point	Water to Container	Measured Volume	Outside Temperature	Water Temperature	Real volume
		Depth (cm)	**Depth (cm)**	**m^3**	**°C**	**°C**	**m^3**
26.03.2013	11:30	135	45	0.299	8.6	9.3	
28.03.2013	12:00	75	105	0.698			
31.03.2013	11:00	65	115	0.764	4.2	4.1	
01.04.2013	10:00	65	115	0.764			
20.04.2013	20:45	61	119	0.791			
20.04.2013	21:15:00	131	49	0.326	12	8	
21.04.2013	10:15:00	110	70	0.465	12	8	
22.04.2013	09:30:00	80	100	0.665	8.5	7	
22.04.2013	14:30:00	77	103	0.685	8	7	
22.04.2013	20:30:00	75	105	0.698	7	7	
23.04.2013	07:00:00	68	112	0.745	8	7	
24.04.2013	20:45:00	63	117	0.778	9	8	
25.04.2013	11:30:00	63	117	0.778	9	8	
21.05.2013	11:00:00	72	108	0.718	11	9	
01.06.2013	20:00:00	23	157	1.044	10	9	
14.06.2013	10:30:00	36	144	0.957	12	10	
06.07.2013	21:00:00	72	108	0.718	14	11	
19.07.2013	21:15:00	80	100	0.665	13	13	
25.07.2013	14:30:00	78	102	0.678	16	13	
07.08.2013	20:00:00	78	102	0.678	17	14	
17.08.2013	19:00:00	81	99	0.658	15	13	
09.10.2013	18:00:00	80	100	0.665	11	11.5	
16.11.2013	10:00:00	73	107	0.711	8	10	
15.12.2013	16:00:00	69	111	0.738	8	8	
04.01.2014	13:00:00	77	103	0.685	6	8	
24.01.2014	17:15:00	75	105	0.698	7	8	
28.02.2014	21:00:00	73	107	0.711	6	8	
28.02.2014	21:30:00	77.5	102.5	0.681			
28.02.2014	22:00:00	82	98	0.651			
28.02.2014	22:30:00	85	95	0.632			
28.02.2014	00:15:00	97	83	0.552			0.258
01.03.2014	09:30:00	157	23	0.153			0.95
01.03.2014	10:30:00	161	19	0.126			1.026
01.03.2014	11:30:00	165	15	0.100			1.098
01.03.2014	12:30:00	170	10	0.066			1.173
01.03.2014	18:30:00	160	20	0.133			
02.03.2014	10:00:00	133	47	0.312			
01.04.2014	15:40:00	79	101	0.671			
01.04.2014	16:00:00	82	98	0.651			
01.04.2014	17:30:00	95	85	0.565			
01.04.2014	18:30:00	102	78	0.519			
01.04.2014	20:10:00	114	66	0.439			
01.04.2014	22:00:00	125	55	0.366			0.468
04.04.2014	13:30:00	89	91	0.605			
04.04.2014	15:15:00	103	77	0.512			0.135
04.04.2014	17:30:00	120	60	0.399			0.298
04.04.2014	19:55:00	137	43	0.286			0.48
04.04.2014	23:00:00	155	25	0.166			0.719
05.04.2014	12:00:00	136	44	0.292			
05.04.2014	13:20:00	145	35	0.233			0.096
05.04.2014		154	26	0.173			0.218
05.04.2014	17:20:00	165	15	0.100			0.389
05.04.2014	18:20:00	170	10	0.066			0.461
06.04.2014	09:00:00	147	33	0.219			0.461
06.04.2014	11:00:00	156	24	0.160			0.587

Appendix Table 8: PRC in VO in ng/sample (first trial, Chapter 2.4)

all values in ng/SPMD	Average Blank	pah0907238 Frozen	pah0907240 Frozen	pah1103176 Field R	pah1304074 Field L	pah0907241 20.07.12-23.07.12 3 days	pah0907252 20.07.12-07.08.12 18 days
Naphthalene-13C6	127%	135%	123%	123%	12%	99%	77%
Acenaphthylene-13C6	122%	131%	119%	116%	12%	107%	96%
Acenaphthene-13C6	127%	135%	124%	124%	12%	104%	104%
Fluorene-13C6	122%	129%	118%	120%	11%	101%	103%
Phenanthrene-13C6	119%	127%	111%	118%	11%	104%	103%
Anthracene-13C6	117%	124%	113%	114%	11%	101%	101%
Fluoranthene-13C6	141%	148%	131%	145%	13%	115%	125%
Pyrene-13C3	131%	137%	126%	130%	13%	113%	112%
Benzo(a)anthracene- 13C6	119%	137%	93%	125%	15%	118%	101%
Chrysene-13C6	148%	154%	143%	147%	17%	126%	126%
Benzo(b)fluoranthene-13C6	131%	140%	126%	127%	15%	114%	118%
Benzo(k)fluoranthene-13C6	143%	150%	139%	141%	18%	127%	127%
Benzo(a)pyrene-13C4	137%	145%	131%	135%	17%	122%	127%
Indeno(1,2,3-cd)pyrene-13C6	132%	141%	124%	131%	14%	113%	120%
Benzo(g,h,i)perylene-13C12	117%	125%	105%	120%	15%	111%	108%
Dibenz(a,h)anthracene-13C6	140%	146%	134%	141%	18%	119%	129%

all values in ng/SPMD	pah1103174 20.07.12-11.09.12 53 days	pah1103169 20.07.12-21.10.12 93 days	pah1103167 20.07.12-04.01.13 168 days	pah1103172 20.07.12-08.03.13 262 days	pah1103176 20.07.12-08.03.13 262 days
Naphthalene-13C6	51%	34%	9%	2%	
Acenaphthylene-13C6	92%	78%	49%	29%	
Acenaphthene-13C6	109%	96%	71%	54%	
Fluorene-13C6	111%	101%	83%	65%	67%
Phenanthrene-13C6	121%	116%	107%	97%	98%
Anthracene-13C6	114%	110%	96%	87%	87%
Fluoranthene-13C6	128%	133%	130%	117%	120%
Pyrene-13C3	127%	129%	129%	119%	125%
Benzo(a)anthracene- 13C6	140%	140%	136%	137%	134%
Chrysene-13C6	145%	150%	151%	142%	145%
Benzo(b)fluoranthene-13C6	132%	130%	140%	127%	136%
Benzo(k)fluoranthene-13C6	146%	144%	146%	138%	143%
Benzo(a)pyrene-13C4	141%	140%	147%	134%	138%
Indeno(1,2,3-cd)pyrene-13C6	132%	133%	143%	129%	137%
Benzo(g,h,i)perylene-13C12	122%	122%	113%	121%	123%
Dibenz(a,h)anthracene-13C6	145%	139%	145%	133%	143%

Appendix Table 9: PRC in VO in ng/sample (second trial, Chapter 2.4)

all values in ng/SPMD	pah1103168 26.03.13-28.02.14 339 days BWL	pah1103171 26.03.13-28.02.14 339 days BWR	pah1103162 26.03.13-20.04.13 25 days	pah1103203 26.03.13-20.04.13 25 days	pah1103204 26.03.13-01.03.14 340days	pah1103161 26.03.13-01.03.14 340days
Naphthalene-13C6	100%	101%	44%	39%	75%	73%
Acenaphthylene-13C6	116%	123%	89%	84%	106%	106%
Acenaphthene-13C6	114%	117%	102%	95%	110%	110%
Fluorene-13C6	105%	110%	103%	89%	104%	98%
Phenanthrene-13C6	113%	117%	113%	107%	117%	113%
Anthracene-13C6	111%	112%	112%	104%	113%	110%
Fluoranthene-13C6	107%	111%	108%	103%	109%	108%
Pyrene-13C3	104%	106%	109%	102%	108%	106%
Benzo(a)anthracene- 13C6	87%	87%	89%	83%	84%	84%
Chrysene-13C6	91%	93%	93%	85%	92%	90%
Benzo(b)fluoranthene-13C6	84%	80%	58%	79%	83%	80%
Benzo(k)fluoranthene-13C6	89%	93%	63%	90%	95%	93%
Benzo(a)pyrene-13C4	79%	84%	48%	78%	85%	82%
Indeno(1,2,3-cd)pyrene-13C(	77%	81%	82%	73%	78%	80%
Benzo(g,h,i)perylene-13C12	65%	63%	69%	56%	63%	64%
Dibenz(a,h)anthracene-13C6	87%	88%	89%	83%	78%	85%

BWL: Blank left BWR: Blank right

Appendix Table 10: Calculation procedure of PAH concentration at 25 d in VO after exposure in well (Chapter 2.4)

pah1103203, 25 d

	MW	*MW* labelled	log K_{ow}	Blank N0	%PRC retention (*N*)	% *N/N0*	*ke*, $_{PRC}$	
Naphthalene	128	134	3.38	1.01	39%	0.39	0.04	d^{-1}
Acenaphthylene	152	158	4.07	1.19	84%	0.71	0.01	d^{-1}
Acenaphthene	154	160	3.92	1.15	95%	0.83	0.01	d^{-1}
Fluorene	166	172	4.1	1.07	89%	0.84	0.01	d^{-1}
Phenanthrene	178	184	4.46	1.15	107%	0.93	0.00	d^{-1}
Anthracene	178	184	4.54	1.12	104%	0.93	0.00	d^{-1}
Fluoranthene	202	208	4.84	1.09	103%	0.94	0.00	d^{-1}
Pyrene	202	208	5.18	1.05	102%	0.97	0.00	d^{-1}
Benzo(a)anthracene	228	234	5.6	0.87	83%	0.96	0.00	d^{-1}
Chrysene	228	234	5.84	0.92	85%	0.92	0.00	d^{-1}
Benzo(b)fluoranthene	252	258	6.44	0.82	79%	0.97	0.00	d^{-1}
Benzo(k)fluoranthene	252	258	6.44	0.91	90%	0.99	0.00	d^{-1}
Benzo(a)pyrene	252	256	6.42	0.82	78%	0.95	0.00	d^{-1}
Indeno(1,2,3-cd)pyrene	276	282	6.42	0.79	73%	0.92	0.00	d^{-1}
Benzo (ghi) perylene	276	288	6.63	0.64	56%	0.88	0.01	d^{-1}
Dibenzo(a,h)anthracene	278	284	6.5	0.87	83%	0.95	0.00	d^{-1}

V_{LDPE} (cm3)	0.7475	V_T (cm3)	0.661474	(mit 0.95 g/cm3 the density of Triolein)
Trioleineinwaage Schläuche	0.6284	*Vs* (cm3)	1.408974	
µl Standard/g Triolein	2.933268			
Deployment time:		25 days		

log K_{TW}	K_{TW}	log K_{LDPEW}	K_{LDPEW}	K_{VO_W}	log K_{VO_W}	*Rs*, $_{PRC}$	
3.485	3055	2.96	910	1917	3.28	103	cm^3d^{-1}
4.175	14962	3.68	4825	9584	3.98	188	cm^3d^{-1}
4.025	10593	3.53	3357	6754	3.83	73	cm^3d^{-1}
4.205	16032	3.72	5188	10279	4.01	104	cm^3d^{-1}
4.565	36728	4.09	12388	23815	4.38	99	cm^3d^{-1}
4.645	44157	4.18	15031	28705	4.46	119	cm^3d^{-1}
4.945	88105	4.49	31046	57833	4.76	192	cm^3d^{-1}
5.285	192752	4.85	70632	127964	5.11	231	cm^3d^{-1}
5.705	506991	5.29	194984	341463	5.53	843	cm^3d^{-1}
5.945	881049	5.54	348337	598430	5.78	2760	cm^3d^{-1}
6.545	3507519	6.17	1485936	2435012	6.39	4794	cm^3d^{-1}
6.545	3507519	6.17	1485936	2435012	6.39	1512	cm^3d^{-1}
6.525	3349654	6.15	1415794	2323687	6.37	6662	cm^3d^{-1}
6.525	3349654	6.15	1415794	2323687	6.37	10893	cm^3d^{-1}
6.735	5432503	6.37	2352339	3798390	6.58	27508	cm^3d^{-1}
6.605	4027170	6.24	1717908	2802042	6.45	8572	cm^3d^{-1}

pah1103203, 25 d

	N/N0 , max	*ke, min*	*Rs, min*	*Rs analyte (N)* cm^3d^{-1}	Masse pg/SPMD	***Cw*** **pg/cm^3=ng/L**
Naphthalene	0.98	0.00 d-1	2 cm^3d^{-1}	103	1264	**0.76**
Acenaphthylene	0.99	0.00 d-1	3 cm^3d^{-1}	188	70	**0.02**
Acenaphthene	0.99	0.00 d-1	3 cm^3d^{-1}	73	118	**0.07**
Fluorene	0.99	0.00 d-1	6 cm^3d^{-1}	104	52	**0.02**
Phenanthrene	0.99	0.00 d-1	9 cm^3d^{-1}	99	1288	**0.54**
Anthracene	0.99	0.00 d-1	9 cm^3d^{-1}	119	146	**0.05**
Fluoranthene	0.98	0.00 d-1	68 cm^3d^{-1}	192	662	**0.14**
Pyrene	0.98	0.00 d-1	122 cm^3d^{-1}	231	1649	**0.29**
Benzo(a)anthracene	0.97	0.00 d-1	527 cm^3d^{-1}	843	98	**0.00**
Chrysene	0.97	0.00 d-1	1014 cm^3d^{-1}	2760	193	**0.00**
Benzo(b)fluoranthene	0.97	0.00 d-1	4152 cm^3d^{-1}	4794	943	**0.01**
Benzo(k)fluoranthene	0.97	0.00 d-1	3992 cm^3d^{-1}	3992	972	**0.01**
Benzo(a)pyrene	0.97	0.00 d-1	4299 cm^3d^{-1}	6662	1056	**0.01**
Indeno(1,2,3-cd)pyrene	0.97	0.00 d-1	4314 cm^3d^{-1}	10893	603	**0.00**
Benzo (ghi) perylene	1.00	0.00 d-1	418 cm^3d^{-1}	27508	446	**0.00**
Dibenzo(a,h)anthracene	0.97	0.00 d-1	4761 cm^3d^{-1}	8572	702	**0.00**

Appendix Table 11: Comparison of PAH and OCP water concentration in VO at 25 days, VO at 340 days and XAD-2 after exposure in well (Chapter 2.4)

	Cw (ng/L)		
	VO, t_{25}	VO, t_{340}	XAD
Naphthalene	0.763	1.758	0.411
Acenaphthylene	0.018	0.047	0.153
Acenaphthene	0.071	0.256	0.086
Fluorene	0.022	0.047	0.114
Phenanthrene	0.540	0.75	0.521
Anthracene	0.051	0.200	0.041
Fluoranthene	0.142	0.303	0.404
Pyrene	0.290	0.251	1.043
Benzo(a)anthracene	0.005	0.006	0.011
Chrysene	0.003	0.008	0.024
Benzo(b)fluoranthene	0.008	0.010	0.023
Benzo(k)fluoranthene	0.010	0.010	0.038
Benzo(a)pyrene	0.007	0.010	0.024
Indeno(1,2,3-cd)pyrene	0.003	0.006	0.015
Benzo (ghi) perylene	0.010	0.019	0.021
Dibenzo(a,h)anthracene	0.003	0.006	0.002

	VO, t_{25}	VO, t_{340}	XAD
γ-HCH	332.92	547.68	422.83
PeCB	2.44	4.19	5.87
2,4'-DDT	5.82	7.79	10.49
2,4'-DDE	0.69	0.85	0.93
Dieldrin	26.55	33.17	55.07
Methoxychlor	6.02	7.60	8.12

Appendix Table 12: Comparison of water concentrations in ng/L, using Huckins method ($C_W(H)$) and the new procedure ($C_W(N)$), of four.-, five-, six-ring PAH with log K_{ow} range from 5.18 to 6.63 during 26 days of deployment (17.3°C - 23.9°C) at twelve different sampling sites along the Three Gorges Reservoir (Chapter 3)

pg/L	Maoping		Guojiaba		Xiangxi I		Xiangxi II		Daning I		Daning II	
	Cw(H)	*Cw(N)*	*Cw(H)*	*Cw(N)*	*Cw(H)*	*Cw(N)*	*Cw(H)*	*Cw(N)*	*Cw(H)*	*Cw(N)*	*Cw(H)*	*Cw(N)*
6 Ring	274	4	449	4	213	11	198	11	263	21	268	14
5 Ring	1452	23	3081	70	1570	37	1960	89	2621	287	2848	240
4 Ring	6825	1591	15013	2279	16918	2135	10700	2751	14718	6856	30838	10020

Fendji		Xiaojiang I		Xiaojiang II		Wanzhou		Changshou		Chongqing	
Cw(H)	*Cw(N)*	*Cw(H)*	*Cw(N)*	*Cw(H)*	*Cw(N)*	*Cw(H)*	*Cw(N)*	*Cw(H)*	*Cw(N)*	*Cw(H)*	*Cw(N)*
330	21	518	36	624	40	852	24	950	7	383	55
3265	328	4116	406	4441	419	7290	300	6244	208	3080	224
18514	8026	25589	17015	28106	21847	74177	33006	52144	62217	12084	14550

Appendix Table 13: Comparison of in situ Rs and Huckins Rs estimated using release values of PRC compounds from previous studies (see chapter 2.2)

	log K_{ow}	**in situ $Rs_{,PRC}$**	**$R_{sanalyte}$ (H)**
Naph-$^{13}C_6$	3.22	420	2626
Ace-$^{13}C_6$	3.93	1163	2510
Acy-$^{13}C_6$	3.78	431	2467
Fle-$^{13}C_6$	3.96	1002	2390
Fen-$^{13}C_6$	4.33	1383	2336
Ant-$^{13}C_6$	4.41	1704	2347
Flo-$^{13}C_6$	4.72	1504	2258
Pyr-$^{13}C_3$	5.07	1735	2272
BaA-$^{13}C_6$	5.50	3171	2144
Chr-$^{13}C_6$	5.74	6413	2135
BbF-$^{13}C_6$	6.36	27532	2078
BkF-$^{13}C_6$	6.36	9107	2078
BaP-$^{13}C_4$	6.34	15161	2096
IND-$^{13}C_6$	6.34	5022	2036
BghiP-$^{13}C_{12}$	6.55	23604	2053
DahA-$^{13}C_6$	6.42	29838	1991

Appendix Table 14: Radioactivity ^{14}C –OCDD data in VO and in LPDE

VO - Migration experiment with ^{14}C-OCDD

Sample	Exposure time of VO mounted in frames (h)	Exposure time of VO in glass (h)	Date of withdrawal at storage at -80°C	Recovery based on ^{14}C Radioactivity %	^{14}C Radioactivity DPM in LDPE-tubing, where measured, calculated
1107047	0	0	01.08.2011	90.41	
1107069	0	0	01.08.2011	94.12	
1107081	0	0	01.08.2011	91.26	
0907236	0	0	01.08.2011	100.56	1009
0907237	0	0	01.08.2011	76.02	
1107042	8		01.08.2011	78.11	
1107043	8		01.08.2011	84.09	
1107045	8		01.08.2011	90.18	
1107046		8	01.08.2011	97.38	
1107048		8	01.08.2011	96.98	
1107049		8	01.08.2011	91.01	
1107050	24		02.08.2011	90.18	
1107051	24		02.08.2011	85.17	
1107052	24		02.08.2011	97.37	
1107053		24	02.08.2011	94.40	
1107054		24	02.08.2011	96.22	
1107055		24	02.08.2011	97.39	
1107056	48		03.08.2011	98.78	
1107057	48		03.08.2011	94.72	
1107058	48		03.08.2011	95.41	
1107059		48	03.08.2011	95.68	
1107060		48	03.08.2011	97.67	
1107061		48	03.08.2011	93.02	
1107062	96		05.08.2011	97.28	
1107063	96		05.08.2011	93.15	
1107064	96		05.08.2011	94.68	
1107065		96	05.08.2011	96.06	
1107066		96	05.08.2011	96.28	
1107067		96	05.08.2011	95.65	
1107068	192		09.08.2011	106.69	1031
1107070	192		09.08.2011	96.44	
1107071	192		09.08.2011	96.81	
1107072		192	09.08.2011	94.42	
1107073		192	09.08.2011	94.54	
1107074		192	09.08.2011	95.34	
1107075	384		17.08.2011	101.65	1232
1107076	384		17.08.2011	97.66	1324
1107077	384		17.08.2011	99.48	1300
1107078		384	17.08.2011	106.00	1776
1107079		384	17.08.2011	106.73	
1107080		384	17.08.2011	96.76	

Appendix Table 15**:** Rs_{min} (L.d^{-1}) was applied if a direct measurement of Rs_{PRC} (L.d^{-1}) was not obtainable for the estimation of $Rs_{PRC}(N)$ (L.d^{-1}) during sampling campaign in 2011 in Three Gorges Reservoir in China**.** The campaign covered twelves sampling sites: Maoping (MP) Guojiaba(GJB), Xiangxi I/II (XX1/2), Daning I/II (DN1/2), Fendji (FJ), Xiaojiang I/II (XJ1/2), Wanzhou (WZ), Changshou (CS), Chongqing (CQ). $Rs,_{PRC}(N)$ were directly used as the native PAHs sampling rates $Rs,_{PAH}(N)$ (L.d^{-1}) with similar physicochemical properties

		MP				GJB				XX1			
PAH-PRC compounds	**log K_{ow}**	**Rs_{PRC}**	**Rs_{min}**	**$Rs_{PRC}(N)$**	**$Rs_{PAH}(N)$**	**Rs_{PRC}**	**Rs_{min}**	**$Rs_{PRC}(N)$**	**$Rs_{PAH}(N)$**	**Rs_{PRC}**	**Rs_{min}**	**$Rs_{PRC}(N)$**	**$Rs_{PAH}(N)$**
Naphthalin-13C6	3.38	0.674	0.004	0.674	0.674		0.005			0.735	0.004	0.735	0.735
Acenaphthylen-13C6	4.07	1.715	0.026	1.715	1.715	3.037	0.036	3.037	3.037	2.448	0.026	2.448	2.448
Acenaphthen-13C6	3.92	0.742	0.022	0.742	0.742	1.543	0.031	1.543	1.543	1.167	0.022	1.167	1.167
Fluoren-13C6	4.1	1.085	0.030	1.085	1.085	2.032	0.043	2.032	2.032	2.104	0.031	2.104	2.104
Phenanthren-13C6	4.46	1.464	0.066	1.464	1.464	2.148	0.092	2.148	2.148	2.421	0.067	2.421	2.421
Anthracen-13C6	4.54	1.582	0.117	1.582	1.582	2.314	0.165	2.314	2.314	2.514	0.120	2.514	2.514
Fluoranthen-13C6	4.84	1.119	0.070	1.119	1.119	2.040	0.098	2.040	2.040	1.399	0.072	1.399	1.399
Pyren-13C3	5.18	1.765	0.194	1.765	1.765	2.450	0.270	2.450	2.450	4.141	0.198	4.141	4.141
Benzo(a)anthracen- 13C6	5.6	4.574	0.911	4.574	4.574	3.020	1.264	3.020	3.020	3.253	0.931	3.253	3.253
Chrysen-13C6	5.84	8.847	1.451	8.847	8.847	8.010	2.010	8.010	8.010	7.068	1.484	7.068	7.068
Benzo(b)fluoranthen-13C6	6.44	33.753	6.129	33.753	33.753	12.235	8.441	12.235	12.235	27.003	6.267	27.003	27.003
Benzo(k)fluoranthen-13C6	6.44	32.119	6.189	32.119	32.119	19.412	8.524	19.412	19.412	22.288	6.328	22.288	22.288
Benzo(a)pyren-13C4	6.42	30.890	6.385	30.890	30.890	33.971	8.794	33.971	33.971	25.262	6.528	25.262	25.262
Indeno(1,2,3-cd)pyren-13C6	6.42	21.245	6.015	21.245	21.245	17.907	8.285	17.907	17.907	-1.470	6.150	6.150	6.150
Benzo(g,h,i)perylen-13C12	6.63	57.909	14.310	57.909	57.909	127.072	19.669	127.072	127.072	69.526	14.631	69.526	69.526
Dibenz(a,h)anthracen-13C6	6.5	29.833	8.418	29.833	29.833	-1.183	11.587	11.587	11.587	22.263	8.608	22.263	22.263

PAH-PRC compounds	log K_{ow}	XX2				DN1				DN2			
		Rs_{PRC}	Rs_{min}	$Rs_{PRC}(N)$	$Rs_{PAH}(N)$	Rs_{PRC}	Rs_{min}	$Rs_{PRC}(N)$	$Rs_{PAH}(N)$	Rs_{PRC}	Rs_{min}	$Rs_{PRC}(N)$	$Rs_{PAH}(N)$
Naphthalin-13C6	3.38	0.731	0.004	0.731	0.731		0.004				0.004		
Acenaphthylen-13C6	4.07	2.735	0.026	2.735	2.735		0.026				0.026		
Acenaphthen-13C6	3.92	1.150	0.022	1.150	1.150		0.022			1.431	0.022	1.431	1.431
Fluoren-13C6	4.1	2.584	0.031	2.584	2.584	2.568	0.031	2.568	2.568	2.985	0.031	2.985	2.985
Phenanthren-13C6	4.46	2.867	0.067	2.867	2.867	3.076	0.066	3.076	3.076	3.055	0.066	3.055	3.055
Anthracen-13C6	4.54	2.965	0.119	2.965	2.965	3.267	0.118	3.267	3.267	3.181	0.118	3.181	3.181
Fluoranthen-13C6	4.84	1.591	0.071	1.591	1.591	1.707	0.070	1.707	1.707	1.358	0.070	1.358	1.358
Pyren-13C3	5.18	2.736	0.197	2.736	2.736	2.760	0.195	2.760	2.760	3.542	0.195	3.542	3.542
Benzo(a)anthracen- 13C6	5.6	2.748	0.926	2.748	2.748	3.250	0.916	3.250	3.250	5.920	0.916	5.920	5.920
Chrysen-13C6	5.84	4.821	1.476	4.821	4.821	9.590	1.461	9.590	9.590	10.460	1.461	10.460	10.460
Benzo(b)fluoranthen-13C6	6.44	16.538	6.232	16.538	16.538	1.068	6.170	6.170	6.170	16.170	6.170	16.170	16.170
Benzo(k)fluoranthen-13C6	6.44	17.750	6.294	17.750	17.750	-2.425	6.231	6.231	6.231	16.230	6.231	16.230	16.230
Benzo(a)pyren-13C4	6.42	8.232	6.492	8.232	8.232	9.434	6.428	9.434	9.434	18.208	6.428	18.208	18.208
Indeno(1,2,3-cd)pyren-13C6	6.42	5.826	6.116	6.116	6.116	-2.890	6.055	6.055	6.055	-1.912	6.055	6.055	6.055
Benzo(g,h,i)perylen-13C12	6.63	53.725	14.552	53.725	53.725	10.831	14.408	14.408	14.408	43.242	14.408	43.242	43.242
Dibenz(a,h)anthracen-13C6	6.5	14.769	8.561	14.769	14.769	0.286	8.475	8.475	8.475	9.454	8.475	9.454	9.454

PAH-PRC compounds	log K_{ow}	FJ				XJ1				XJ2			
		Rs_{PRC}	Rs_{min}	$Rs_{PRC}(N)$	$Rs_{PAH}(N)$	Rs_{PRC}	Rs_{min}	$Rs_{PRC}(N)$	$Rs_{PAH}(N)$	Rs_{PRC}	Rs_{min}	$Rs_{PRC}(N)$	$Rs_{PAH}(N)$
Naphthalin-13C6	3.38		0.004				0.004				0.004		
Acenaphthylen-13C6	4.07	3.044	0.026	3.044	3.044	3.065	0.026	3.065	3.065	2.959	0.026	2.959	2.959
Acenaphthen-13C6	3.92		0.022				0.022				0.022		
Fluoren-13C6	4.1	2.375	0.031	2.375	2.375	2.406	0.030	2.406	2.406	2.371	0.031	2.371	2.371
Phenanthren-13C6	4.46	2.889	0.066	2.889	2.889	2.934	0.066	2.934	2.934	2.940	0.066	2.940	2.940
Anthracen-13C6	4.54	3.193	0.119	3.193	3.193	3.221	0.117	3.221	3.221	3.254	0.119	3.254	3.254
Fluoranthen-13C6	4.84	1.632	0.071	1.632	1.632	1.470	0.070	1.470	1.470	1.463	0.071	1.463	1.463
Pyren-13C3	5.18	2.930	0.196	2.930	2.930	2.920	0.194	2.920	2.920	2.760	0.196	2.760	2.760
Benzo(a)anthracen- 13C6	5.6	4.060	0.922	4.060	4.060	4.910	0.910	4.910	4.910	4.920	0.920	4.920	4.920
Chrysen-13C6	5.84	8.470	1.470	8.470	8.470	8.840	1.450	8.840	8.840	8.470	1.466	8.470	8.470
Benzo(b)fluoranthen-13C6	6.44	16.210	6.210	16.210	16.210	16.130	6.126	16.130	16.130	16.190	6.193	16.190	16.190
Benzo(k)fluoranthen-13C6	6.44	19.490	6.271	19.490	19.490	16.190	6.187	16.190	16.190	16.250	6.254	16.250	16.250
Benzo(a)pyren-13C4	6.42	17.080	6.469	17.080	17.080	16.380	6.382	16.380	16.380	12.660	6.451	12.660	12.660
Indeno(1,2,3-cd)pyren-13C6	6.42	-5.284	6.094	6.094	6.094	-7.815	6.012	6.012	6.012	-2.274	6.078	6.078	6.078
Benzo(g,h,i)perylen-13C12	6.63	28.773	14.500	28.773	28.773	-19.759	14.306	14.306	14.306	-14.413	14.461	14.461	14.461
Dibenz(a,h)anthracen-13C6	6.5	3.037	8.530	8.530	8.530	-16.919	8.415	8.415	8.415	-12.279	8.507	8.507	8.507

PAH-PRC compounds	log K_{ow}	WZ				CS				CQ			
		Rs_{PRC}	Rs_{min}	$Rs_{PRC}(N)$	$Rs_{PAH}(N)$	Rs_{PRC}	Rs_{min}	$Rs_{PRC}(N)$	$Rs_{PAH}(N)$	Rs_{PRC}	Rs_{min}	$Rs_{PRC}(N)$	$Rs_{PAH}(N)$
Naphthalin-13C6	3.38		0.004				0.004			0.733	0.004	0.733	0.733
Acenaphthylen-13C6	4.07	2.028	0.027	2.028	2.028	1.651	0.027	1.651	1.651	3.110	0.027	3.110	3.110
Acenaphthen-13C6	3.92	0.983	0.023	0.983	0.983	1.081	0.023	1.081	1.081	1.313	0.023	1.313	1.313
Fluoren-13C6	4.1	1.515	0.032	1.515	1.515	1.986	0.032	1.986	1.986	3.029	0.031	3.029	3.029
Phenanthren-13C6	4.46	1.832	0.068	1.832	1.832	2.236	0.068	2.236	2.236	6.201	0.068	6.201	6.201
Anthracen-13C6	4.54	2.031	0.122	2.031	2.031	2.406	0.122	2.406	2.406	7.908	0.121	7.908	7.908
Fluoranthen-13C6	4.84	1.660	0.073	1.660	1.660	1.091	0.073	1.091	1.091	6.635	0.072	6.635	6.635
Pyren-13C3	5.18	2.430	0.201	2.430	2.430	2.200	0.201	2.200	2.200	2.233	0.200	2.233	2.233
Benzo(a)anthracen- 13C6	5.6	4.950	0.945	4.950	4.950	4.950	0.945	4.950	4.950	11.304	0.941	11.304	11.304
Chrysen-13C6	5.84	8.510	1.506	8.510	8.510	8.510	1.506	8.510	8.510	38.577	1.499	38.577	38.577
Benzo(b)fluoranthen-13C6	6.44	-13.269	6.358	6.358	6.358	7.842	6.358	7.842	7.842	109.619	6.329	109.619	109.619
Benzo(k)fluoranthen-13C6	6.44	-10.029	6.421	6.421	6.421	10.067	6.421	10.067	10.067	41.975	6.391	41.975	41.975
Benzo(a)pyren-13C4	6.42	2.336	6.623	6.623	6.623	100.439	6.623	100.439	100.439	74.642	6.593	74.642	74.642
Indeno(1,2,3-cd)pyren-13C6	6.42	-4.227	6.240	6.240	6.240	22.676	6.240	22.676	22.676	18.653	6.211	18.653	18.653
Benzo(g,h,i)perylen-13C12	6.63	-11.970	14.843	14.843	14.843	63.282	14.843	63.282	63.282	116.983	14.775	116.983	116.983
Dibenz(a,h)anthracen-13C6	6.5	-3.896	8.733	8.733	8.733	28.528	8.733	28.528	28.528	151.517	8.693	151.517	151.517

Appendix Table 16: Determination of the contribution of m_{SP}, m_{DOC} and m_W to estimate the total mass distribution of PAHs concentration in 1L of water

(C_T =VO(N))

Analytes	**m_w [ng]**	**m_{ss} [ng]**	**m_{DOC} [ng]**	**m_T [ng]**	**C_T ng/L**
Naph	9.03732	0.00211	0.02892	9.06835	9.06835
Acy	0.04089	0.00005	0.00066	0.04160	0.04160
Ace	0.20402	0.00017	0.00231	0.20650	0.20650
Fle	0.78831	0.00127	0.01741	0.80699	0.80699
Fen	3.36287	0.00951	0.13040	2.50000	2.50000
Ant	0.29527	0.00102	0.01394	0.31022	0.31022
Flo	1.32156	0.01650	0.22625	1.56431	1.56431
Pyr	1.43002	0.01752	0.24024	1.68779	1.68779
BaA	0.06517	0.00303	0.04150	0.90969	0.90969
Chr	0.09536	0.00443	0.06072	0.16051	0.16051
BbF	0.11436	0.00206	0.02825	1.19000	1.19000
BkF	0.20314	0.00045	0.00617	0.22976	0.22976
BaP	0.50420	0.00050	0.00686	0.61156	0.61156
IND	0.60300	0.00122	0.01667	0.72088	0.72088
BghiP	0.30126	0.00048	0.00663	0.38373	0.38373
DahA	0.07095	0.00042	0.00580	0.08718	0.08718